

A Giovanna, Adelma e Peppe

Dad what is the mind? Is it just a system of impulses or something tangible?

Bart Simpson

Acknowledgements

First I would like to thank my supervisor, Rüdiger Kein, for giving me the opportunity to work in his group and most importantly for the freedom he has given me to develop my own ideas. I greatly appreciate his support as well as all the scientific inputs that have helped pursuing my own interests.

I am very grateful to all collaborators working at the MPI of Neurobiology and at other institutes without whom this project could not have been completed. A special thank goes to Sonia Paixao who performed all the biochemistry experiments presented in this thesis. She also generated and analyzed the mice overexpressing ephrinA3 in astrocytes. I would like to thank Silke Honsek and Christine Rose at the Heinrich Heine University of Düsseldorf for performing the astrocyte electrophysiology experiments; Lore Becker, Berend Feddersen and Thomas Klopstock at the Friedrich Baur Institute of Neurology of the University of Munich for performing the seizure analysis; Klas Kullander at the Uppsala University, York Rudhard, Ralf Schoepfer at the University College London and Elena Pasquale at the Burnham Institute for medical research in La Jolla for providing mouse lines.

Very special thanks go to Volker Staiger at the MPI of Neurobiology for helping me with the electrophysiology experiments at the beginning of my PhD. I would like also to thank Valentin Stein for suggestions for patch-clamping experiments, Marielle Klein for technical help and all the people working in the service units of the MPI of Neurobiology for making my life in the lab easier.

I would like to thank the members of the Klein group for scientific and non-scientific discussions and comments. I would like also to acknowledge the people working in the IMPRS coordination office, especially Hans-Joerg Schaeffer, for managing a fantastic graduate school. I wish to thank Onur Gökce for being a great student and friend.

I would like finally to thank some very special people that have been (and always be) part of my life, without whom I would not have been the person I am now: Suphansa, my parents Giovanna and Algerino, my brother Giuseppe and my friends Stefano, Gabriele, Cico, "lo Zio", Marianna, Marco, Eva, Maria, Simona and Giulio.

**Neuron-glia communication
via EphA4-ephrinA3
modulates LTP through glial
glutamate transport**

Dissertation

Der Fakultät für Biologie
der Ludwig-Maximilians-Universität
München

Vorgelegt von
Alessandro Filosa
München, März 2010

Erstgutachter: Prof. Dr. Rüdiger Klein

Zweitgutachter: Prof. Dr. Christian Leibold

Tag der mündlichen Prüfung: 07/06/2010

The work presented in this thesis was performed in the laboratory of Prof. Dr. Rüdiger Klein, Department of Molecular Neurobiology, Max Planck Institute of Neurobiology, Martinsried, Germany.

Ehrenwörtliche Versicherung

Ich versichere hiermit ehrenwörtlich, dass die vorgelegte Dissertation von mir selbständig und ohne unerlaubte Beihilfe angefertigt ist.

Hiermit erkläre ich, dass ich mich anderweitig einer Doktorprüfung ohne Erfolg nicht unterzogen habe.

München, den

.....

(Unterschrift)

Table of contents

List of figures and tables v

Abbreviations viii

Abstract..... 1

1 Introduction..... 5

1.1 Anatomy of the hippocampus 6

1.2 Structural and functional properties of hippocampal synapses 8

 1.2.1 Presynaptic compartment and mechanism of neurotransmitter release 8

 1.2.2 Postsynaptic compartment 10

 1.2.2.1 Glutamate receptors 10

 1.2.2.2 Scaffold and signaling proteins..... 12

1.3 Synaptic Plasticity 13

 1.3.1 Short term plasticity 14

 1.3.2 Long term plasticity 14

 1.3.2.1 Long term potentiation 15

 1.3.2.2 Long term depression 17

 1.3.3 Structural plasticity 18

 1.3.4 Metaplasticity 18

 1.3.5 Homeostatic synaptic scaling 19

1.4 Contributions of glia to synaptic transmission and plasticity 20

 1.4.1 The role of glia in synaptogenesis 21

 1.4.2 Gliotransmission and its effect on synaptic function..... 22

 1.4.3 Glial glutamate transporters 23

 1.4.4 Impact of synaptic changes on glia physiology..... 25

1.5 Eph receptors and ephrin ligands 25

1.5.1 Eph forward signaling mechanisms	27
1.5.2 Ephrin reverse signaling mechanisms	29
1.5.2.1 EphrinB reverse signaling.....	29
1.5.2.1 EphrinA reverse signaling	31
1.5.3 Cis versus trans interactions	32
1.5.4 The role of Eph receptors and ephrins in synaptic plasticity	33
1.5.4.1 Modulation of structural plasticity by Ephs and ephrins.....	33
1.5.4.2 Modulation of functional plasticity by Ephs and ephrins.....	36
1.6 Summary of the thesis project.....	38
2 Results	40
2.1 Characterization of a novel <i>Epha4</i> conditional allele.....	41
2.2 Hippocampal long term synaptic plasticity is not altered in <i>Epha4^{lox/-}</i> mice....	42
2.3 Efficient subregion-specific elimination of EphA4 in adult hippocampus.....	43
2.4 Normal basal synaptic transmission in <i>Epha4</i> mutants	45
2.5 EphA4 is required for LTP in postsynaptic CA1 cells.....	48
2.6 Tetanus-induced LTP does not require EphA4	50
2.7 EphrinA3 is required for TBS-induced LTP	51
2.8 Normal basal synaptic transmission in <i>Efna3</i> null mutants.....	52
2.9 Astrocytic glutamate transporter upregulation in <i>Epha4</i> mutants	54
2.10 Normal astrocytic glutamate transporter abundance in <i>Epha4^{EGFP/EGFP}</i> mice...56	
2.11 Increased glutamate uptake in <i>Efna3^{-/-}</i> astrocytes	57
2.12 Low glutamate concentration near synapses in <i>Epha4^{-/-}</i> mice.....	59
2.13 Reduced neuronal depolarization during high frequency stimulation in <i>Epha4</i> and <i>Efna3</i> mutants.....	61
2.14 Blockade of glutamate transport rescues LTP defects in <i>EphA4</i> and <i>Efna3</i> mutants	62
2.15 Transgenic mice overexpressing ephrinA3 in astrocytes	64

2.16 EphrinA3 overexpression in astrocytes reduces glial glutamate transporter abundance66

2.17 EphrinA3 overexpression in astrocytes causes excitotoxicity and increases seizure susceptibility67

3 Discussion..... 70

3.1 Postsynaptic EphA4 modulates LTP at the CA3-CA1 synapse73

3.2 EphA4 and ephrinBs promotes LTP through different mechanisms74

3.3 LTP induced by diverse stimulation patterns is differently affected by EphA4-ephrinA3 signaling75

3.4 Does EphA4-ephrinA3 interaction control metaplasticity?75

3.5 Does EphA4-ephrinA3 interaction regulate plasticity of glutamate uptake?....76

3.6 Possible molecular mechanisms mediating ephrinA3 control of glial glutamate transporter abundance76

3.7 Could there be a link between synaptic plasticity and dendritic spine morphology defects in *Epha4* and *Efna3* mutant mice?78

3.8 Does EphA4-ephrinA3 interaction control morphology and/or motility of astrocytic processes?78

3.9 Potential pathological consequence of EphA4-ephrinA3 signaling malfunction79

4 Materials and methods 81

4.1 Materials.....82

4.1.1 Chemicals and drugs82

4.1.2 Genotyping oligonucleotides82

4.1.3 Primary antibodies.....83

4.1.4 Buffers and solutions.....84

4.1.5 Mouse lines90

4.2 Methods92

4.2.1 Molecular biology	92
4.2.2 Biochemistry.....	95
4.2.3 Histology and image analysis	96
4.2.4 Assessment of seizure susceptibility	98
4.2.5 Electrophysiology	98
4.2.6 Statistical analysis.....	101
5 Bibliography	102
<i>Curriculum vitae</i>	121

List of figures and tables

Introduction

Figure 1.1 Anatomy of the mouse hippocampus 7

Figure 1.2 Morphology and main molecular components
of the CA3-CA1 synapse 9

Figure 1.3 Stimulation patterns used for LTP induction 15

Figure 1.4 Astrocyte-mediated modulation of synaptic function..... 20

Figure 1.5 Eph receptors and ephrin ligands..... 26

Figure 1.6 Eph receptor forward signaling 28

Figure 1.7 EphrinB reverse signaling 30

Figure 1.8 Mechanisms of ephrinA reverse signaling 32

Figure 1.9 Molecular pathways regulating spine morphogenesis
downstream of EphB receptors 34

Figure 1.10 Regulation of spine morphogenesis by EphA4-ephrinA3
interaction at the neuro-glia interface..... 35

Figure 1.11 Eph receptors and ephrins promote LTP and
LTD at the CA3-CA1 synapse 37

Results

Figure 2.1 Validation of the *Epha4^{lx}* allele 41-42

Figure 2.2 Normal LTP in *Epha4^{lx/-}* mice..... 43

Figure 2.3 Efficient sub-region-specific recombination of *Epha4*
floxed allele in the hippocampus 44

Figure 2.4 Normal axonal function and postsynaptic
responses in *Epha4* mutants 46

Figure 2.5 Normal PPF in *Epha4* mutants..... 47

Figure 2.6	Normal AMPAR- and NMDAR-mediated currents in <i>Epha4</i> ^{-/-} mice	48
Figure 2.7	EphA4 is required for TBS-induced LTP in postsynaptic CA1 cells	49
Figure 2.8	EphA4 is dispensable for tetanus-induced LTP	50
Figure 2.9	Impaired TBS-induced LTP in <i>Efna3</i> null mutants.....	52
Figure 2.10	Normal basal synaptic transmission in <i>Efna3</i> null mutants.....	53
Figure 2.11	Normal mEPSC amplitudes and frequency in <i>Efna3</i> ^{-/-} mice	53-54
Figure 2.12	Increased GLAST and GLT1 protein abundance in <i>Epha4</i> mutants.....	55
Figure 2.13	The EphA4 cytoplasmic domain is dispensable for regulating GLAST and GLT1 abundance.....	57
Figure 2.14	Increased astrocytic glutamate transporter currents in <i>Efna3</i> ^{-/-} mice.....	58-59
Figure 2.15	Reduced glutamate concentration near synapses in <i>Epha4</i> ^{-/-} mice	60
Figure 2.16	Decreased neuronal depolarization during high frequency stimulation in <i>Epha4</i> and <i>Efna3</i> mutants	61
Figure 2.17	Rescue of LTP defects in presence of the glutamate transporter inhibitor TFB-TBOA.....	63
Figure 2.18	Rescue of LTP defects in presence of the broad spectrum glutamate transporter inhibitor tPDC.....	64
Figure 2.19	Transgenic mice overexpressing ephrinA3 in astrocytes	65
Figure 2.20	EphrinA3 overexpression in astrocytes reduces abundance of glial glutamate transporters.....	66-67
Figure 2.24	EphrinA3 overexpression in astrocytes causes excitotoxicity and increases susceptibility to seizures.....	68
 Discussion		
Figure 3.1	Model describing the function of EphA4-ephrinA3 interaction at the neuro-glia interface.....	72

Materials and methods

Table 4.1 Summary of the primary antibodies used for the experiments described in this thesis83

Table 4.2 Summary of the primers and PCR programs used to amplify the indicated alleles.....93

Abbreviations

ACSF	artificial cerebrospinal fluid
ALS	amyotrophic lateral sclerosis
AMPA	α -amino-3-hydroxy-5-methyl-4-isoxazole propionic acid
AMPA	AMPA receptor
ANCOVA	analysis of covariance
ANOVA	analysis of variance
Arc	activity regulated cytoskeletal-associated protein
CA1	<i>cornu ammonis</i> (region) 1
CA3	<i>cornu ammonis</i> (region) 2
CaMKII	calcium-calmodulin-dependent protein kinase II
Cas	Crk-associated substrate
Cdk5	cyclin-dependent kinase 5
CNS	central nervous system
CREB	cyclic AMP responsive element-binding protein
DG	dentate gyrus
EAAC1	excitatory amino acid carrier-1
EAAT	excitatory amino acid transporter
Eph	erythropoietin-producing hepatocellular (carcinoma cell)
ephrin	Eph receptor interacting (protein)
<i>Efn</i>	ephrin (gene symbol)
EPSC	excitatory postsynaptic current
FAK	focal adhesion kinase
fEPSP	field excitatory postsynaptic potential
FV	fiber volley
GAP	GTPase-activating protein

GDNF	glial cell line-derived neurotrophic factor
GEF	guanine nucleotide exchange factor
GFAP	glial fibrillary acidic protein
GKAP	guanylate kinase-associated protein
GIT1	G protein-coupled receptor kinase interacting protein 1
GLAST	glial glutamate/aspartate transporter
GLT1	glutamate transporter subtype 1
GPI	glycosyl-phosphatidyl-inositol
GRIP	glutamate receptor-interacting proteins
HA	hemagglutinin
ISI	interstimulus interval
KS	Kolmogorov-Smirnov
LTD	long term depression
LTP	long term potentiation
MAPK	mitogen-activated protein kinases
mEPSC	miniature excitatory postsynaptic current
mGluR	metabotropic glutamate receptor
NMDA	N-methyl-D-aspartate
NMDAR	NMDA receptor
P	postnatal (day)
PAK	p21-activated kinases
PCR	polymerase chain reaction
PDZ	<u>P</u> SD-95/ <u>D</u> LG/ <u>Z</u> O-1
PI3K	phosphatidylinositol 3-kinase
PKA	protein kinase A
PKC	protein kinase C

PKM ζ	protein kinase M zeta
PLC	phospholipase C
PP1	protein phosphatase 1
PPF	paired pulse facilitation
PSD	postsynaptic density
PTZ	pentylentetrazole
PTX	picrotoxin
Pyk2	prolyne-rich tyrosine kinase 2
RTK	receptor tyrosine kinase
SAM	sterile alpha-motif
s.e.m.	standard error of the mean
SH2	Src-homology-2 (domain)
<i>Slc1a2</i>	GLT1 (gene symbol)
<i>Slc1a3</i>	GLAST (gene symbol)
SNARE	SNAP(S-nitroso-N-acetylpenicillamine) receptors
SOD1	Cu/Zn superoxide dismutase
TBS	theta burst stimulation
TFB-TBOA	(2S, 3S)-3-{3-[4-(trifluoromethyl)benzoylamino]benzyloxy}aspartate
TNF α	tumor necrosis factor α
tPDC	L-trans-pyrrolidine-2,4-dicarboxylic acid
TTX	tetrodotoxin
VAPB	VAMP-associated membrane protein B
wt	wild type
γ -DGG	γ -D-glutamylglycine

Abstract

Synaptic plasticity is the ability of neuronal connections to change in strength. Long lasting modifications of synaptic strength, such as long term potentiation (LTP), are considered as the cellular mechanism mediating learning and memory.

Synaptic transmission has been classically considered as a plot with two actors: the presynaptic neuron carrying the message and the postsynaptic neuron receiving and integrating it. Although a circuit composed of these two elements is the minimal requirement for synaptic communication, also glia cells, and in particular astrocytes, play important roles not only in sustaining neural function but also in actively shaping synaptic transmission and plasticity. For example, astrocytes detect glutamate released from the presynaptic terminal and respond to this stimulus with the release of molecules that modulate the activity of both pre- and postsynaptic compartments. Moreover, astrocytes regulate synaptic glutamate concentration through uptake of extracellular glutamate by specific glutamate transporters. The molecular mechanisms regulating neuro-glia communication are not fully understood.

Eph receptor tyrosine kinases and their ephrin ligands are critical modulators of synaptic plasticity. It has been shown that the EphA4 receptor promotes long term plasticity at the CA3-CA1 synapse in the hippocampus independently of its cytoplasmic domain. However, it was not known which specific synaptic compartment requires EphA4, or which molecular mechanisms mediate its action. By removing EphA4 from pre- or postsynaptic neurons, I now show that only postsynaptic EphA4 is required for LTP modulation.

EphrinA3 is a high affinity ligand for EphA4 expressed in astrocytes. Here I demonstrate that *EfnA3* null mutants also have impaired LTP, raising the possibility that EphA4 function involves astrocytes. Interestingly, both *Epha4* and *EfnA3* null mutant mice show increased expression of glial glutamate transporters and glutamate uptake is enhanced in astrocytes lacking ephrinA3. The LTP deficit observed in *Epha4* and *EfnA3* mutants is rescued by applying glutamate transporter inhibitors, providing a direct link between the altered glial glutamate transporter expression and LTP deficiency. In a gain-of-function experiment, transgenic mice overexpressing ephrinA3

specifically in astrocytes presented a reduction in glial glutamate transporter expression. Moreover, overexpression of ephrinA3 in astrocytes caused glutamate excitotoxicity and increases susceptibility to seizures *in vivo*.

Taken together, these results suggest that the interaction between dendritic EphA4 and astrocytic ephrinA3 modulates long term synaptic plasticity by negatively regulating the expression of glial glutamate transporters and consequently controlling glutamate concentration near synapses. On the other hand, increased activation of EphA4-ephrinA3 signaling leads to pathological conditions caused by enhanced glutamatergic transmission.

Zusammenfassung

Als synaptische Plastizität bezeichnet man die Fähigkeit neuronaler Verbindungen, ihre Übertragungsstärke zu verändern. Lang anhaltende Veränderungen der synaptischen Übertragungsstärke, wie z.B. Langzeit-Potenzierung (LTP), werden als die zellulären Mechanismen angesehen, die Lernen und Gedächtnis vermitteln.

Synaptische Plastizität wurde klassischerweise als ein Vorgang mit zwei Akteuren angesehen: Das präsynaptische Neuron, das die Information trägt und das postsynaptische Neuron, welches die Information empfängt und weiterverarbeitet. Obwohl ein Schaltkreis aus diesen beiden Elementen die kleinstmögliche Einheit für synaptische Kommunikation ist, spielen auch Gliazellen, vor allem Astrozyten, eine wichtige Rolle, nicht nur bei der Aufrechterhaltung neuronaler Funktion. Sie sind auch aktiv an der Gestaltung der von neuronaler Transmission und synaptischer Plastizität beteiligt. Astrozyten können zum Beispiel von der präsynaptischen Endigung freigesetztes Glutamat erkennen und auf diesen Stimulus mit der Freisetzung von Molekülen reagieren, welche die prä- und postsynaptische Aktivität regulieren. Ausserdem regulieren Astrozyten die synaptische Glutamatkonzentration über die Aufnahme extrazellulären Glutamats mithilfe spezifischer Glutamattransporter. Die molekularen Mechanismen, welche Neuron-Glia Interaktionen regulieren, sind noch nicht vollständig verstanden.

Eph Rezeptor Tyrosin Kinasen und ihre Ephrin Liganden sind entscheidende Regulatoren synaptischer Plastizität. Es konnte gezeigt werden, dass der EphA4 Rezeptor unabhängig von seiner cytoplasmischen Domäne an der Langzeitplastizität an der CA3-CA1 Synapse im Hippocampus beteiligt ist. Allerdings war weder bekannt, welches spezifische synaptische Kompartiment hierbei EphA4 benötigt, noch welche molekularen Mechanismen diese Funktion vermitteln. Durch Entfernen von EphA4 aus den prä- und postsynaptischen Zellen konnte ich jetzt zeigen, dass nur postsynaptisches EphA4 nötig ist, um LTP zu modulieren.

EphrinA3 ist ein hochaffiner Ligand für EphA4 und ist in Astrozyten exprimiert. Ich zeige hier, dass *Efna3* null Mutanten auch eine Beeinträchtigung im LTP haben, was

die Möglichkeit nahelegt, dass die Funktion von EphA4 auch Astrozyten umfasst. Interessanterweise zeigen sowohl *Epha4* als auch *Efna3* knock out Mäuse erhöhte Expression des glialen Glutamatransporters und Astrozyten, welchen ephrinA3 fehlt, zeigen eine gesteigerte Glutamataufnahme. Das in *Epha4* und *Efna3* Mutanten beobachtete LTP Defizit kann durch die Zugabe von Glutamatransporterinhibitoren verhindert werden, was eine direkte Verbindung zwischen veränderter Expression von Glutamatransportern in Gliazellen und Fehlen von LTP aufzeigt. In einem gain-of-function Experiment zeigten Mäuse, die ephrinA3 spezifisch in Astrozyten überexprimieren, reduzierte Expression des glialen Glutamatransporters. Des Weiteren führte die Überexpression von ephrinA3 in Astrozyten zu Excitotoxizität und einer erhöhten Neigung zu Krämpfen *in vivo*.

Zusammengenommen legen diese Ergebnisse nahe, dass die Interaktion zwischen dendritischem EphA4 und ephrinA3 in Astrozyten durch die negative Regulation des glialen Glutamatransporters und die daraus folgende Kontrolle der Glutamatkonzentration in der Nähe der Synapsen die synaptische Langzeitplastizität moduliert. Andererseits führt die erhöhte Aktivierung von EphA4-ephrinA3 Signaltransduktion zu pathologischen Veränderungen, verursacht durch verstärkte glutamaterge Neurotransmission.

1

Introduction

1.1 Anatomy of the hippocampus

The hippocampus is a structure in the brain of vertebrates involved in spatial navigation and certain types of learning and memory (Andersen, 2007; O'Keefe and Nadel, 1978). The hippocampal region that includes *cornu ammonis* (CA) fields, dentate gyrus and subiculum together with the adjacent entorhinal, perirhinal and parahippocampal cortices constitute the medial temporal lobe (Squire et al., 2004).

The mammalian hippocampus is a three-layered structure, also known as archicortex, with a central layer of densely packed neuronal somata that lies between two relatively cell-sparse layers (figure 1.1). The layers of the dentate gyrus are termed molecular layer (*stratum moleculare*), granule cell layer and polymorphic layer (also known as hilus). The cytoarchitectonics of CA3 and CA1 is more complex and five to six layers can be recognized. They are termed, from deep to superficial, *stratum lacunosum-moleculare*, *stratum radiatum*, *stratum lucidum* (present only in CA3), *stratum pyramidale*, *stratum oriens* and *stratum alveus*. The subiculum is an even more complex structure, with different areas with four or five cell body layers, because it is a transition region between the three-layered archicortex and the six-layered entorhinal cortex.

The major inputs to the hippocampus are carried by axons of the perforant path, which connect neurons in layer II of the entorhinal cortex to granule cells in the dentate gyrus. In addition, layer III cells of the entorhinal cortex are connected to the distal apical dendrites of CA1 pyramidal cells in the *stratum lacunosum-moleculare*. Granule cells project their axons (mossy fibers) to the apical dendrites of CA3 pyramidal cells which, in turn, are connected to the apical dendrites of CA1 pyramidal cells in the *stratum radiatum*, and to a minor extent with basal dendrites of *stratum oriens*, through Schaffer collaterals. In addition, CA3 neurons project to contralateral CA3 and CA1 pyramidal cells through commissural connections and there is also an associative network connecting CA3 cells ipsilaterally. Finally, CA1

pyramidal neurons project their axons back to the entorhinal cortex both directly and indirectly via the subiculum. The circuit connecting entorhinal cortex and hippocampus is therefore a closed loop of glutamatergic excitatory synapses. The hippocampus receives also modulatory inputs from other brain regions including the septum, amygdala, thalamus, hypothalamus and brainstem monoaminergic nuclei. The activity of hippocampal circuits is controlled by a complex network of γ -aminobutyric acid (GABA)-releasing interneurons (Klausberger and Somogyi, 2008).

Because of its well characterized and relatively simple circuitry, the hippocampus offers many advantages for electrophysiological analysis and has provided important details about the mechanisms underlying synaptic transmission and plasticity.

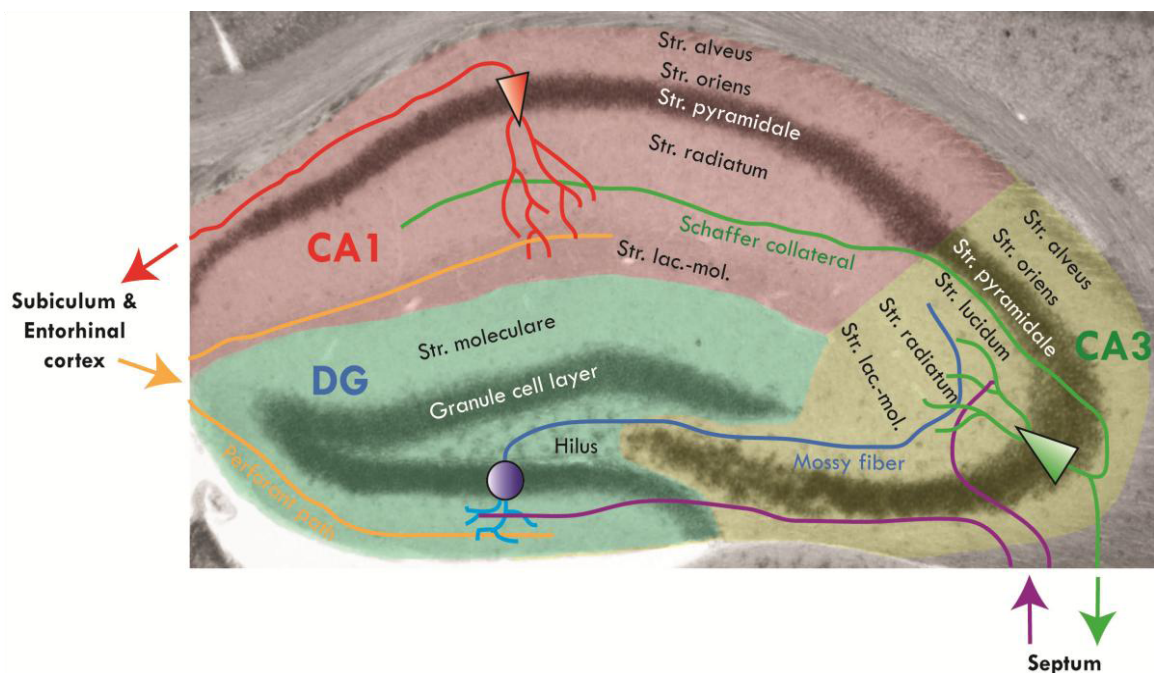


Figure 1.1 Anatomy of the mouse hippocampus. Transversal section of an adult mouse hippocampus showing the layer organization and schematic representation of the main internal and external axonal pathways. Abbreviations: CA1, *cornus ammonis* 1; CA3, *cornus ammonis* 3; DG, dentate gyrus; lac.-mol, *lacunosum-moleculare*; Str., *stratum*.

1.2 Structural and functional properties of hippocampal synapses

Synapses are specialized intercellular junctions between neurons or between neurons and other excitable cells where signals are transmitted from one cell to another (Cowan et al., 2001). Electrical synapses are gap junctions that allow the propagation of electrical signals through connected cells. At chemical synapses electrical signals carried by the axon induce release of molecules (neurotransmitters) from the presynaptic terminal into the synaptic cleft. This chemical signal is then reconverted postsynaptically into an electrical signal through binding of neurotransmitters to specific receptors. In vertebrates most of the synapses are chemical. Electrical synapses do not allow significant modulation of signal propagation. On the contrary, chemical synapses, hereafter referred to simply as synapses, are flexible in morphology and function and finely tune the information flow between neurons (Cowan et al., 2001). Synapses of different regions of the central nervous system (CNS) share some common basic features. However, neuronal connections in different neural circuits also have structural and physiological differences. For this reason the following description will focus on the characteristics of the excitatory Schaffer collateral synapse in the hippocampus (hereafter referred to as CA3-CA1 synapse).

1.2.1 Presynaptic compartment and mechanism of neurotransmitter release

Schaffer collateral fibers from CA3 pyramidal neurons make *en passant* (non-terminal) synapses on CA1 pyramidal neuron dendrites. For this reason these axons contact many neurons along their path in the *stratum radiatum* of CA1. Presynaptic boutons appear as axonal expansions containing mitochondria, endosomal membranes and synaptic vesicles filled with glutamate (figure 1.2). Synaptic vesicles are distributed in two distinct pools; those situated more distally from the synaptic junction are part of a reserve pool while others found in direct contact with the presynaptic cell membrane in an area known as active zone

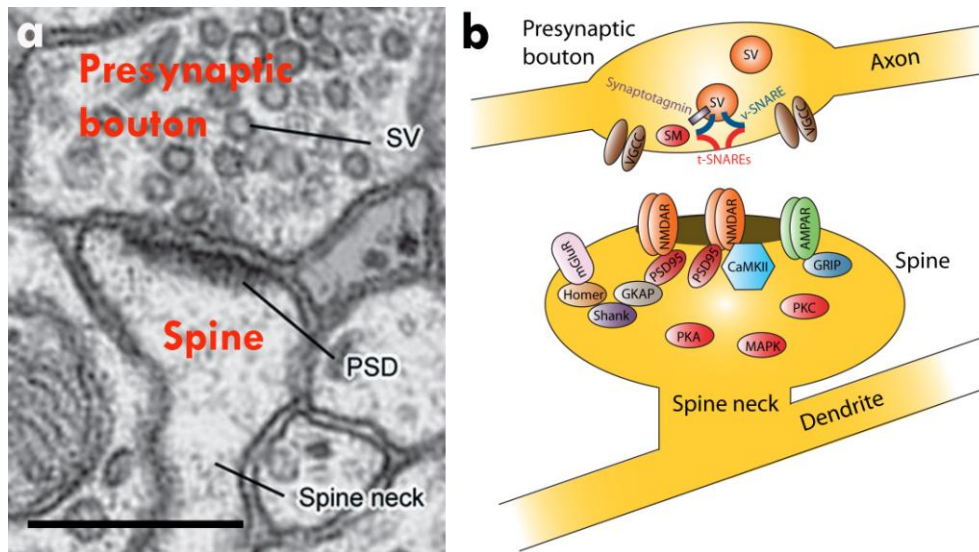


Figure 1.2 Morphology and main molecular components of the CA3-CA1 synapse. **a)** Electron microscopy image of a synapse between a CA3 neuron axon and a CA1 pyramidal cell dendrite. The presynaptic bouton filled with synaptic vesicles (SV) and the dendritic spine with the electron dense postsynaptic density (PSD) are visible. Scale bar 0.5 μm . **b)** Schematic representation of a CA3-CA1 synapse with some of the proteins required for neuronal transmission and plasticity. VGCC, voltage-gated calcium channel; SM, Sec1/Munc18-like proteins. Figure 1.2a is modified from (Sheng and Hoogenraad, 2007).

belong to the readily releasable pool (Murthy and De Camilli, 2003). The release of synaptic vesicles is a highly regulated process involving a complex molecular machinery triggered by calcium influx through voltage-gated calcium channels during axonal depolarization (Murthy and De Camilli, 2003; Sudhof, 2004). The synaptic vesicle release process can be divided in different steps. First, synaptic vesicles have to be attached to the active zone through the formation of a docking complex between the synaptic vesicle and plasma membrane proteins called vesicle (v) and target (t) SNAREs (SNAP(S-nitroso-N-acetylpenicillamine) receptors). Synaptic exocytosis is mediated by one v-SNARE (synaptobrevin/VAMP (vesicle-associated membrane protein)) and two t-SNAREs on the presynaptic plasma membrane (syntaxin 1 and SNAP-25). It has been proposed that the SNARE complex creates an unstable membrane fusion intermediate without opening the

fusion pore. The SNARE complex formation is regulated by other players including complexins and Sec1/Munc18-like (SM) proteins. The next step is the exocytosis of synaptic vesicles triggered by the detection of calcium influx into the presynaptic bouton by the vesicle-associated proteins synaptotagmins through a mechanism not fully understood. After exocytosis, synaptic vesicles undergo endocytosis, recycle and refill with glutamate for a new round of exocytosis.

1.2.2 Postsynaptic compartment

Opposite to the axonal bouton is the postsynaptic reception apparatus that in the hippocampal glutamatergic synapse is located in small thorny-like protrusions of dendrites enriched in actin called spines (figure 1.2) (Bourne and Harris, 2008; Nimchinsky et al., 2002). Dendritic spines provide biochemical compartmentalization that allows local control of individual synapses. The distal tip of the spine contains a dense network of proteins termed postsynaptic density (PSD) juxtaposed to the presynaptic active zone (Sheng and Hoogenraad, 2007). The main function of the PSD is to anchor glutamate receptors at the postsynaptic plasma membrane and to ensure that the proper signaling cascade is started following receptor activation.

1.2.2.1 Glutamate receptors

Glutamate receptors can be ion channels (ionotropic receptors) or transmembrane proteins without intrinsic ion permeability coupled to intracellular signal transduction complexes (metabotropic receptors) (Cowan et al., 2001). Fast synaptic transmission at the CA3-CA1 synapse is mainly mediated by the ionotropic α -amino-3-hydroxy-5-methyl-4-isoxazole propionic acid (AMPA) and N-methyl-D-aspartate (NMDA) receptors. Metabotropic glutamate receptors (mGluRs) function as modulators that fine tune synaptic transmission.

AMPA receptors (AMPA receptors) are composed of four subunits (GluR1-4, also known as GluRA-D) (Shepherd and Huganir, 2007). Most AMPA receptors in hippocampal pyramidal neurons are GluR1-2 and GluR2-3 tetramers (Wenthold et al., 1996). At resting potential sodium influx accounts for most of the AMPAR current and is the main driving force for postsynaptic depolarization at the CA3-CA1 synapse. However, also NMDA receptors (NMDARs) contribute significantly to synaptic transmission but in a more complex way.

NMDARs exist as heteromultimers of two glycine-binding NR1 subunits and two glutamate-binding NR2A-D subunits. NR2C and D and two other subunits, NR3A and B, do not appear to play a relevant role in hippocampal pyramidal cells (Andersen, 2007). The subunit composition and compartmental localization of NMDARs are developmentally regulated and affect channel activity and downstream signaling (Cull-Candy and Leszkiewicz, 2004; Kohr, 2006). NR1 is the essential subunit of all NMDARs and can be assembled together with different NR2 or NR3 subunits that determine the electrophysiological characteristics of the channel, affecting its conductance, opening time and magnesium sensitivity. In hippocampal pyramidal neurons NR2B is abundant at early developmental stages and NR2A progressively appears during postnatal development and plays a major role in adult hippocampal synapses. NR2A and NR2B appear to be preferentially localized in different subcellular compartments, with NR2A enriched in the PSD and NR2B mostly present in perisynaptic/extrasynaptic membranes (Janssen et al., 2005). The NMDAR channel is doubly gated, opening only when two conditions are simultaneously satisfied: glutamate must be bound to the receptor and the postsynaptic membrane must be depolarized. The second condition is required for releasing the magnesium atom that blocks the channel at resting potential. This means that NMDARs are activated only when there is a conjunction of presynaptic glutamate release and postsynaptic depolarization. In this way NMDARs act as coincidence detectors of pre- and postsynaptic activity (Cull-Candy and Leszkiewicz, 2004; Kohr, 2006).

mGluRs contain seven transmembrane segments and are assembled as dimers. They are coupled to G proteins, which mediate most of their action (Anwyl, 1999). mGluRs are divided in three classes based on differences in downstream signaling and pharmacological properties. Group I receptors tend to be localized in postsynaptic membranes in the perisynaptic compartment (Baude et al., 1993; Lujan et al., 1996). They activate phospholipase C (PLC) via G proteins, leading to an increase in inositol triphosphate and diacylglycerol (Fagni et al., 2000). Group II and group III receptors are localized in presynaptic membranes and are negatively coupled to adenylate cyclase through G proteins (Anwyl, 1999).

1.2.2.2 Scaffold and signaling proteins

Glutamate receptors contain interaction domains in their cytoplasmic regions that allow them to contact intracellular scaffold and signaling proteins. Most of the scaffold proteins in the PSD contain PSD-95/DLG/ZO-1 (PDZ) domains, modular protein-interaction domains specialized for binding to short peptide motif at the carboxy termini of other proteins (Kim and Sheng, 2004). AMPARs, NMDARs and mGluRs contain such PDZ interacting motifs in their cytoplasmic domains that mediate binding to scaffold proteins such as PSD-95, glutamate receptor-interacting proteins (GRIPs), guanylate kinase-associated protein (GKAP), Shank and Homer (figure 1.2) (Kim and Sheng, 2004; Sheng and Kim, 2002). These scaffold molecules, in turn, interact with cytoplasmic signaling proteins allowing the coupling of glutamate receptor activation to downstream signaling pathways. Different classes of proteins are engaged in signal transduction processes in the PSD, including kinases such as calcium-calmodulin-dependent protein kinase II (CaMKII), protein kinase A and C (PKA and PKC); phosphatases, such as calcineurin; and a plethora of other proteins that modulate the activity of kinases and phosphatases (Kennedy et al., 2005). Scaffold molecules not only interact with glutamate receptors but also, directly or indirectly, with other transmembrane proteins including receptor tyrosine kinases and adhesion molecules that coordinate

trans-synaptic communication and modulate postsynaptic function (Dalva et al., 2007; Kim and Sheng, 2004). This complex network of proteins is responsible not only for mediating basal synaptic transmission, but also for triggering, maintaining and integrating experience-dependent changes in synaptic strength.

1.3 Synaptic Plasticity

Living organisms are embedded in an unpredictable environment and they must modify their behaviors accordingly to changes of their surroundings. For this reason evolution has favored strategies directed toward the development of flexible neural networks. Synaptic transmission can be modified by different patterns of neuronal activity, correlated with different environmental stimuli, through complex mechanisms collectively grouped under the name of synaptic plasticity (Kandel, 2001; Kim and Linden, 2007; Nelson and Turrigiano, 2008). Synaptic changes can last from some milliseconds to few minutes (short term plasticity) or can be maintained for days and possibly for the entire life of an organism (long term plasticity). Long lasting changes in synaptic strength associated with specific patterns of stimulation, such as long term potentiation (LTP) and long term depression (LTD), are considered as the cellular mechanisms responsible for the formation and storage of memories (Martin et al., 2000; Pastalkova et al., 2006; Whitlock et al., 2006). These changes can also be associated with structural rearrangements such as gain or loss of synaptic connections and dendritic spine remodeling (Alvarez and Sabatini, 2007; Yuste and Bonhoeffer, 2001). The direction and amount of changes in synaptic strength are controlled by another process called metaplasticity (Abraham, 2008). Finally, the overall level of synaptic excitability is kept in a constant range by homeostatic synaptic scaling processes (Turrigiano, 2008).

1.3.1 Short term plasticity

Short term forms of synaptic plasticity last at most few minutes and can be divided, on the basis of their duration, in facilitation or depression (few hundreds of milliseconds), augmentation (several tens of seconds) and post-tetanic potentiation (few tens of seconds to several minutes) (Zucker and Regehr, 2002). Facilitatory processes are usually attributed to a residual elevation of presynaptic concentration of calcium during brief trains of stimuli. However, other molecular events, including phosphorylation, could play a role especially in post-tetanic potentiation (Brager et al., 2003). Repeated stimulation of axons can induce synaptic enhancement or depression at different synapses depending on the intrinsic characteristics of the synapse. For example the amount of facilitation, also referred to as paired pulse facilitation (PPF), is inversely related to the initial release probability of the synapse (Dobrunz and Stevens, 1997). At synapses with high release probability depression prevails due to depletion of the pool of readily releasable vesicles. Depression can also be a consequence of feedback activation of presynaptic receptors and/or postsynaptic events such as glutamate receptor desensitization (Zucker and Regehr, 2002).

1.3.2 Long term plasticity

LTP and LTD can be triggered and expressed by a variety of different mechanisms at different synapses. In some synapses, such as the hippocampal mossy fiber-CA3 synapse, long term plasticity is expressed presynaptically, as a change of the probability of neurotransmitter release (Malenka and Bear, 2004; Nicoll and Schmitz, 2005). In other synapses, like the CA3-CA1 synapse, LTP and LTD are expressed as changes in number and unitary conductance of AMPARs and/or NMDARs (Malenka and Bear, 2004; Nicoll, 2003). Here I will focus on the mechanism of induction and expression of LTP and LTD at the CA3-CA1 synapse.

1.3.2.1 Long term potentiation

Long lasting enhancement of synaptic strength can be induced at the CA3-CA1 synapse by applying a train of stimuli at high frequency to Schaffer collaterals. Different stimulation patterns can be used (Albenis et al., 2007). A commonly used LTP induction protocol consists of a single 100 Hz train of one second duration (tetanus, figure 1.3). However, this kind of stimulation is probably different from naturally occurring firing patterns of hippocampal neurons (Albenis et al., 2007). For this reason other stimulation protocols, such as theta burst stimulation (TBS, figure 1.3), that resemble more closely the neuronal firing in the hippocampus during episodes of learning and memory were developed (Morgan and Teyler, 2001). Such stimulation patterns lead to calcium influx through NMDARs

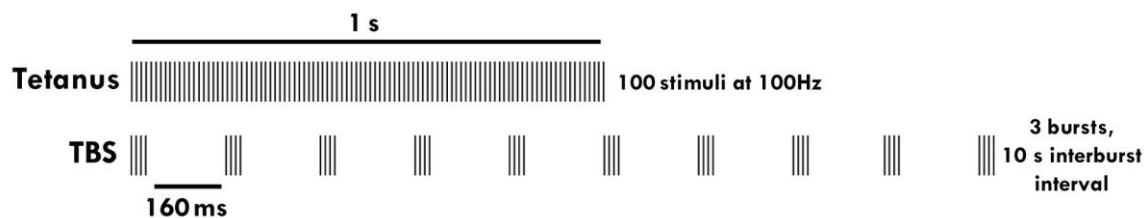


Figure 1.3 Stimulation patterns used for LTP induction. Schematic representation of a tetanus and theta burst stimulation (TBS) used in experiments described in this thesis. Three trains of TBS with intervals of 10 s were used. Each vertical line represents one electrical stimulus.

and to a rise in calcium concentration in dendritic spines. This step is an absolute requirement for LTP induction at the CA3-CA1 synapse and pharmacological inhibition or genetic ablation of NMDARs prevents LTP (Malenka and Bear, 2004; Nicoll, 2003). On the other hand, overexpression of NMDARs enhances LTP (Tang et al., 1999). Calcium influx into the spine triggers a cascade of molecular events that result in potentiation of synaptic transmission. A plethora of proteins have been shown to be involved in LTP induction and/or expression. Some of them are absolutely required for LTP induction (mediators) while others can alter LTP but are not essential for its occurrence (modulators) (Malenka and Bear, 2004; Sanes and

Lichtman, 1999). An important mediator is CaMKII and genetic deletion of a crucial CaMKII subunit blocks the induction of LTP (Lisman et al., 2002; Silva et al., 1992). Several other kinases play key roles in LTP induction. PKA is required for LTP induction during early postnatal life but its action is less relevant in the adult (Malenka and Bear, 2004; Yasuda et al., 2003). Different isoforms of PKC, in particular the atypical isozyme protein kinase M zeta (PKM ζ), are also important for LTP (Malenka and Bear, 2004; Pastalkova et al., 2006). Other important players are Src family kinases (Lu et al., 1998) and mitogen-activated protein kinases (MAPKs) (Thomas and Huganir, 2004). These enzymes phosphorylate different substrates in the postsynaptic compartment, including glutamate receptors. Phosphorylation of specific amino acids regulates the unitary conductance and surface expression of glutamate receptors (Salter and Kalia, 2004; Sheng and Kim, 2002; Shepherd and Huganir, 2007). A major mechanism for expression of LTP at the CA3-CA1 synapse involves the increase of surface expression of AMPARs (Shepherd and Huganir, 2007).

Different phases of LTP can be distinguished based on their duration and molecular mechanisms required for their maintenance (Kelleher et al., 2004). While protein phosphorylation events can sustain LTP for circa one hour (early LTP), new mRNAs and proteins must be synthesized to sustain enhanced synaptic transmission for longer periods (late LTP). Late LTP initially needs translation of mRNAs, often stored locally in dendrites (Kelleher et al., 2004; Sutton and Schuman, 2006). After few more hours new mRNAs must be transcribed (Kelleher et al., 2004). This last phase involves signaling from the potentiated synapses to the cell nucleus through the action of kinases, such as PKA, CaMKIV and MAPKs, that converges on the key transcription factor cyclic AMP responsive element-binding protein (CREB) (Adams and Dudek, 2005; Flavell and Greenberg, 2008). CREB, in turn, initiates the transcription of mRNAs, such as the one coding for the activity regulated cytoskeletal-associated protein (Arc), and consequently the production of new proteins that must be transported back specifically to potentiated synapses through

a mechanism that probably requires the presence of a “synaptic tag” applied to synapses after LTP induction (Martin and Kosik, 2002).

1.3.2.2 Long term depression

Prolonged low frequency (0.5-5 Hz) stimulation of Schaffer collaterals induces long lasting depression of synaptic transmission in CA1 pyramidal cells (Dudek and Bear, 1992). Two distinct forms of LTD coexist at the CA3-CA1 synapse, one triggered by activation of NMDARs (NMDAR-LTD) and another one requiring signaling downstream of group I mGluRs (mGluR-LTD) (Malenka and Bear, 2004; Oliet et al., 1997).

NMDAR-LTD is induced by influx of calcium through NMDARs during low frequency stimulation. The quantitative and temporal characteristics of the calcium influx determine direction of synaptic changes, with fast calcium entry leading to LTP and slower and more prolonged influx triggering LTD (Bi and Poo, 2001; Sheng and Kim, 2002). LTD is correlated with dephosphorylation of postsynaptic PKA and PKC, but not CaMKII, substrates (Malenka and Bear, 2004). Important phosphatases involved in this process are calcineurin and protein phosphatase 1 (PP1) (Sheng and Kim, 2002). Dephosphorylation events are accompanied by decreased AMPAR open channel probability and reduced AMPAR surface expression (Shepherd and Huganir, 2007).

mGluR-LTD can be induced in presence of NMDAR inhibitors (Oliet et al., 1997). Like NMDAR-LTD, it also requires rise in postsynaptic calcium but T-type calcium channels are involved instead of NMDARs (Oliet et al., 1997). PKC activation is involved in mGluR-LTD while phosphatase activity is dispensable (Oliet et al., 1997). Similarly to NMDAR-LTD, mGluR-LTP induction triggers internalization of postsynaptic AMPARs (Malenka and Bear, 2004; Snyder et al., 2001).

1.3.3 Structural plasticity

Patterns of neuronal activity that induce long term synaptic plasticity can also trigger changes in dendritic spine morphology (Alvarez and Sabatini, 2007; Yuste and Bonhoeffer, 2001). Induction of LTP is associated with the growth of new spines (Engert and Bonhoeffer, 1999) and persistent volume increase of the existing ones (Matsuzaki et al., 2004). On the other hand, stimulation protocols that trigger LTD induce spine retraction (Nagerl et al., 2004). Structural changes of neuronal connections have been observed also *in vivo*. Sensory deprivation increases spine motility in the primary visual and somatosensory cortices in rodents (Hofer et al., 2009; Majewska et al., 2006; Zuo et al., 2005), and environmental enrichment increases dendritic branching, spine density and number of synapses in rodents (Alvarez and Sabatini, 2007) and primates (Kozorovitskiy et al., 2005). Remodeling of the actin cytoskeleton is responsible for structural changes associated with synaptic plasticity (Bourne and Harris, 2008).

1.3.4 Metaplasticity

The capability of neurons to generate changes of synaptic strength and the quantitative control of these changes is affected by prior patterns of synaptic activity through modulatory mechanisms collectively termed metaplasticity (Abraham, 2008; Abraham and Bear, 1996). The difference between metaplasticity and other forms of synaptic modulation is that while the latter overlap in time with the regulated event, the former can persist for prolonged periods after priming signal. Events capable of inducing metaplastic changes include specific patterns of electrical stimulation, pharmacological activation of neurotransmitter receptors, release of hormones and sensory deprivation (Abraham, 2008). The major consequence of the priming activity is modification of the thresholds for induction of LTP and LTD, without itself causing persistent synaptic plasticity. For example, in the visual cortex of light-deprived rats the threshold for

induction of LTP is reduced while the one for LTD is increased as a consequence of reduced synaptic activity (Kirkwood et al., 1996). One of the mechanisms mediating metaplastic effects involves modification of the intrinsic excitability of neurons, for example through modifications of voltage-gated potassium channels (Chen et al., 2006; Kim and Linden, 2007). Metaplasticity can be considered as a homeostatic mechanism that preserves stability in the network and prevents runaway potentiation or depression (Abraham, 2008).

1.3.5 Homeostatic synaptic scaling

The global activity of neural networks has to be tightly controlled and kept within a particular range otherwise processes like LTP and LTD could drive synapses to their limits of potentiation and depression, respectively. Metaplasticity represents a mechanism to achieve this objective. Another way is through homeostatic synaptic scaling, a processes employed by neurons to adjust their own firing rate depending on the overall activity of the network (Turrigiano, 2008; Turrigiano and Nelson, 2004). Neurons tend to increase their firing rate in response to prolonged inhibition of synaptic transmission, for example in presence of tetrodotoxin, while they compensate in the opposite direction when network activity is increased, for example in presence of the GABA_A receptor inhibitor picrotoxin. Homeostatic synaptic scaling takes place not only *in vitro* but also *in vivo* (Goel and Lee, 2007; Maffei et al., 2004) and without this form of plasticity neural networks can become unstable and perform suboptimally (Abbott and Nelson, 2000; Turrigiano and Nelson, 2004).

1.4 Contributions of glia to synaptic transmission and plasticity

The volume of mammalian brains is mostly occupied by nonneuronal cells called glia. During evolution the density and morphology of these cells have remarkably increased (Kettenmann and Verkhratsky, 2008; Sherwood et al., 2006). Glial cells in the mature CNS are commonly divided in three major families: oligodendrocytes, astrocytes and microglia (Barres, 2008). A new class of glia, the

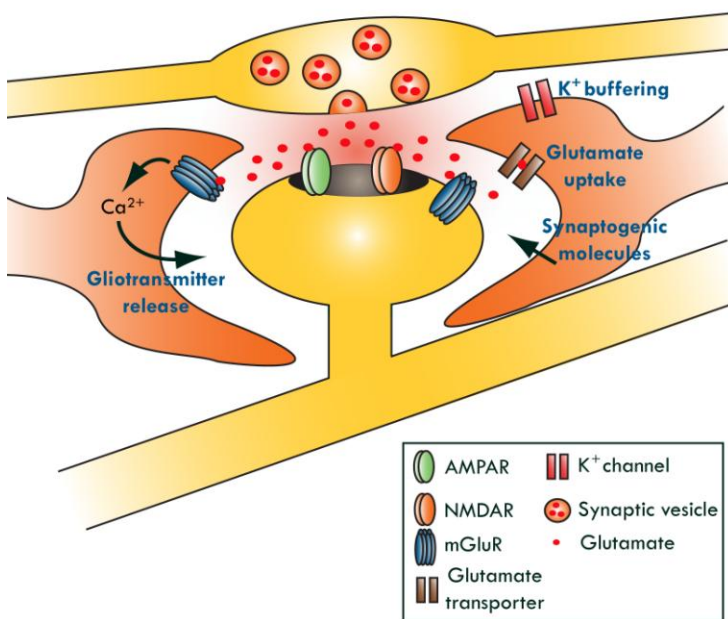


Figure 1.4 Astrocyte-mediated modulation of synaptic function. Scheme summarizing some of the mechanisms used by astrocytes to regulate synaptic transmission and plasticity. Binding of glutamate to receptors present on astrocytic processes (orange) induces increase of intracellular calcium that, in turn, triggers release of gliotransmitters. Astrocytes control extracellular concentration of glutamate and potassium through specific transporters and channels. Molecules released by astrocytes promote synaptogenesis.

NG2-glia or polydendrocytes, which has some neuronal features and receives synaptic inputs, has been recently described (Nishiyama et al., 2009). The main function of oligodendrocytes is to wrap axons with myelin allowing fast impulse conduction and to support axon functional integrity (Nave and Trapp, 2008). Microglia are the resident immune cells of the brain and share many properties with macrophages (Soulet and Rivest, 2008). Astrocytes play many roles in brain physiology and they will be the focus of this introduction.

For a long time glial

cells have been regarded as passive bystanders with the only function of providing trophic support to neurons (Kettenmann and Verkhratsky, 2008). For example, astrocytes are responsible for homeostatic and trophic regulation of the CNS by affecting extracellular concentration of ions, water movements, blood brain barrier function and supply of energetic substrates for neurons (Hertz and Zielke, 2004). However, glial cells, and in particular astrocytes, can also actively modulate synaptic function by controlling the genesis and maintenance of synapses and by participating in different forms of synaptic plasticity (Barres, 2008; Halassa et al., 2007; Perea et al., 2009). Astrocytic processes are in close contact with synapses and can sense synaptic activity by detecting neurotransmitter release or by direct contact with pre- or postsynaptic membranes (Perea et al., 2009; Ventura and Harris, 1999). In this way astrocytes can monitor the activity of neuronal circuits and provide feedback signals to fine tune the properties of the network (figure 1.4). On the other hand, changes in neuronal activity and synaptic strength can also affect glia physiology (Genoud et al., 2006; Pita-Almenar et al., 2006). The astrocytic processes together with the pre- and postsynaptic compartments constitute therefore a functional unit characterized by bidirectional communications between the single elements. Alterations of the physiological properties of glial cells have been involved in numerous pathologies that affect the CNS, including epilepsy and amyotrophic lateral sclerosis (ALS), a disease characterized by progressive loss of motor neurons (Seifert et al., 2006).

1.4.1 The role of glia in synaptogenesis

Factors released by glial cells are critical regulators of synaptogenesis. It was originally observed that the addition of glia to purified ganglion cells in cultures promotes the formation of synapses and strongly enhances pre- and postsynaptic function (Pfrieger and Barres, 1997; Ullian et al., 2001). Astrocytes release large matrix-associated proteins called thrombospondins that are sufficient to induce the formation of synapses with normal pre- and postsynaptic

ultrastructures. These synapses, however, lack AMPAR mediated currents. Astrocytes secrete an additional and still unknown factor that promotes full synaptic maturation (Christopherson et al., 2005). The secretion of thrombospondins by astrocytes may be controlled by neuronal activity (Barres, 2008). Thrombospondin expression in the CNS has greatly increased during evolution from primates to humans suggesting a contribution of glia to the enhanced complexity of the human brain (Caceres et al., 2007).

1.4.2 Gliotransmission and its effect on synaptic function

Astrocytes can sense synaptic activity through glutamate receptors present on their plasma membrane and respond by releasing neuroactive molecules (gliotransmitters), such as glutamate, D-serine, GABA and ATP, which bind to receptors localized in neuronal pre- and postsynaptic compartments (Perea et al., 2009; Volterra and Meldolesi, 2005). Gliotransmission can be triggered by calcium transients in astrocytes induced by synaptic activity (Perea et al., 2009; Volterra and Meldolesi, 2005). The mechanisms responsible for the release of gliotransmitters are still under debate. Vesicle exocytosis, release from secretory lysosomes and transport across the plasma membrane through channels and transporters have been proposed (Perea et al., 2009; Volterra and Meldolesi, 2005).

Glutamate was one of the first molecules recognized as a gliotransmitter. Binding of glutamate released by astrocytes to presynaptic NMDARs or group I mGluRs increases the frequency of excitatory postsynaptic currents (Fiacco and McCarthy, 2004; Jourdain et al., 2007). Astrocytic glutamate can also induce network synchronization by binding to NMDARs in postsynaptic neurons (Fellin et al., 2004). Temporally coincident release of glutamate from astrocytes and postsynaptic depolarization can induce long lasting changes in synaptic strength at the CA3-CA1 synapse (Perea and Araque, 2007).

D-serine is a coagonist for NMDARs produced and released by astrocytes (Mothet et al., 2000; Mothet et al., 2005). In the supraoptic nucleus of the hypothalamus astrocytes undergo drastic morphological changes in different physiological conditions (Oliet and Piet, 2004). In basal conditions astrocytic processes tightly enwrap the synapses between the neurons that control release of hormones oxytocin and vasopressin into the bloodstream. During physiological events that require high concentrations of these hormones the processes of astrocytes retract and the concentration of astrocyte-released D-serine decreases. As a consequence activation of NMDARs is reduced and the threshold for induction of LTP is increased (Panatier et al., 2006). This metaplastic mechanism allows the selective potentiation of synaptic connections that are highly active during the physiologically relevant event.

Glia can modulate neuronal activity also by releasing larger molecules. For example, glial cells control homeostatic synaptic scaling by secreting the cytokine tumor necrosis factor α (TNF α) (Beattie et al., 2002; Stellwagen and Malenka, 2006).

1.4.3 Glial glutamate transporters

Glutamate transporters are membrane proteins that use the electrochemical gradient to transport glutamate from the extracellular space into the cell (Beart and O'Shea, 2007; Tzingounis and Wadiche, 2007). They are also known as excitatory amino acid transporters (EAATs). Different subtypes of glutamate transporters coded by different loci have specific and diverse expression patterns. EAAT1, also known as glutamate/aspartate transporter (GLAST), and EAAT2, also known as glutamate transporter 1 (GLT1), are predominantly expressed in glia. EAAT3, alternatively called excitatory amino acid carrier 1 (EAAC1), is expressed by neurons throughout the brain. EAAT4 and EAAT5 display more restricted expression, being localized only in cerebellar Purkinje cells and in retinal rod

photoreceptors and bipolar cells respectively. Glial specific transporters are responsible for most of the glutamate uptake at the CA3-CA1 synapse (Bergles and Jahr, 1998). The structural properties of glutamate transporters are not fully understood. Some evidences suggest that functional transporters are homotrimeric complexes (Tzingounis and Wadiche, 2007). Glutamate transport is coupled to the cotransport of three Na⁺ ions and one H⁺ ion, and the countertransport of one K⁺ ion (Tzingounis and Wadiche, 2007).

Glutamate uptake by astrocytes is a relatively slow process and it cannot account by itself for regulation of fast synaptic transmission (Tzingounis and Wadiche, 2007; Wadiche et al., 1995). However, glutamate transporters can modulate fast synaptic currents by buffering extracellular glutamate on a submillisecond time scale through rapid binding of the neurotransmitter (Diamond and Jahr, 1997; Tzingounis and Wadiche, 2007). Acute inhibition of glutamate transporters in hippocampal slices causes only very subtle changes of the kinetics and amplitude of synaptic currents induced with low frequency stimulation (Diamond and Jahr, 1997; Sarantis et al., 1993; Tzingounis and Wadiche, 2007). However, glutamate transporters control activation of peri- and extrasynaptic glutamate receptors and postsynaptic responses during trains of high frequency stimulation (Arnth-Jensen et al., 2002; Mulholland et al., 2008; Wadiche and Jahr, 2005) with consequences also on synaptic plasticity. For example, neuronal EAAT4 in Purkinje cells modulates LTD by controlling activation of perisynaptic mGluRs (Brasnjo and Otis, 2001; Wadiche and Jahr, 2005). In the hippocampus astrocyte glutamate transporters regulate mGluR-mediated excitation of interneurons (Huang et al., 2004). In the supraoptic nucleus of the hypothalamus changes of synaptic wrapping by astrocytes modify the amount of glutamate uptake and consequently alter synaptic transmission (Oliet et al., 2001). The impact of astrocytic glutamate uptake on synaptic plasticity at the CA3-CA1 synapse is not known.

The presence of glial glutamate transporters is essential for the proper functionality of glutamatergic synapses and dysfunction of glutamate transport results in excitotoxicity and may be involved in pathological conditions, such as

epilepsy and ALS (Beart and O'Shea, 2007; Seifert et al., 2006). For example, genetic elimination of GLT1 and GLAST in mice causes neuronal cell death and increases susceptibility to seizures (Tanaka et al., 1997; Watase et al., 1998).

1.4.4 Impact of synaptic changes on glia physiology

So far only the influence of astrocytes on neuronal functions has been discussed. However, the communication between neurons and glia is bidirectional and changes in neuronal activity can also modify glial physiology. For example, stimulation patterns capable of triggering LTP at the CA3-CA1 synapse simultaneously induce upregulation of glutamate transport in astrocytes by increasing the expression of GLT1 in a PKA dependent manner (Ge and Duan, 2007; Pita-Almenar et al., 2006). Sensory experience *in vivo* can also impact on astrocytes (Genoud et al., 2006). Whisker stimulation in mice induces an increase of GLAST and GLT1 expression in the corresponding cortical columns of the barrel cortex. The same sensory stimulation also causes an increase in astrocytic envelopment of excitatory synapses on dendritic spines.

1.5 Eph receptors and ephrin ligands

Eph receptors (from erythropoietin-producing hepatocellular carcinoma cell, the cell line from which their cDNAs were first isolated) constitute the largest family of receptor tyrosine kinases (RTKs) (Egea and Klein, 2007; Kullander and Klein, 2002; Pasquale, 2008). They are divided into two subclasses on the basis of sequence similarity and binding affinity for their ephrin (Eph receptor interacting protein) ligands (Gale et al., 1996; Kullander and Klein, 2002). A-type receptors (nine members in mammals, EphA1-EphA8 and EphA10) typically bind to ephrinA ligands, while B-type receptors (five members in mammals, EphB1-B4 and EphB6) bind to ephrinBs. Exceptions to this rule are EphA4 receptor, which binds both

groups of ephrins (Kullander and Klein, 2002; Qin et al., 2010), and EphB2 that can bind ephrinA5, in addition to ephrinB ligands (Himanen et al., 2004). Eph receptors and ephrins have been identified in a wide variety of animal phyla including Porifera, Arthropoda (including *Drosophila melanogaster*), Nematoda (*Cenorhabditis elegans*) and Chordata (including *Xenopus laevis*, *Danio rerio*, *Mus musculus* and *Homo sapiens*) (Drescher, 2002). Invertebrates have a lower number

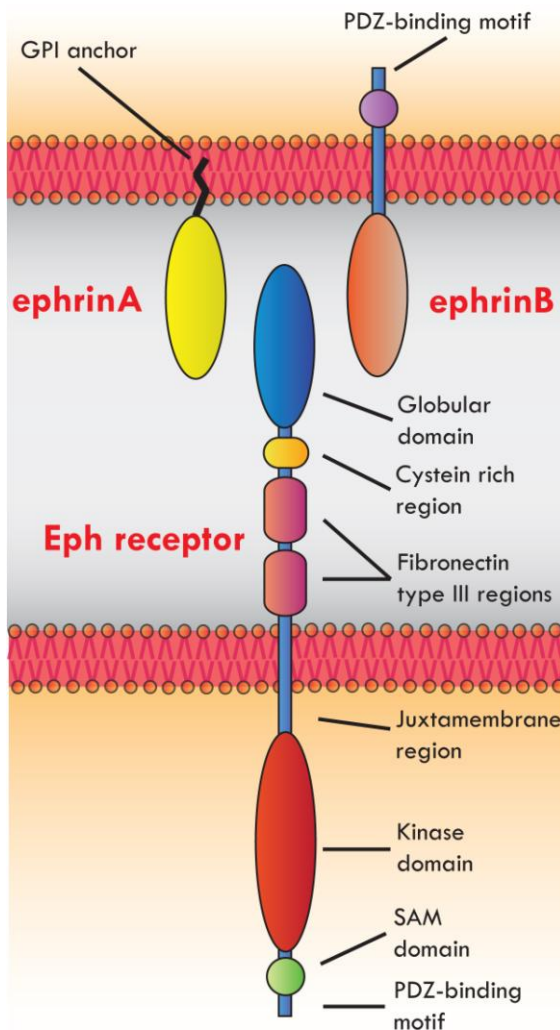


Figure 1.5 Eph receptors and ephrin ligands. Schematic representation of the structural organization of Eph receptors and ephrin ligands.

of Eph receptors and ephrins compared to vertebrates. For example in *D. melanogaster* there is one Eph receptor (D-Eph) and one ephrin (D-ephrin), and *C. elegans* has one Eph (VAB-1) and four ephrins (EFN1-4) (Drescher, 2002). The genomic amplification of loci coding for Ephs and ephrins during evolution has probably mirrored the increased numbers and complexity of physiological roles of these proteins.

The Eph receptor extracellular region contains a ligand binding globular domain, a cysteine-rich region and two fibronectin type III repeats (figure 1.5). The intracellular region is composed of a juxtamembrane region containing two conserved tyrosines, a protein tyrosine kinase domain, a sterile alpha-motif (SAM) and a PDZ-domain binding motif.

EphrinB ligands are transmembrane proteins with an

extracellular receptor binding domain and an intracellular region containing a PDZ-binding motif. EphrinAs, on the other hand, have only an extracellular globular domain tethered to the cell membrane by a glycosylphosphatidylinositol (GPI) anchor (figure 1.5). Ephrin ligands lack intrinsic enzymatic activity.

Three peculiar characteristics make Eph and ephrins unique among other RTKs. First, unlike many other RTKs, they are activated by membrane bound ligands but not by soluble monomeric ligands (Davis et al., 1994). Second, while other RTKs are fully activated after dimerization, Eph receptors usually need to form high-order clusters to induce robust downstream signal transduction (Stein et al., 1998). Third, since ephrins are membrane bound molecules, upon binding receptor and ligand can transduce signals bidirectionally into both the receptor-expressing cell (known as forward signaling) and the ligand-expressing cell (known as reverse signaling) (Egea and Klein, 2007; Kullander and Klein, 2002; Pasquale, 2008).

1.5.1 Eph forward signaling mechanisms

The first step for the activation of Eph receptors is the transphosphorylation of several tyrosines that are located in the intracellular region of other Eph receptors that are recruited into the cluster (Kalo and Pasquale, 1999). In particular, phosphorylation of the two tyrosine residues in the juxtamembrane region is a crucial event to convert the kinase domain into its fully active conformation (Binns et al., 2000; Kullander et al., 2001a). Once the receptor is activated, adaptor proteins bind to it and regulate signal transduction into the cell (Kullander and Klein, 2002; Pasquale, 2008). These adaptor proteins often lack intrinsic enzymatic activity but contain protein-interaction domains, such as Src-homology-2 (SH2) and SH3 domains, that are important for formation of signaling protein complexes (Pawson and Scott, 1997). The best characterized signaling pathway downstream of Eph receptors is the one that leads to changes in the actin cytoskeleton (figure 1.6). Small Rho family GTPases, including Rho, Rac and Cdc42, are key players in this pathway. These proteins function as bistable switches,

cycling between an active GTP-bound form and an inactive GDP-bound form (Heasman and Ridley, 2008). The balance between the two forms is regulated by guanine nucleotide-exchange factors (GEFs), that activate Rho GTPases by promoting the release of GDP and the binding of GTP, and GTPase-activating proteins (GAPs), that inactivate Rho GTPases by increasing the intrinsic GTPase activity of Rho proteins (Rossman et al., 2005). Eph receptors regulate the activity

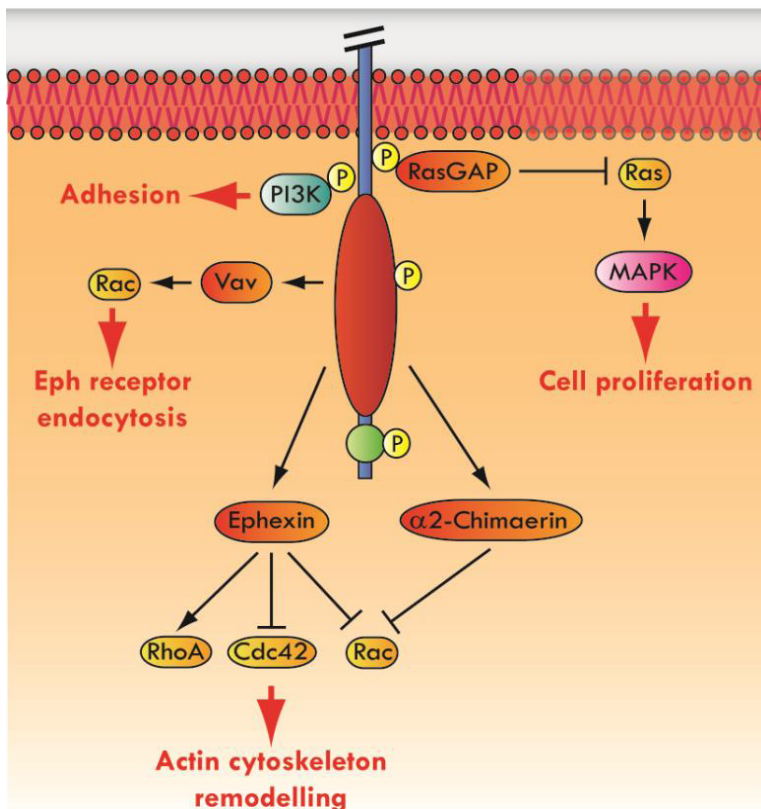


Figure 1.6 Eph receptor forward signaling. Schematic representation of some of the signaling pathways triggered by activation of Eph receptors. The scheme in the center of the figure represents the cytoplasmic domain of an Eph receptor. Red oval, kinase domain; green circle, SAM domain. The yellow circles marked with P represent phosphorylated tyrosines.

of Rho family GTPases by acting on GEFs, like ephexin (Sahin et al., 2005; Shamah et al., 2001) and Vav (Cowan et al., 2005), and GAPs like α 2-Chimaerin (Beg et al., 2007; Iwasato et al., 2007; Shi et al., 2007; Wegmeyer et al., 2007). Activation of RhoA by Eph receptors induces local depolymerization of actin filaments. At the same time Eph receptors inhibit Rac and Cdc42 and consequently block actin polymerization. These two pathways act in parallel to generate local collapse of the cytoskeleton. Other important signaling hubs, such as the phosphatidyl-

inositol 3-kinase (PI3K), Src family kinases and MAPKs, regulate a vast variety of cellular processes, including mitogenesis and cell adhesion, downstream of Eph receptor forward signaling (figure 1.6) (Kullander and Klein, 2002; Pasquale, 2008).

In some physiological contexts Eph receptor function does not require forward signaling. In some cases the ectodomain of the receptor is sufficient to activate ephrin-mediated reverse signaling in neighboring cells (Grunwald et al., 2004; Henkemeyer et al., 1996; Kullander et al., 2001b). In other situations the ectodomain of Eph receptors interacts in cis with other membrane proteins, promoting their clustering in localized cellular compartments and modulating their function (Dalva et al., 2000; Takasu et al., 2002).

1.5.2 Ephrin reverse signaling mechanisms

While EphA and EphB receptors share very similar downstream pathways, the molecular signaling mechanisms downstream ephrinA and ephrinB ligands are mostly divergent due to the structural differences between the two families of proteins (Egea and Klein, 2007).

1.5.2.1 EphrinB reverse signaling

The mechanisms involved in ephrinB reverse signaling that have been described so far invariably depend on the protein cytoplasmic domain (figure 1.7) (Cowan and Henkemeyer, 2002; Egea and Klein, 2007; Kullander and Klein, 2002). The signal transduction cascade is triggered by clustering of ephrinBs after binding to Eph receptors on adjacent cells. This event induces the recruitment and activation of Src family kinases that phosphorylate specific tyrosine residues of the ephrinB intracellular region (Palmer et al., 2002). The phospho-tyrosines function as docking sites for proteins with SH2 domains, such as Grb4, that in turn activate downstream signaling pathways regulating different physiological processes,

including remodeling of the actin cytoskeleton and cell adhesion (Cowan and Henkemeyer, 2001; Segura et al., 2007; Xu and Henkemeyer, 2009). EphrinBs can also activate downstream molecular targets independently from phosphorylation of the tyrosine residues by interactions of the PDZ-binding motif with PDZ domain-containing proteins. These proteins can be adaptors without intrinsic enzymatic activity like GRIPs and syntenin (Bruckner et al., 1999; Grootjans et al., 2000), or proteins containing functional units, such as PDZ-RGS3 (Lu et al., 2001). These interactions can be relevant for clustering and stabilizing other membrane proteins on the cell surface (Essmann et al., 2008) or can modulate signaling cascades downstream of other receptors (Lu et al., 2001). For example activation of ephrinB1 inhibits G-protein-coupled receptor CXCR4 signaling through recruitment of PDZ-RGS3. This protein contains a regulator of heterotrimeric G-protein-coupled receptor (RGS3) domain that acts as a GAP for the α subunit of trimeric G proteins, catalyzing the hydrolysis of GTP to GDP and therefore inactivating the molecular cascade downstream of CXCR4 (Lu et al., 2001).

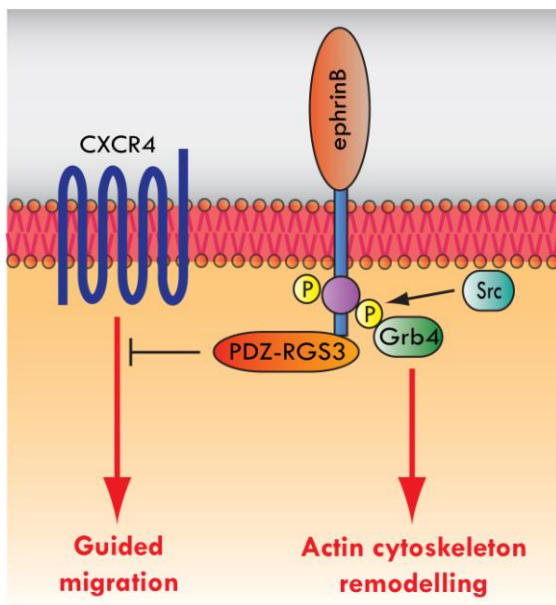


Figure 1.7 EphrinB reverse signaling.

Schematic representation of some of the pathways downstream of ephrinBs. Src phosphorylates specific tyrosines in the cytoplasmic domain of ephrinBs allowing the docking of adaptor proteins, such as Grb4. Interactions of these adaptors with specific enzymes trigger biochemical changes downstream of ephrinBs. Signaling molecules, such as PDZ-RGS3, interact with the PDZ-binding motif at the C-terminus of ephrinBs and modulate intracellular signaling pathways.

1.5.2.2 EphrinA reverse signaling

EphrinA reverse signaling has been implicated in a wide variety of physiological processes including axon guidance (Knoll et al., 2001; Lim et al., 2008b; Marquardt et al., 2005), cell migration (Coate et al., 2009), neurogenesis (Holmberg et al., 2005), insulin secretion (Konstantinova et al., 2007) and cell adhesion (Davy et al., 1999; Davy and Robbins, 2000; Huai and Drescher, 2001). However, the molecular mechanisms mediating ephrinA reverse signaling are poorly understood. Since ephrinA ligands lack a cytoplasmic domain, the mechanisms of signal transduction are radically different from ephrinB signaling. EphrinAs can use two different strategies for activating downstream molecular pathways (figure 1.8). First, they can interact in cis with a coreceptor (Lim et al., 2008b; Marler et al., 2008), similarly to other GPI-membrane bound proteins, such as the glial cell line-derived neurotrophic factor (GDNF) receptors (Airaksinen and Saarma, 2002). In this case ephrinA clustering modulates the intrinsic activity of associated transmembrane proteins. For example, in the axons of ganglion cells of the retina ephrinA repulsive effect during retinotopic map formation is mediated by the neurotrophin receptor p75 (Lim et al., 2008b). At later stages of development ephrinAs interact with TrkB in the axons of ganglion cells to control branching and synaptogenesis (Marler et al., 2008). The second mechanism used by ephrinA ligands to trigger reverse signaling may involve local modification of the membrane physical properties that causes the recruitment and activation of intracellular membrane-bound proteins. GPI-linked proteins, including ephrinAs, are often localized in specialized cell membrane microdomains rich in cholesterol and sphingolipids called lipid rafts (Brown and London, 1998; Tsui-Pierchala et al., 2002). It has been proposed that clustering of GPI-anchored proteins induces the formation of larger raft domains, which allows the interaction with signaling molecules attached to the inner surface of the rafts (Brown and London, 1998). Such a mechanism has been suggested for the ephrinA dependent activation of Src family kinases (Davy et al., 1999).

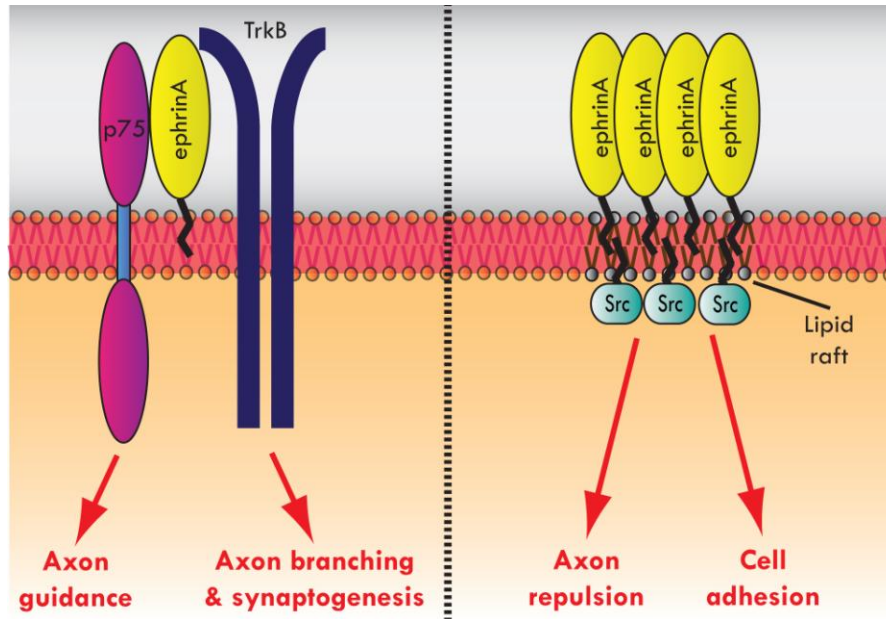


Figure 1.8 Mechanisms of ephrinA reverse signaling. Scheme showing two different mechanisms proposed for ephrinA signaling transduction. Left: ephrinAs interact with transmembrane proteins (coreceptors), such as p75 and TrkB. Right: ephrinA clustering induces local plasma membrane changes that, in turn, trigger recruitment of Src family kinases.

1.5.3 Cis versus trans interactions

Very often Eph receptors and ephrins are coexpressed in the same cells (Egea and Klein, 2007). The physiological implications of this observation are still controversial. It has been suggested that receptors and ligands can interact in cis. Such a scenario has been described for EphA3 and ephrinA5 in the growth cones of axons of retinal ganglion cells (Carvalho et al., 2006). In this case the interaction between receptor and ligand on the same cell membrane inhibits Eph forward signaling, probably by preventing the interaction between EphA3 and ephrinAs in trans. Other studies instead suggested that coexpressed receptors and ligands do not interact in cis. For example, it has been proposed that ephrinAs and EphAs in the growth cones of axons of spinal cord motor neurons segregate in distinct microdomains where they mediate opposing cellular responses, with ephrinAs

signaling attraction and EphAs inducing repulsion (Marquardt et al., 2005). Opposing functions and at least partial segregation of coexpressed Ephs and ephrins were also shown in pancreatic β cells, where EphA forward signaling inhibits, while ephrinA reverse signaling enhances insulin secretion (Konstantinova et al., 2007).

1.5.4 The role of Eph receptors and ephrins in synaptic plasticity

Eph receptors and ephrin ligands have been shown to be involved in a wide variety of processes during nervous system development including axon guidance, cell migration, proliferation and apoptosis (Kullander and Klein, 2002; Pasquale, 2008). However, the function of Ephs and ephrins is not restricted to embryonic development. Indeed, most of the receptors and ligands are highly expressed in the adult nervous system (Grunwald et al., 2001; Liebl et al., 2003), where they regulate structural and functional synaptic plasticity (Klein, 2009).

1.5.4.1 Modulation of structural plasticity by Ephs and ephrins

Different Eph receptors and ephrins are involved in the regulation of spine morphogenesis. Modulation of spine shape can involve both forward and reverse signaling (Klein, 2009). It has been shown that molecular events downstream of multiple EphB receptors and EphA4 are required for proper maturation of dendritic spines (Carmona et al., 2009; Henkemeyer et al., 2003; Murai et al., 2003). Neurons lacking EphB1-3 display loss and defective maturation of spines *in vitro* and *in vivo*. However, neurons lacking only one of the receptors have normal spines suggesting that EphBs are functionally redundant (Henkemeyer et al., 2003). EphB receptors clustering initiate parallel molecular pathways that lead to the remodeling of the actin cytoskeleton in spines (figure 1.9). For example the Rho-GEF Kalrinin is recruited into the EphB clusters and induces the Rac1 mediated

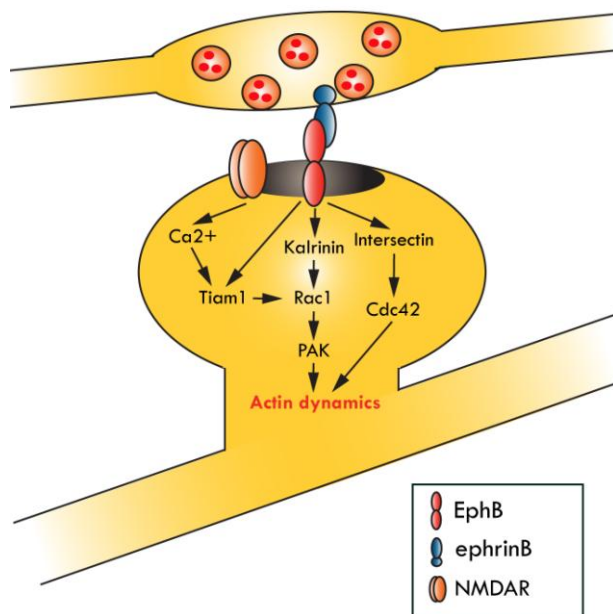


Figure 1.9 Molecular pathways regulating spine morphogenesis downstream of EphB receptors. EphBs regulate actin dynamics by activating small GTPases, such as Rac1 and Cdc42, through GEFs, including Kalrinin and Tiam1 or by recruiting multidomain scaffold proteins, such as Intersectin. Some of the pathways are influenced by synaptic activity. For example the GEF Tiam1 requires calcium entry through NMDARs to be activated.

activation of p21-activated kinases (PAKs), which ultimately trigger actin depolymerization (Penzes et al., 2003). This pathway is influenced by NMDAR activity. EphB receptors activation by ephrinBs induces the phosphorylation and recruitment of the Rac1-GEF Tiam1 to EphB complexes that also contain NMDARs (Tolias et al., 2005; Tolias et al., 2007). Tiam1 is phosphorylated in a calcium-dependent manner in response to NMDAR activity (Tolias et al., 2005). Another way for EphBs to influence spine morphology is to recruit the multi-domain scaffold protein Intersectin that controls local formation and branching of actin filaments by regulating the activity of Cdc42 (Irie and Yamaguchi, 2002).

Stimulation of EphA4 forward signaling in hippocampal slice cultures by application of preclustered ephrinA3 decreases spine length and density (Murai et al., 2003). On the contrary, *Epha4* and *EfnA3* null mutant mice display spine elongation and shape distortions *in vivo*, although the phenotype is much milder than *in vitro* (Carmona et al., 2009; Murai et al., 2003). Since EphA4 is enriched in dendritic spines and ephrinA3 is mainly localized in astrocytes in the adult mouse hippocampus, EphA4-ephrinA3 mediated neuroglia interaction has been proposed to regulate dendritic spine shape. Similarly to EphB receptors, EphA4 controls spine

morphology by affecting the dynamics of actin cytoskeleton (figure 1.10). EphA4 clustering induces the recruitment and activation of cyclin-dependent kinase 5 (Cdk5) that phosphorylates the Rho-GEF ephexin1, causing the RhoA-mediated rearrangement of actin filaments (Fu et al., 2007). In addition, binding of ephrinA3 to EphA4 induces the activation of the actin depolymerizing/severing factor cofilin mediated by phospholipase C γ 1 (PLC γ 1) (Zhou et al., 2007). Modulation of spine morphology by EphA4 involves also inhibition of β 1-integrin-dependent adhesion. Activation of EphA4 by ephrinA3 triggers the disassembling of integrin signaling complexes containing the Crk-associated substrate (Cas) the focal adhesion kinase (FAK) and the proline-rich tyrosine kinase 2 (Pyk2) (Bourgin et al., 2007). An additional mechanism used by EphA4 to modulate integrin function involves the recruitment, through its PDZ interacting motif, of the spine-associated RapGAP that inactivates Rap1 and consequently inhibits integrin-mediated adhesion (Richter et al., 2007).

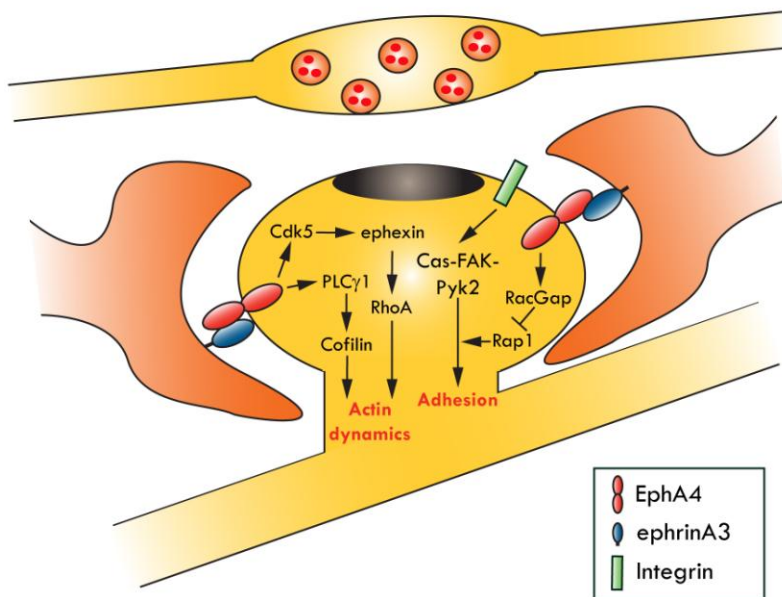


Figure 1.10 Regulation of spine morphogenesis by EphA4-ephrinA3 interaction at the neuro-glia interface.

Binding of astrocytic ephrinA3 to EphA4 on dendritic spines triggers parallel pathways that lead to actin cytoskeleton remodeling and inhibition of integrin-mediated cell adhesion.

Also ephrinB reverse signaling has been implicated in modulation of structural plasticity. Clustering of ephrinBs promotes the maturation of spines *in vitro* through a signaling pathway involving Grb4, G protein-coupled receptor kinase interacting protein 1 (GIT1) and the Rac-GEF β -PIX (Segura et al.,

2007; Zhang et al., 2005).

1.5.4.2 Modulation of functional plasticity by Ephs and ephrins

Eph receptors and ephrins not only control spine morphogenesis but also modulate functional synaptic plasticity (figure 1.11) (Klein, 2009). It has been shown that EphB2 directly interacts with NMDARs (Dalva et al., 2000; Grunwald et al., 2001) and modulates their function (Takasu et al., 2002). Activation of EphB2 induces phosphorylation of NMDARs by Src family kinases thereby potentiating NMDAR-dependent influx of calcium (Takasu et al., 2002). These events result in enhanced NMDAR-dependent gene expression and require EphB2 kinase activity. *Ephb2* null mutant mice have impaired LTP and LTD at the CA3-CA1 synapse and impaired LTP at the perforant path-dentate granule synapse (Grunwald et al., 2001; Henderson et al., 2001). Moreover, they display reduced NMDAR synaptic currents and NMDAR density in postsynaptic compartments (Henderson et al., 2001). However, EphB2 kinase activity is dispensable for long term synaptic plasticity modulation, suggesting that EphB2-dependent clustering of NMDARs may be sufficient to regulate their function. Alternatively, EphB2 could be required in the presynaptic bouton to activate postsynaptic ephrinB reverse signaling.

Similarly to EphB2, EphA4 modulates LTP and LTD at the CA3-CA1 synapse in a kinase-independent fashion (Grunwald et al., 2004). However, differently from EphB2, EphA4 does not interact with NMDARs (Dalva et al., 2000) and the molecular mechanisms involved in its function have been elusive. EphA4 is localized in both presynaptic bouton and postsynaptic spine (Tremblay et al., 2007) and it could be required in both or only one of the two compartments.

Also ephrinB reverse signaling modulates functional synaptic plasticity. EphrinB2 and ephrinB3 are enriched in CA1 region and dentate gyrus of the hippocampus (Grunwald et al., 2004; Grunwald et al., 2001). *Efnb2* conditional knockouts and *Efnb3* null mutant mice have impaired LTP and LTD at the CA3-CA1 synapse (Grunwald et al., 2004). Tyrosine phosphorylation sites in the ephrinB2

cytoplasmic domain are necessary to promote LTP but not LTD, while the ephrinB2 PDZ binding motif is required for both forms of plasticity (Bouzioukh et al., 2007). It has been suggested that one mechanism used by ephrinB2 to control synaptic plasticity may involve stabilization of AMPARs at the synapse through a mechanism mediated by GRIPs (Essmann et al., 2008). EphrinB3 reverse signaling appears to be dispensable for regulation of synaptic plasticity at the CA3-CA1 synapse but is required at the mossy fiber-CA3 synapse (Armstrong et al., 2006). At this synapse tetanic stimulation of mossy fibers induces clustering of postsynaptic EphB2 through a mechanism requiring GRIPs (Contractor et al., 2002). Clustering of postsynaptic EphB2 triggers ephrinB reverse signaling in the presynaptic compartment that, in turn, promotes LTP possibly by activating PKA signaling and ultimately by

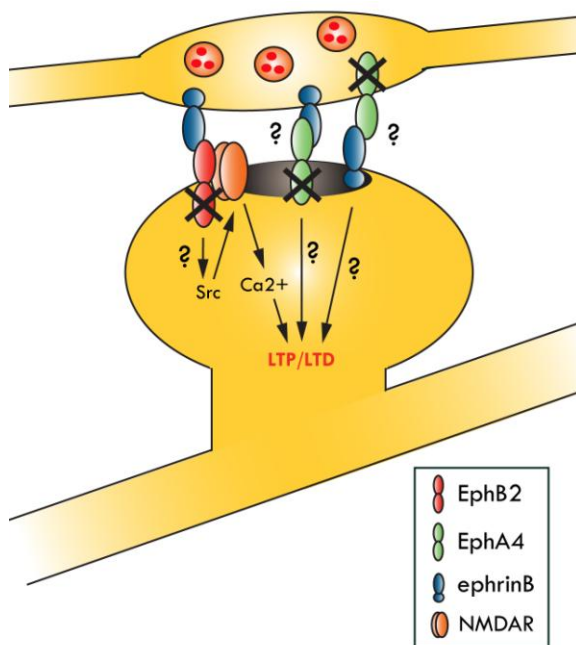


Figure 1.11 Eph receptors and ephrins promote LTP and LTD at the CA3-CA1 synapse. The EphB2 receptor interacts with NMDARs and regulates their clustering and activity. Activation of EphB2 forward signaling, most likely by presynaptic ephrinBs, induces phosphorylation of NMDARs by Src, regulating in this way their calcium permeability. However, EphB2 promotes LTP and LTD in a kinase-independent fashion. EphA4 modulates LTP and LTD in a forward signaling-independent fashion. EphA4 could be required in the presynaptic bouton to activate postsynaptic ephrinB reverse signaling or could act in the dendritic spine through an unknown

mechanism. EphrinB2, but not ephrinB3, reverse signaling promotes long term synaptic plasticity at the CA3-CA1 synapse. It is not clear yet if ephrinBs are required in the pre- or postsynaptic compartment.

increasing glutamate release from mossy fiber boutons. EphrinB reverse signaling has also been involved in the modulation of synaptic function in the retinotectal circuit of *Xenopus laevis* tadpoles (Lim et al., 2008a). Here, activation of ephrinB1 reverse signaling in axon terminals induces rapid increase of transmitter release and delayed enhancement of postsynaptic currents.

While the mechanisms underlying the functions of Eph receptors and ephrin ligands in structural plasticity are well characterized, the details of their roles in functional plasticity are still elusive.

1.6 Summary of the thesis project

As outlined in the introduction it was already known that EphA4 is involved in LTP modulation at the CA3-CA1 synapse (Grunwald et al., 2004). However, the molecular mechanism underlying EphA4 function in LTP regulation was not understood. It was suggested that EphA4 in the presynaptic bouton could modulate LTP by activating ephrinB reverse signaling in the postsynaptic compartment (figure 1.11) (Grunwald et al., 2004). This conclusion was based on three evidences: i) EphA4 forward signaling is dispensable for this function; ii) the ephrinB2 and ephrinB3 ligands also promote LTP at the CA3-CA1 synapse; iii) the two ligands are mostly localized in the postsynaptic side at the CA3-CA1 synapse. However, this model could not be rigorously proven because EphA4 is expressed in both CA3 and CA1 pyramidal neurons. For this reason I analyzed mice with conditional *Epha4* alleles in combination with CA1- and CA3-specific Cre lines. Contrary to the initial working model, I found that postsynaptic EphA4 is important for modulating LTP, while EphA4 localized in the presynaptic axon is dispensable.

It was known that dendritic EphA4 can bind ephrinA3 present in astrocytes (Murai et al., 2003). This idea was further strengthened by a recent study showing that EphA4 is mostly localized in the perisynaptic region of dendritic spines and presynaptic boutons where it cannot be engaged in a transsynaptic interaction but

could easily interact with astrocytic membrane proteins (Tremblay et al., 2007). These evidences led me to hypothesize that the interaction between dendritic EphA4 and glial ephrinA3 could be important for LTP modulation. In agreement with this hypothesis I found that *EfnA3* null mutant mice have impaired LTP. Further work showed that EphA4-ephrinA3 interaction at the neuro-glia interphase modulates LTP by controlling the amount of glial glutamate transporters present in astrocytes and as a consequence the concentration of glutamate near synapses.

2

Results

2.1 Characterization of a novel *Epha4* conditional allele

To investigate the function of EphA4 in the pre- or postsynaptic compartment at the CA3-CA1 synapse a new conditional allele of *Epha4* (hereafter referred to as *Epha4^{lx}*) was used (Filosa et al., 2009; Klas Kullander, unpublished results). Western blot analysis of hippocampal protein extracts revealed that EphA4 expression in *Epha4^{lx/lx}* mice was reduced to 15-20% when compared to *Epha4^{+/+}* mice (figure 2.1a). However, this reduction did not cause phenotypic alterations, such as anterior commissure and dorsal funiculus defects and synchronous hindlimb locomotion that were previously described in *Epha4* null mutants (Kullander et al., 2001b) (figure 2.1b,d,f). These phenotypes were instead evident when EphA4 was ubiquitously removed in *PGK-cre;Epha4^{lx/lx}* mice (Lallemand et al., 1998) (figure 2.1c,e,g).

These results demonstrated that the *Epha4^{lx}* allele, although hypomorphic, does not cause any major phenotypes present in *Epha4* null mice and that it can be efficiently recombined in presence of Cre.

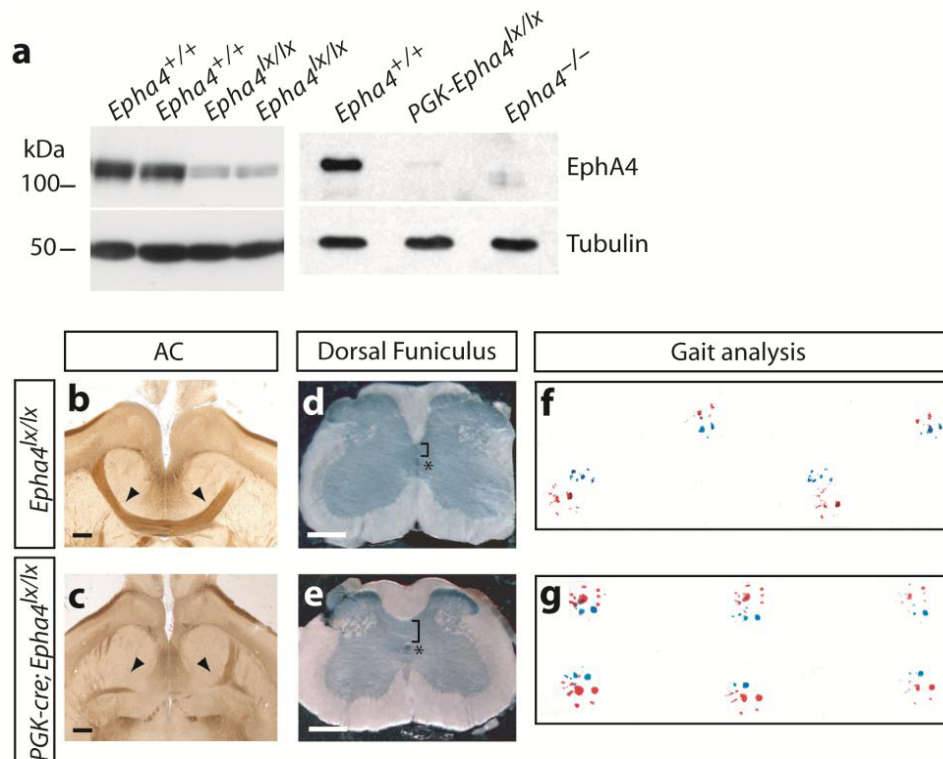


Figure 2.1 (previous page) Validation of the *Epha4^{lx}* allele. **(a)** EphA4 protein level analysis by western blot in P40 hippocampal protein extracts from two *Epha4^{+/+}* and two *Epha4^{lx/lx}* mice (left blot) and from *Epha4^{+/+}*, *PGK-cre;Epha4^{lx/lx}* and *Epha4^{-/-}* mice (right blot); tubulin was used as loading control. **(b,c)** Bright-field microscopy images of horizontal adult brain sections showing normal anterior commissure (AC, arrowheads) in *Epha4^{lx/lx}* mice **(b)** but not in *PGK-cre;Epha4^{lx/lx}* mutants **(c)**. **(d,e)** Dark-field images of cross sections of adult lumbar spinal cord. The ventral part of the dorsal funiculus containing corticospinal tract axons was normal in *Epha4^{lx/lx}* mice **(d)**, but greatly reduced in *PGK-cre;Epha4^{lx/lx}* mutants **(e)** as revealed by the increased distance (black square bracket) between the dorsal funiculus to the central canal (*). Scale bars: 500 μ m. **(f,g)** Gait analysis; to evaluate placement of paws during walking forepaws and hindpaws were coated in blue and red ink, respectively. *Epha4^{lx/lx}* mice show normal gait with alternative steps **(f)**, whereas *PGK-cre;Epha4^{lx/lx}* mice show a hopping gait characteristic of *Epha4^{-/-}* mice **(g)**. Data generated by S. Paixao.

2.2 Hippocampal long term synaptic plasticity is not altered in *Epha4^{lx/-}* mice

Because of the reduced expression of EphA4, the hypomorphic *Epha4^{lx}* allele may cause alterations of hippocampal long term synaptic plasticity that have been previously shown in *Epha4* null mutants (Grunwald et al., 2004). To test this possibility I analyzed LTP at the CA3-CA1 synapse in acute hippocampal slices obtained from *Epha4^{lx/-}* and *Epha4^{lx/+}* mice. Extracellular recordings did not reveal LTP defects in *Epha4^{lx/-}* mice, which had only one intact *Epha4* allele, compared to *Epha4^{lx/+}* mice up to 1 h after application of TBS or one tetanus to Schaffer collaterals (figure 2.2).

These results indicated that *Epha4^{lx/-}* mice could be used as controls in experiments investigating the role of EphA4 in LTP at the CA3-CA1 synapse. *Epha4^{lx/-}* and not *Epha4^{lx/lx}* mice were used as controls in the experiments described in this thesis to avoid variability of EphA4 expression due to potential Cre-mediated germ line recombination.

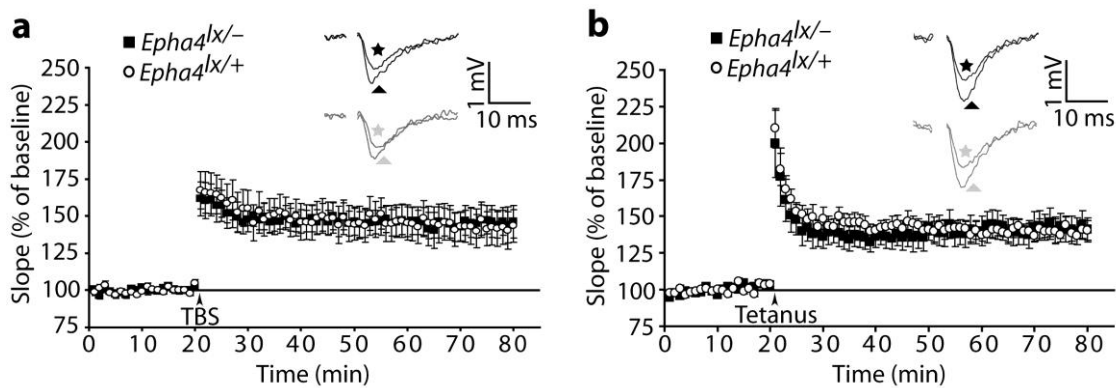


Figure 2.2 Normal LTP in *Epha4^{lox/-}* mice. **(a,b)** Graphs displaying LTP, represented as percentage of the baseline, induced with three TBSs **(a)** or one tetanus **(b)**. Insets: representative traces from controls (black traces) and mutants (gray traces) recorded before (stars) and 55-60 min after (triangles) LTP induction. The stimulation artifacts were removed. *Epha4^{lox/+}* and *Epha4^{lox/-}* mice had similar amount of potentiation at 55-60 min after LTP induction (TBS: 142.1 ± 11.8 % in *Epha4^{lox/+}*, $n = 8$ slices, 5 mice, versus 145.4 ± 10.3 % in *Epha4^{lox/-}*, $n = 8$ slices, 5 mice, t -test, $P = 0.8$; tetanus: 140.2 ± 5.7 % in *Epha4^{lox/+}*, $n = 10$ slices, 8 mice, versus 141.5 ± 8.9 % in *Epha4^{lox/-}*, $n = 10$ slices, 8 mice, t -test, $P = 0.9$). Error bars, s.e.m.

2.3 Efficient subregion-specific elimination of EphA4 in adult hippocampus

To generate CA1 pyramidal cell-specific *Epha4* knockout mice, I used the *R4Ag11CamKII-cre* mouse line (hereafter referred to as *CA1-cre*) which recombines in CA1 cells starting from the second postnatal week (Tsien et al., 1996). To generate CA3 pyramidal cell-specific *Epha4* knockout mice, I used a new knock-in mouse line, which expresses Cre from the endogenous *Grik4* locus (hereafter referred to as *CA3-cre*) starting from the first postnatal week (Filosa et al., 2009). *CA1-cre;Epha4^{lox/-}* and *CA3-cre;Epha4^{lox/-}* mice were viable and fertile, and exhibited no gross developmental abnormalities. The recombination efficiencies in the *CA1-cre;Epha4^{lox/-}* and *CA3-cre;Epha4^{lox/-}* lines were quantified by densitometric

analysis of *Epha4* mRNA *in situ* hybridizations and calculated to be approximately 80% for both lines (figure 2.3).

These results demonstrated that efficient sub-region specific elimination of EphA4 in the hippocampus could be achieved by combining the *Epha4^{lox}* allele with the CA1-cre and CA3-cre lines.

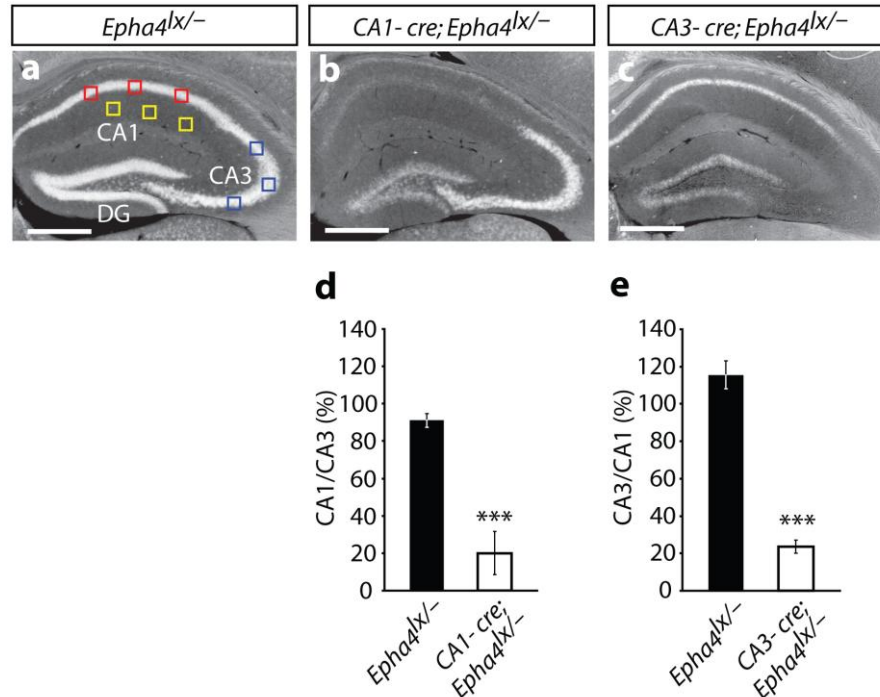


Figure 2.3 Efficient sub-region-specific recombination of *Epha4* floxed allele in the hippocampus. (a) *In situ* hybridization showing *Epha4* mRNA expression in the dentate gyrus (DG), CA3 and CA1 regions of the hippocampus of an adult *Epha4^{lox/-}* mouse. The small squares indicate the regions used for densitometric measurements for calculating the recombination efficiency (details in the materials and methods section). (b,c) *In situ* hybridizations for *Epha4* showing highly reduced expression of the mRNA in CA1 in *CA1-cre; Epha4^{lox/-}* mice (b) and in CA3 in *CA3-cre; Epha4^{lox/-}* mice (c). (d,e) Bar graphs depicting the CA1/CA3 ratio (in percentage) of *Epha4* mRNA hybridization signal strength in *Epha4^{lox/-}* (d, black bar) and *CA1-cre; Epha4^{lox/-}* (d, white bar) mice or the CA3/CA1 ratio (in percentage) in *Epha4^{lox/-}* (e, black bar) and *CA3-cre; Epha4^{lox/-}* (e, white bar) mice (CA1/CA3 ratio: 20% \pm 12% in *CA1-cre; Epha4^{lox/-}* mice, compared to 91% \pm 4% in *Epha4^{lox/-}* controls; CA3/CA1 ratio: 24% \pm 4% in *CA3-cre; Epha4^{lox/-}* animals, compared to 116% \pm 7% in *Epha4^{lox/-}* controls; $n = 3-5$ mice; *t*-test, *** $P < 0.0001$). Scale bars, 500 μ m. Error bars, s.e.m.

2.4 Normal basal synaptic transmission in *Epha4* mutants

Before analyzing LTP, I performed a careful analysis of potential alterations of basal synaptic transmission in *CA1-cre;Epha4^{lox/-}* and *CA3-cre;Epha4^{lox/-}* mice. Extracellular recordings of the CA3-CA1 pathway in acute hippocampal slices from *CA1-cre;Epha4^{lox/-}*, *CA3-cre;Epha4^{lox/-}* and control mice revealed similar amplitudes of the presynaptic fiber volley (FV), which is proportional to the number of axons recruited by electrical stimulation (figure 2.4a,b). Also the slopes of field excitatory postsynaptic potentials (fEPSPs) at various stimulation intensities were not altered in *Epha4* mutants, indicating normal postsynaptic responses to presynaptic stimulation (figure 2.4a,b). These data revealed linear relations between synaptic inputs (FVs) and postsynaptic responses (fEPSPs) in *CA1-cre;Epha4^{lox/-}* and *CA3-cre;Epha4^{lox/-}* mice that were comparable to the ones obtained from control mice.

Furthermore, PPF at various interstimulus intervals (ISIs) was normal in mutant mice, indicating that the probability of synaptic vesicle release was comparable in mutant and control mice (figure 2.5a,b). Fiber volley amplitudes, fEPSP slopes and PPF were normal also in *Camk2a-cre;Epha4^{lox/-}* mice, in which EphA4 was removed from forebrain neurons, including pyramidal cells in CA3 and CA1 regions of the hippocampus, starting from the second postnatal week (Minichiello et al., 1999) (figure 2.4c, 2.5c).

Moreover, whole-cell voltage-clamp analysis showed no alterations in AMPAR/NMDAR current ratio in CA1 pyramidal cells of acute hippocampal slices obtained from *Epha4* null mutants (figure 2.6), revealing normal function of postsynaptic ionotropic glutamate receptors in basal conditions.

Taken together, these data showed that hippocampal basal synaptic transmission is not perturbed in *Epha4* mutants.

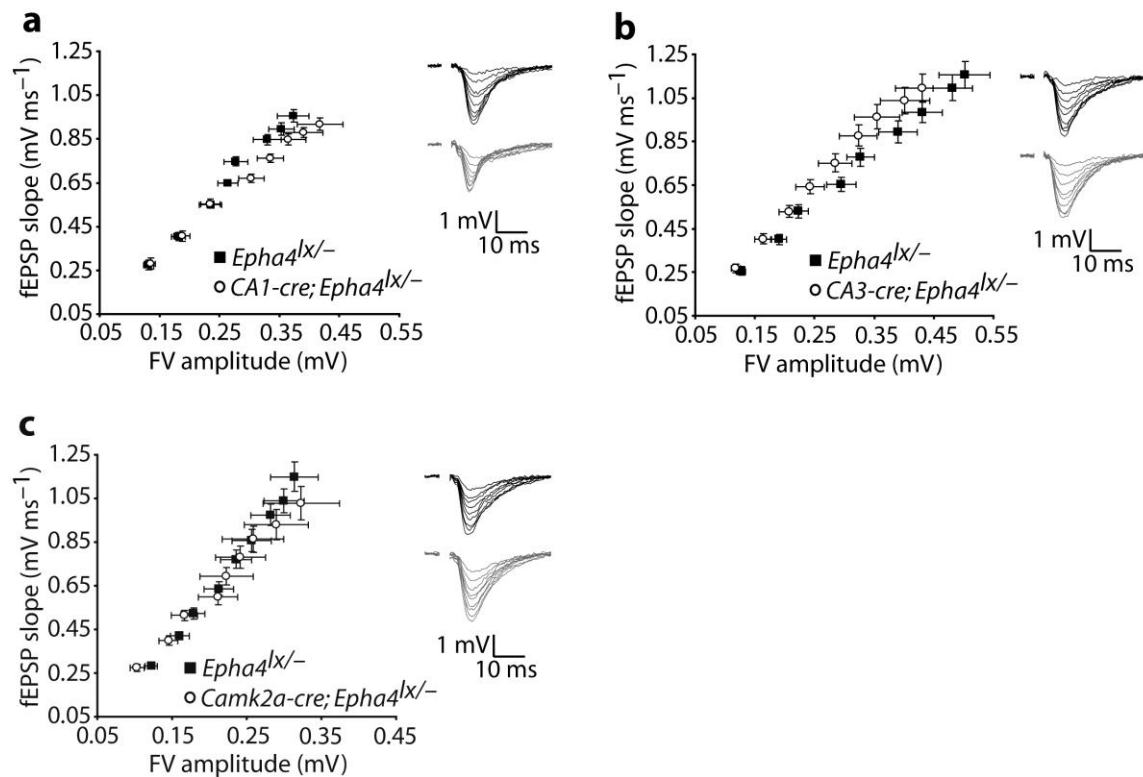


Figure 2.4 Normal axonal function and postsynaptic responses in *Epha4* mutants. **(a,b,c)** Left: relations between presynaptic fiber volley (FV) amplitudes and fEPSP slopes at various stimulus intensities. Right: representative traces of fEPSPs at various stimulation intensities in controls (black traces) and mutants (gray traces). The stimulation artifacts were removed. **(a)** Normal fEPSPs in *CA1-cre;Epha4*^{lox/-} mice (*Epha4*^{lox/-}, $n = 16$ slices, 5 mice, per group, *CA1-cre;Epha4*^{lox/-}, $n = 16$ slices, 5 mice, per group, ANCOVA, $P = 0.1$). **(b)** In the FV range of 0.1-0.3 mV *Epha4*^{lox/-} controls ($n = 17$ slices, 6 mice per group) and *CA3-cre;Epha4*^{lox/-} mutants ($n = 17$ slices, 6 mice per group) showed similar values (ANCOVA, $P = 0.07$). **(c)** *Camk2a-cre;Epha4*^{lox/-} mutants had normal fEPSP slopes at various stimulus intensities compared to *Epha4*^{lox/-} controls ($n = 11$ slices, 4 mice per group, ANCOVA, $P = 0.2$). Error bars, s.e.m.

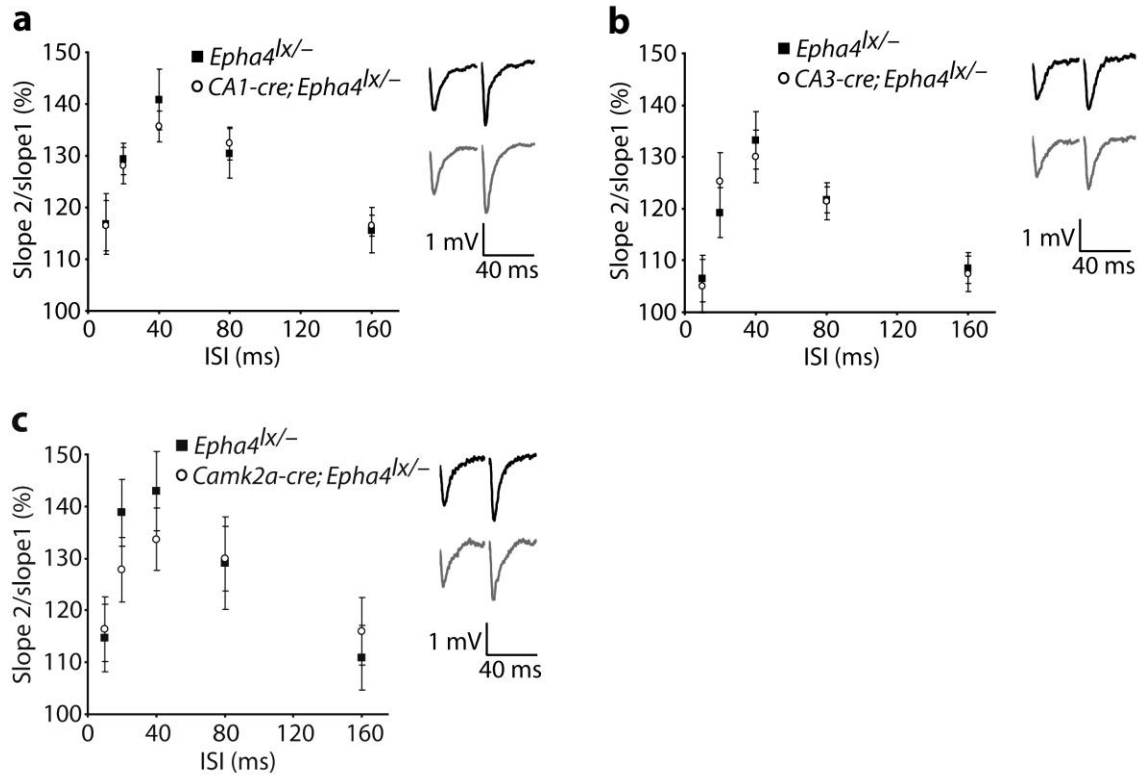


Figure 2.5 Normal PPF in *Epha4* mutants. **(a,b,c)** Left: PPF of the fEPSPs, at various interstimulus intervals (ISIs) from **(a)** *CA1-cre;Epha4^{lox/-}* and *Epha4^{lox/-}* mice ($n = 14$ slices, 5 mice per group, two-way repeated measures ANOVA, between genotypes: $F_{1,130} = 0.09$, $P = 0.8$), from **(b)** *CA3-cre;Epha4^{lox/-}* and *Epha4^{lox/-}* mice ($n = 13$ slices, 4 mice per group, two-way repeated measures ANOVA, between genotypes: $F_{1,120} = 0.2$, $P = 0.9$) and from **(c)** *Camk2a-cre;Epha4^{lox/-}* and *Epha4^{lox/-}* mice ($n = 14$ slices, 7 mice per group, between genotypes: $F_{1,130} = 0.4$, two-way repeated measures ANOVA, $P = 0.6$). Right: representative traces showing PPF at 40 ms ISI in controls (black traces) and mutants (gray traces). The stimulation artifacts were removed. Error bars, s.e.m.

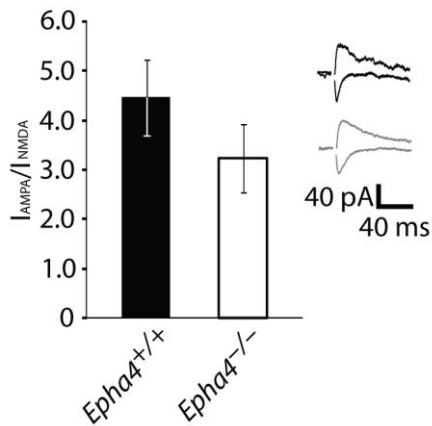


Figure 2.6 Normal AMPAR- and NMDAR-mediated currents in *Epha4*^{-/-} mice. Histogram showing the ratios between AMPAR and NMDAR currents (I) in *Epha4*^{+/+} and *Epha4*^{-/-} mice (*Epha4*^{+/+}: 4.5 ± 0.8 ; *Epha4*^{-/-}: 3.3 ± 0.8 , $n = 6$ cells, 6 mice per group, $P = 0.3$, t -test). Inset: representative average evoked currents recorded at -70 mV (lower traces) or $+40$ mV (upper traces) (*Epha4*^{+/+}: black traces; *Epha4*^{-/-}: gray traces). The stimulation artifacts were removed. Error bars, s.e.m.

2.5 EphA4 is required for LTP in postsynaptic CA1 cells

To investigate a requirement for either postsynaptic or presynaptic EphA4 for LTP modulation at the CA3-CA1 synapse, I induced LTP with TBS in acute hippocampal slices from *Epha4* mutant and control mice. After recording a stable baseline, three TBS were given to fibers of the CA3 presynaptic neurons, and postsynaptic responses were recorded from *stratum radiatum* of CA1 region with an extracellular electrode for up to 60 min post stimulation. *CA1-cre;Epha4*^{lx/-} mice had a marked reduction in LTP compared to littermate *Epha4*^{lx/-} controls (figure 2.7a). A similar LTP reduction was observed also in *Camk2a-cre;Epha4*^{lx/-} mice (figure 2.7b). In contrast, TBS-induced LTP was not altered in *CA3-cre;Epha4*^{lx/-} mice (figure 2.7c).

These results demonstrated that EphA4 functions postsynaptically to regulate LTP at the CA3-CA1 synapse.

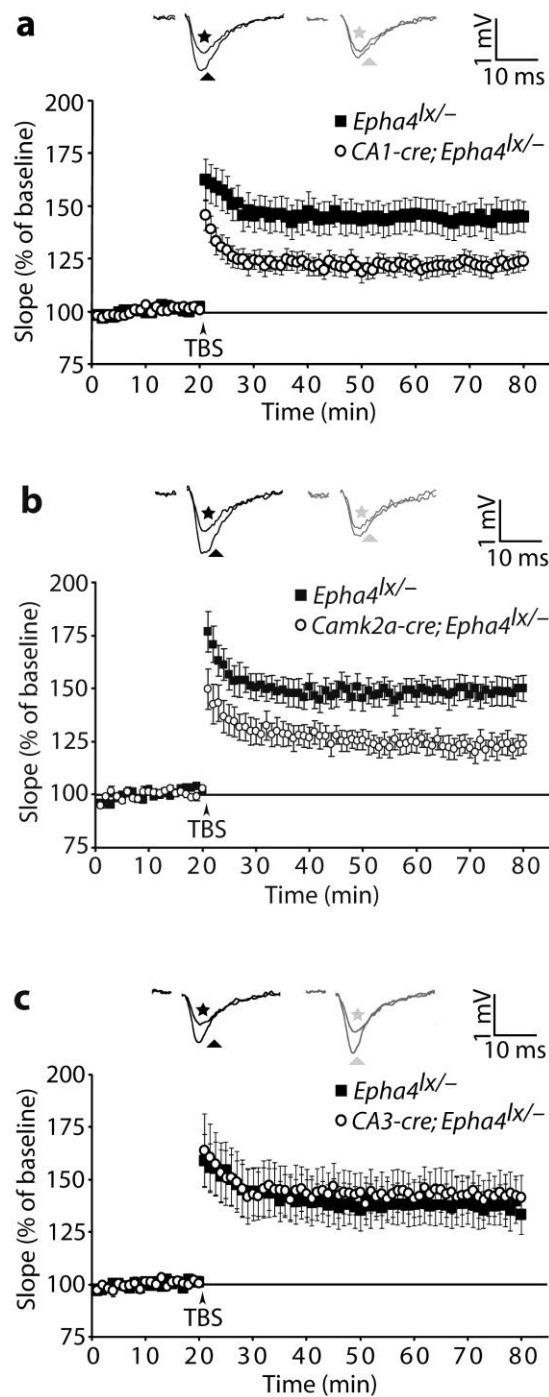


Figure 2.7 EphA4 is required for TBS-induced LTP in postsynaptic CA1 cells. **(a-c)** Scatter plots showing LTP, represented as percentage of the baseline, induced by stimulation of Schaffer collaterals with three TBSs. Insets: representative traces from controls (black) and mutants (gray) recorded before (stars) and 55-60 min after (triangles) LTP induction. The stimulation artifacts were removed. **(a)** CA1-cre;Epha4^{lox/-} mice showed a marked deficit in TBS-induced LTP compared to littermate Epha4^{lox/-} controls ($123.0 \pm 4.4\%$ in mutants, $n = 12$ slices, 7 mice; versus $144.8 \pm 7.6\%$ in controls, $n = 14$ slices, 7 mice; at 55-60 min after induction, t -test, $P = 0.02$). **(b)** Camk2a-cre;Epha4^{lox/-} mice had impaired TBS-induced LTP ($123.4 \pm 4.8\%$ in mutants, $n = 12$ slices, 10 mice, versus $149.0 \pm 6.1\%$ in controls, $n = 13$ slices, 10 mice, at 55-60 min after induction, t -test, $P = 0.003$). **(c)** CA3-cre;Epha4^{lox/-} mice showed normal TBS-induced LTP ($142.9 \pm 10.0\%$ in mutants, $n = 10$ slices, 8 mice; versus $136.9 \pm 9.7\%$ in controls, $n = 10$ slices, 8 mice; at 55-60 min after induction, t -test, $P = 0.7$). Error bars, s.e.m.

2.6 Tetanus-induced LTP does not require EphA4

LTP can be induced at the CA3-CA1 synapse with different patterns of high frequency stimulation (Albenis et al., 2007). Differences in induction protocols can result in diverse outcomes when LTP is analyzed in presence of pharmacological or genetic manipulations (Shalin et al., 2006; Zakharenko et al., 2003). To better

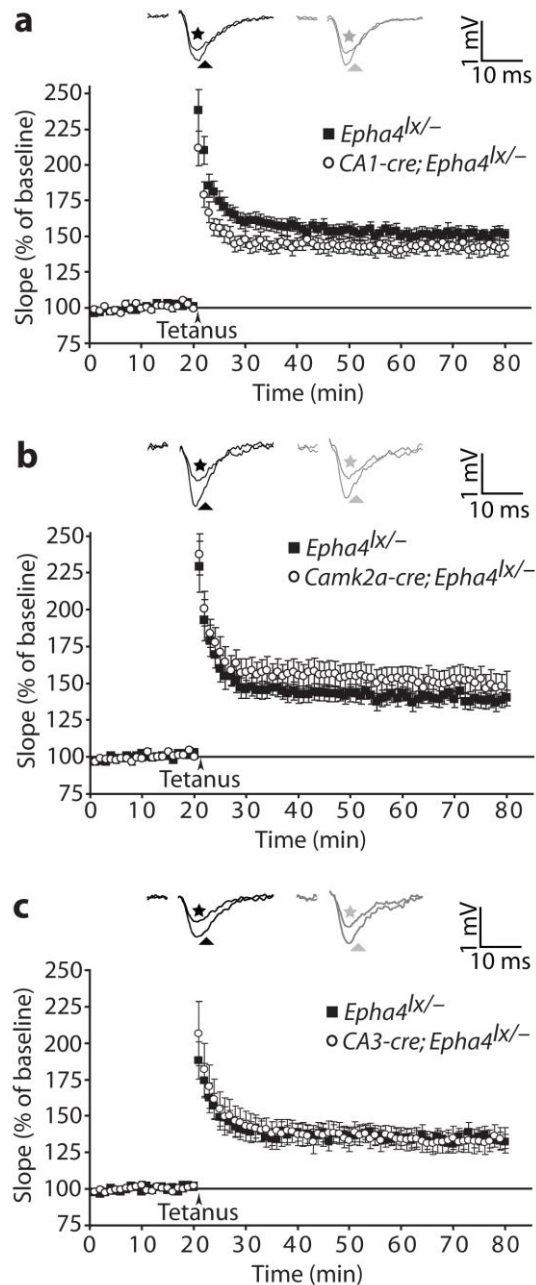


Figure 2.8 EphA4 is dispensable for tetanus-induced LTP. (a-c) Graphs showing LTP, induced by stimulation of Schaffer collaterals with one tetanus. Insets: representative traces from controls (black) and mutants (gray) recorded before (stars) and 55-60 min after (triangles) LTP induction. The stimulation artifacts were removed. *CA1-cre;Epha4*^{lox/-} (a), *Camk2a-cre;Epha4*^{lox/-} (b) and *CA3-cre;Epha4*^{lox/-} (c) mice had normal tetanus-induced LTP (*CA1-cre;Epha4*^{lox/-} mice: $142.8 \pm 6.0\%$ in mutants, $n = 11$ slices, 9 mice; versus $151.0 \pm 11.0\%$ in controls, $n = 12$ slices, 9 mice; at 55-60 min after induction, t -test, $P = 0.5$; *Camk2a-cre;Epha4*^{lox/-}: $148.0 \pm 9.0\%$ in mutants, $n = 13$ slices, 9 mice, versus $138.6 \pm 5.2\%$ in controls, $n = 15$ slices, 9 mice, at 55-60 min after induction, t -test, $P = 0.4$; *CA3-cre;Epha4*^{lox/-} mice: $133.8 \pm 7.9\%$ in mutants, $n = 10$ slices, 8 mice; versus $134.0 \pm 5.4\%$ in controls, $n = 9$ slices, 8 mice; at 55-60 min after induction, t -test, $P = 1.0$). Error bars, s.e.m.

characterize the role of EphA4 in long term synaptic plasticity modulation I analyzed LTP induced with one tetanus in *Epha4* mutants. Surprisingly, *CA1-cre;Epha4^{lox/-}* and *Camk2a-cre;Epha4^{lox/-}* mice did not display any LTP defects under these conditions (figure 2.8a,b). Similar results were obtained with *CA3-cre;Epha4^{lox/-}* mice (figure 2.8c).

These data indicated that EphA4 is dispensable for tetanus-induced LTP. Therefore, EphA4 is differentially engaged in LTP modulation depending on the stimulation pattern used for LTP induction.

2.7 EphrinA3 is required for TBS-induced LTP

The fraction of EphA4 that is localized in dendrites has previously been shown to respond to ephrinA3 present in hippocampal astrocytes (Carmona et al., 2009; Murai et al., 2003). Consistent with such a model, immune electron microscopic studies have suggested that EphA4 is localized mainly perisynaptically (Tremblay et al., 2007) where it could easily interact with proteins on the surface of astrocytic processes rather than with presynaptic binding partners. Therefore EphA4 may modulate LTP by interacting with astrocytic ephrinA3, possibly inducing some biochemical change in astrocytes. Therefore, I examined LTP at the CA3-CA1 synapse in *Efna3* null mutant mice (Carmona et al., 2009). Application of three TBS to Schaffer collaterals in acute hippocampal slices from *Efna3^{-/-}* mice revealed a strong inhibition of LTP compared to *Efna3^{+/+}* controls (figure 2.9a). Interestingly, like *Epha4* mutants, *Efna3^{-/-}* mice displayed reduced TBS-induced LTP but normal tetanus-induced LTP (figure 2.9b).

These findings suggested that EphA4 interacts with ephrinA3 to mediate TBS-induced LTP at the CA3-CA1 synapse.

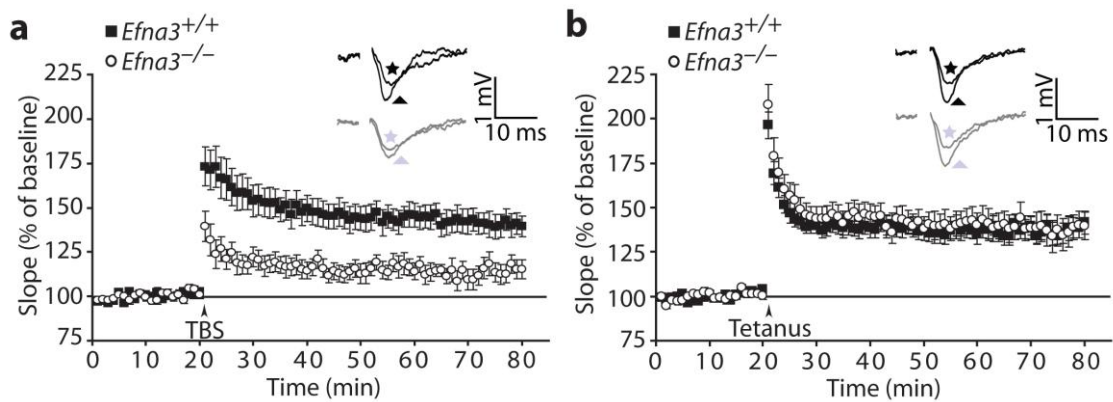


Figure 2.9 Impaired TBS-induced LTP in *Efna3* null mutants. **(a,b)** Scatter plots showing LTP induced by stimulation of presynaptic CA3 neurons with three TBSs **(a)** or a single tetanus **(b)**. **(a)** *Efna3*^{-/-} mice showed a strong deficit in TBS-induced LTP compared to *Efna3*^{+/+} controls (*Efna3*^{+/+}, $140.7 \pm 6.1\%$, $n = 14$ slices, 10 mice; *Efna3*^{-/-}, $114.8 \pm 5.0\%$, $n = 12$ slices, 10 mice, at 55-60 min after stimulus, t -test, $P = 0.004$). **(b)** *Efna3*^{-/-} mice had normal tetanus-induced LTP (*Efna3*^{+/+}, $138.6 \pm 6.0\%$, $n = 13$ slices, 10 mice; *Efna3*^{-/-}, $137.9 \pm 7.7\%$, $n = 12$ slices, 10 mice; at 55-60 min after stimulus, t -test, $P = 0.9$). Insets: representative traces from *Efna3*^{+/+} (black) and *Efna3*^{-/-} (gray) mice recorded before (stars) and 55-60 min after (triangles) LTP induction. The stimulation artifacts were removed. Error bars, s.e.m.

2.8 Normal basal synaptic transmission in *Efna3* null mutants

To rule out the possibility that the LTP deficit in *Efna3*^{-/-} mice is caused by defects in basal synaptic transmission, I analyzed fiber volley amplitudes, fEPSP slopes and PPF. These parameters were comparable in *Efna3*^{-/-} and *Efna3*^{+/+} mice (figure 2.10). Moreover, whole-cell patch-clamp analysis did not reveal alterations in average frequency and amplitude of miniature excitatory postsynaptic currents (mEPSCs) in *Efna3* mutant mice (figure 2.11), confirming comparable probability of synaptic vesicle release and postsynaptic function in mutant and control mice.

These data demonstrated that basal synaptic transmission at the CA3-CA1 synapse is not altered in *Efna3*^{-/-} mice.

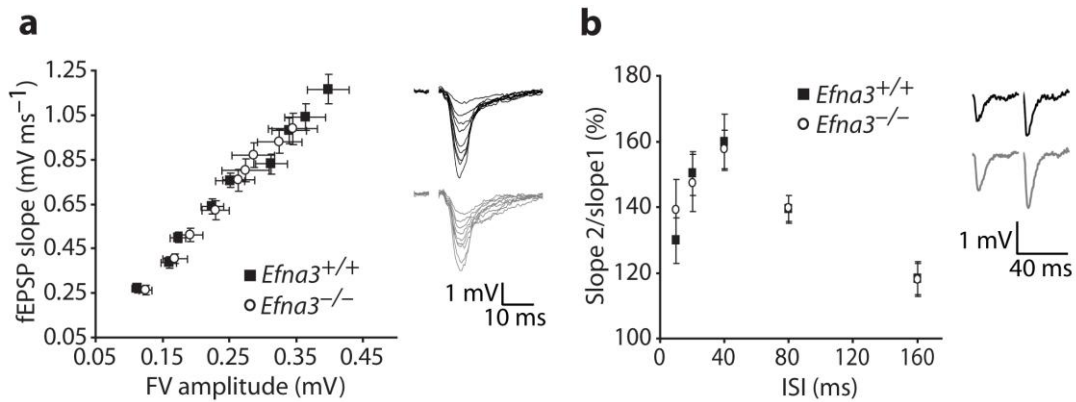


Figure 2.10 Normal basal synaptic transmission in *Efn3* null mutants. **(a)** fEPSP slopes at various stimulus intensities (FV, fiber volley) and representative traces (*Efn3*^{+/+}, black; *Efn3*^{-/-}, gray; $n = 12$ slices, 6 mice per group; ANCOVA, $P = 0.1$). **(b)** PPF at various ISIs and representative traces at 40 ms ISI (*Efn3*^{+/+}, black; *Efn3*^{-/-}, gray; $n = 10$ slices, 5 mice per group, two-way repeated measures ANOVA: between genotypes, $F_{1,90} = 0.03$, $P = 0.9$). The stimulation artifacts were removed. Error bars, s.e.m.

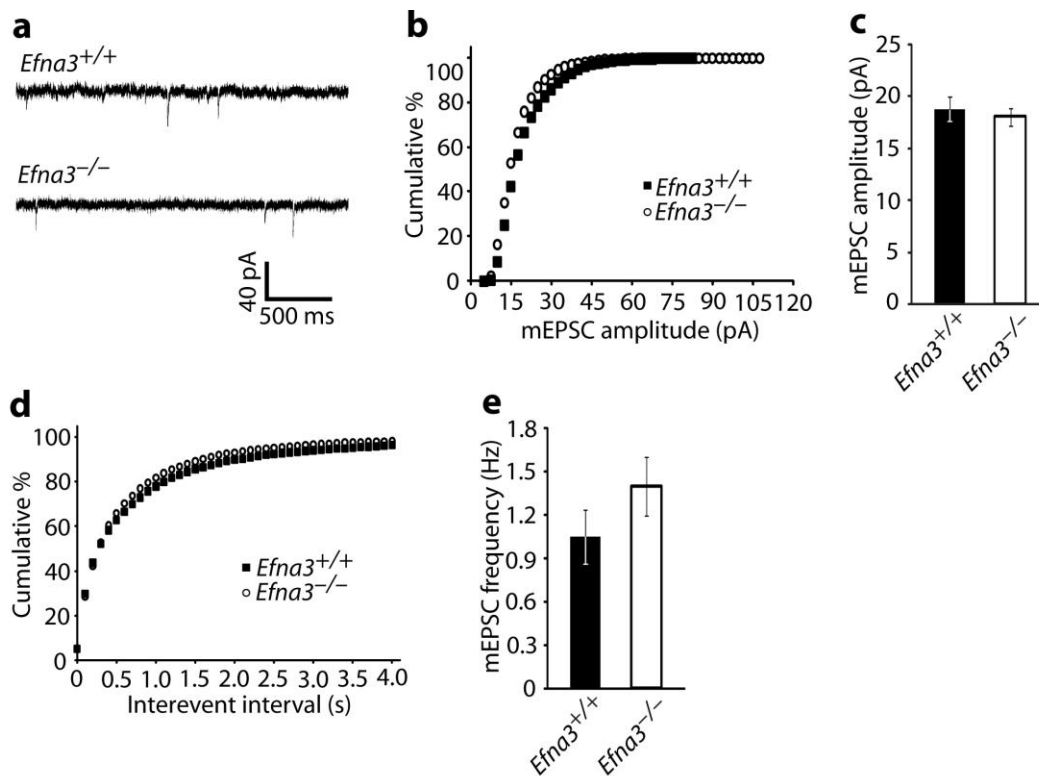


Figure 2.11 (previous page) Normal mEPSC amplitudes and frequency in *Efna3*^{-/-} mice. **(a)** Representative traces of mEPSCs in *Efna3*^{+/+} and *Efna3*^{-/-} mice. **(b,c)** Plots depicting cumulative distribution **(b)** or average values **(c)** of mEPSC amplitudes showed no alterations in *Efna3*^{-/-} mice compared to wild type controls **(b: P = 0.15, two sample Kolmogorov-Smirnov (KS) test; c: P = 0.7, t-test; n=16 mice for *Efna3*^{-/-} and n=15 mice for the control group)**. **(d,e)** Graphs showing the cumulative distributions of interevent interval **(d)** and average frequency **(e)** of mEPSCs in *Efna3*^{+/+} and *Efna3*^{-/-} mice. There were no differences between the two groups **(d: P = 0.09, two sample KS test; e: P = 0.2, t-test; n=16 mice for *Efna3*^{-/-} and n=15 mice for the control group)**. 97% of the total events are shown in **(d)**. Error bars, s.e.m.

2.9 Astrocytic glutamate transporter upregulation in *Epha4* mutants

Since EphA4 forward signaling is dispensable for LTP (Grunwald et al., 2004), the EphA4 ectodomain may activate ephrinA3 reverse signaling in astrocytes, and thereby modulating astrocytic functions that influence LTP. Glial glutamate transporters are known to regulate synaptic transmission by clearing glutamate from the synapse (Beart and O'Shea, 2007; Tzingounis and Wadiche, 2007). This property makes them likely candidates for mediating EphA4- and ephrinA3-dependent modulation of LTP. For this reason, the abundances of the glial glutamate transporters GLAST and GLT1 in brains of *Epha4* mutant mice were analyzed by western blot. Interestingly, a marked upregulation of GLAST abundance and a modest increase in GLT1 abundance were observed in *Epha4*^{-/-} hippocampi and cerebral cortexes compared to littermate controls (figure 2.12a-c). Amounts of glial fibrillary acidic protein (GFAP) and the neuronal glutamate transporter EAAC1 were not altered in *Epha4*^{-/-} brains (Figure 2.12a,c), indicating that the biochemical alterations were restricted to astrocytes. GLAST upregulation was also detected in dissected CA1, but not CA3, regions of *CA1-cre;Epha4*^{lox/-} (figure 2.12d-f). Similar changes in GLAST and GLT1 abundance were observed in *Efna3*^{-/-} mice (Carmona et al., 2009).

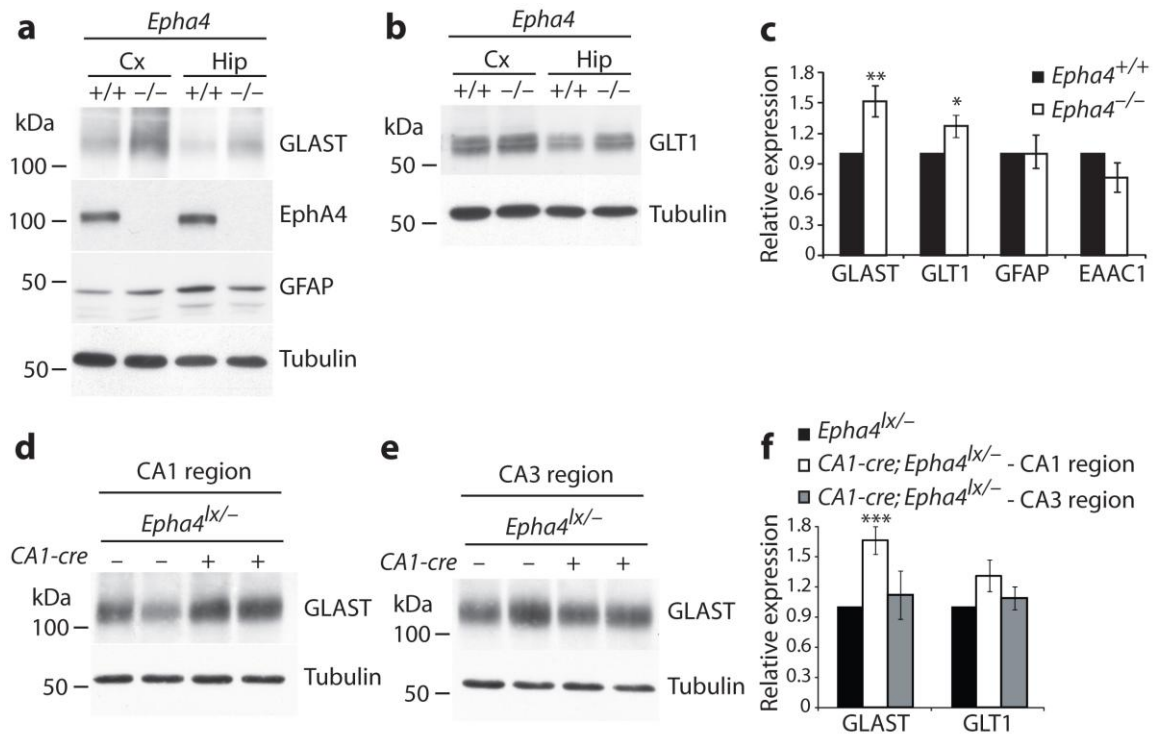


Figure 2.12 Increased GLAST and GLT1 protein abundance in *Epha4* mutants. **(a,b)** Western blot analysis of GLAST, GLT1, GFAP, EAAC1, EphA4 and tubulin protein levels in cerebral cortex (Cx) and hippocampi (Hip) of *Epha4*^{-/-} and *Epha4*^{+/+} mice. **(c)** Bar graph depicting average amount of glutamate transporters and GFAP in hippocampi of *Epha4*^{-/-} and *Epha4*^{+/+} mice, relative to values for *Epha4*^{+/+} protein lysates, determined with densitometric measurements. Expression was normalized to tubulin. GLAST and GLT1 levels were 50% and 25% higher, respectively, in *Epha4*^{-/-} mice than in *Epha4*^{+/+} controls (GLAST, ** $P = 0.009$, $n = 10$ mice per group; GLT1, * $P = 0.03$, $n = 15$ mice; GFAP, $P = 0.2$, $n = 10$ mice; EAAC1, $P = 0.3$, $n = 3$ mice; t -test). **(d,e)** Western blot analysis of protein lysates from dissected CA1 and CA3 regions obtained from *CA1-cre;Epha4*^{lox/-} mice or *Epha4*^{lox/-} controls for their content of GLAST and tubulin. **(f)** Bar graph showing average amount of GLAST and GLT1 in the indicated genotypes and hippocampal regions. GLAST abundance in CA1, but not CA3, was increased (GLAST in CA1, $n = 7$ mice, *** $P = 0.0009$; GLAST in CA3, $n = 6$ mice, $P = 0.7$; GLT1 in CA1, $n = 13$ mice, $P = 0.07$; GLT1 in CA3, $n = 6$ mice, $P = 0.5$). Error bars, s.e.m. Data showed in a-c were generated by S. Paixao. Data represented in d-e were generated by S. Paixao and A. Filosa.

Interestingly, the regulation of glial glutamate transporter abundance does not happen at the posttranscriptional level, since the levels of *Slc1a3* and *Slc1a2* mRNAs, coding for GLAST and GLT1, respectively, in *Epha4*^{-/-} and *Efna3*^{-/-} mice were similar to control mice (Carmona et al., 2009; Filosa et al., 2009).

These results revealed that EphA4, presumably by interacting with ephrinA3 in astrocytes, negatively controls glial glutamate transporter abundance through a post transcriptional mechanism.

2.10 Normal astrocytic glutamate transporter abundance in *Epha4*^{EGFP/EGFP} mice

If EphA4 interaction with ephrinA3 induced a reverse signal that causes changes of glutamate transporter abundance in astrocytes, the EphA4 intracellular domain should be dispensable for this function. To test this hypothesis, glial glutamate transporter abundances were examined in brains of *Epha4*^{EGFP/EGFP} mice, in which the cytoplasmic domain is replaced by EGFP (Grunwald et al., 2004). Interestingly, western blot analysis did not reveal upregulation of GLAST and GLT1 suggesting that the EphA4 ectodomain was sufficient for maintaining normal GLAST and GLT1 levels in astrocytes (figure 2.13a-c). This observation correlates well with the fact that *Epha4*^{EGFP/EGFP} mice have normal LTP (Grunwald et al., 2004).

These results indicated that the EphA4 intracellular domain is dispensable for regulating glial glutamate transporter abundance. Moreover the data point to a role for GLAST and GLT1 in mediating EphA4 and ephrinA3 dependent LTP modulation.

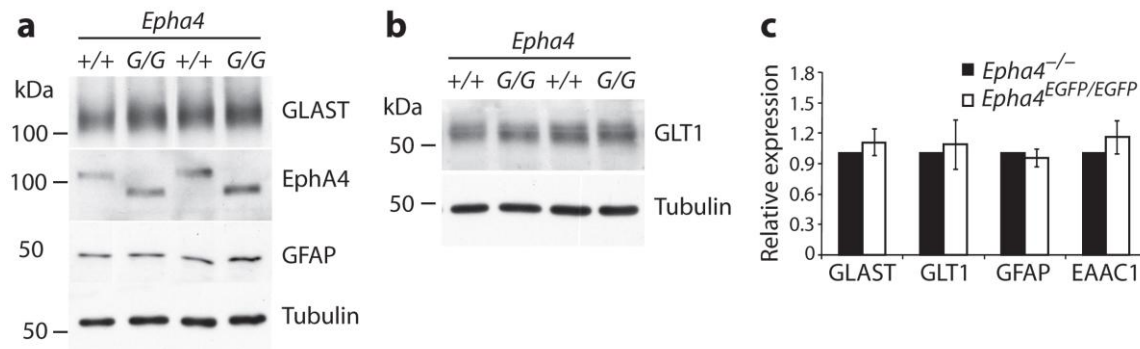


Figure 2.13 The EphA4 cytoplasmic domain is dispensable for regulating GLAST and GLT1 abundance. **(a,b)** Western blot analysis of hippocampal protein lysates from *Epha4*^{EGFP/EGFP} and *Epha4*^{+/+} mice for their content of GLAST, GLT1, GFAP, EphA4 and tubulin. **(c)** Bar graph depicting relative abundance of GLAST, GLT1, GFAP and EAAC1 calculated as in Figure 2.12c ($n = 7-9$ mice per group, $P > 0.3$, t -test). Error bars, s.e.m. Data were generated by S. Paixao.

2.11 Increased glutamate uptake in *Efna3*^{-/-} astrocytes

The upregulation of glial glutamate transporter abundance observed in *Epha4* and *Efna3* mutant mice (this study and (Carmona et al., 2009)) may result in increased glutamate uptake in astrocytes. To test this possibility, whole-cell patch-clamp recordings from astrocytes in *stratum radiatum* of *Efna3*^{-/-} acute hippocampal slices were performed. Sodium inward currents associated with glutamate uptake in astrocytes were evoked by endogenous release of glutamate from presynaptic boutons following stimulation of Schaffer collaterals. The mean peak amplitude of normalized transporter currents in response to single pulse stimulation was significantly higher in *Efna3*^{-/-} mice than in littermate controls (figure 2.14a,b). Notably, similar results were obtained with a TBS protocol (figure 2.14c-e) which had produced a much reduced LTP in *Efna3*^{-/-} mice.

These results indicated that glutamate uptake in response to a single stimulus or a TBS protocol is significantly increased in astrocytes lacking ephrinA3.

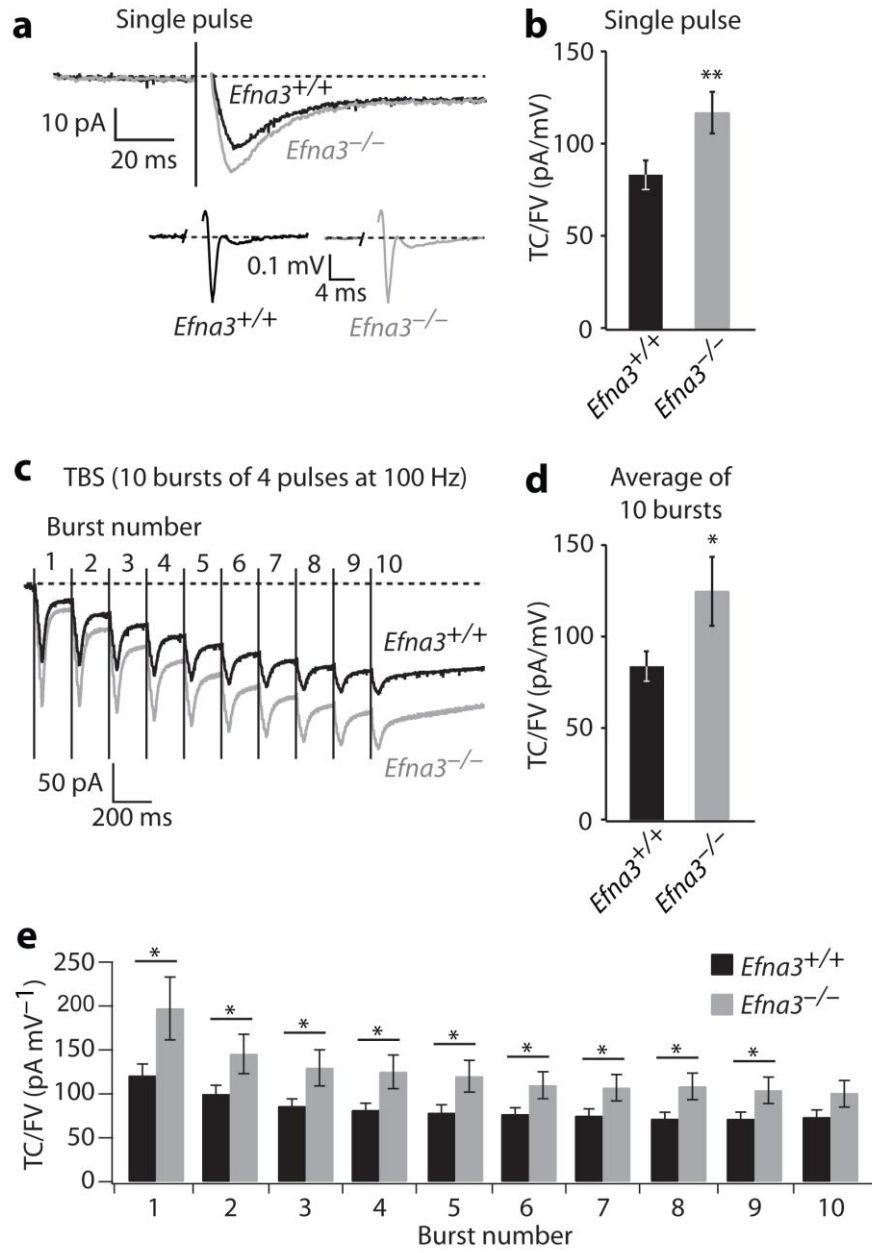


Figure 2.14 (previous page) Increased astrocytic glutamate transporter currents in *Efna3*^{-/-} mice. **(a)** Mean inward currents in response to a single pulse stimulation of Schaffer collaterals in *Efna3*^{+/+} (black) and *Efna3*^{-/-} mice (gray). Inset: mean fiber volleys (FV) in *Efna3*^{+/+} (black) and *Efna3*^{-/-} (gray) mice. **(b)** Bar graph depicting mean glutamate transporter current amplitudes (TC), divided by the amplitude of the corresponding FV to normalize for the numbers of fibers activated. Transporter currents in *Efna3*^{-/-} mice were significantly higher than in *Efna3*^{+/+} controls in response to a single pulse stimulation (117.7 ± 11.1 pA mV⁻¹ in mutants, $n = 42$ recordings, 20 cells; 95.7 ± 8.9 pA mV⁻¹ in *Efna3*^{+/+} controls, 34 recordings, 17 cells; ** $P = 0.01$, *t*-test) **(c)** Mean inward currents in response to TBS in *Efna3*^{+/+} (black) and *Efna3*^{-/-} mice (gray). Traces are averages from all stimulations performed. **(d)** Bar graph showing mean normalized TC amplitudes in response to TBS (124.8 ± 18.8 pA mV⁻¹ in mutants, $n = 20$ measurements, 15 cells; 83.5 ± 8.5 pA mV⁻¹ in *Efna3*^{+/+} controls, $n = 18$ measurements, 10 cells; * $P = 0.03$, *t*-test). **(e)** Bar chart representing average normalized TC amplitudes in response to each of the ten bursts. Current amplitudes were significantly higher in *Efna3*^{-/-} mice compared to *Efna3*^{+/+} controls in 9 out of 10 bursts (* $P < 0.05$, *t*-test). Stimulation artifacts in **a** and **c** were replaced by a vertical line indicating the start of the stimulation. Error bars, s.e.m. Data were generated by Silke Honsek under the supervision of Christine Rose.

2.12 Low glutamate concentration near synapses in *Epha4*^{-/-} mice

Elevated levels of glutamate transporters in astrocytes may decrease glutamate levels in proximity of synapses. To estimate synaptic glutamate concentrations, I performed whole-cell patch-clamp recordings of CA1 pyramidal cells in acute hippocampal slices in presence of the low affinity competitive AMPA receptor antagonist γ -D-glutamylglycine (γ -DGG). γ -DGG binds non-NMDA receptors with low affinity and with rapid dissociation kinetics comparable to the dissociation kinetics of synaptically released glutamate (Liu et al., 1999; Oliet et al., 2001). Thus, the degree of inhibition by γ -DGG is sensitive to the concentration of glutamate. If less glutamate is present, the inhibition by γ -DGG is stronger. Whole-cell patch-clamp recordings revealed normal frequencies and average amplitude of mEPSCs in *Epha4*^{-/-} mice compared to *Epha4*^{+/+} controls (figure

2.15a-e), confirming that basal synaptic transmission was not altered in these mutants. γ -DGG (1 mM) reduced the amplitude of mEPSCs in *Epha4*^{-/-} slices more than the amplitude of mEPSCs in *Epha4*^{+/+} control slices (figure 2.15f), indicating that the levels of glutamate near synapses in *Epha4*^{-/-} slices were reduced.

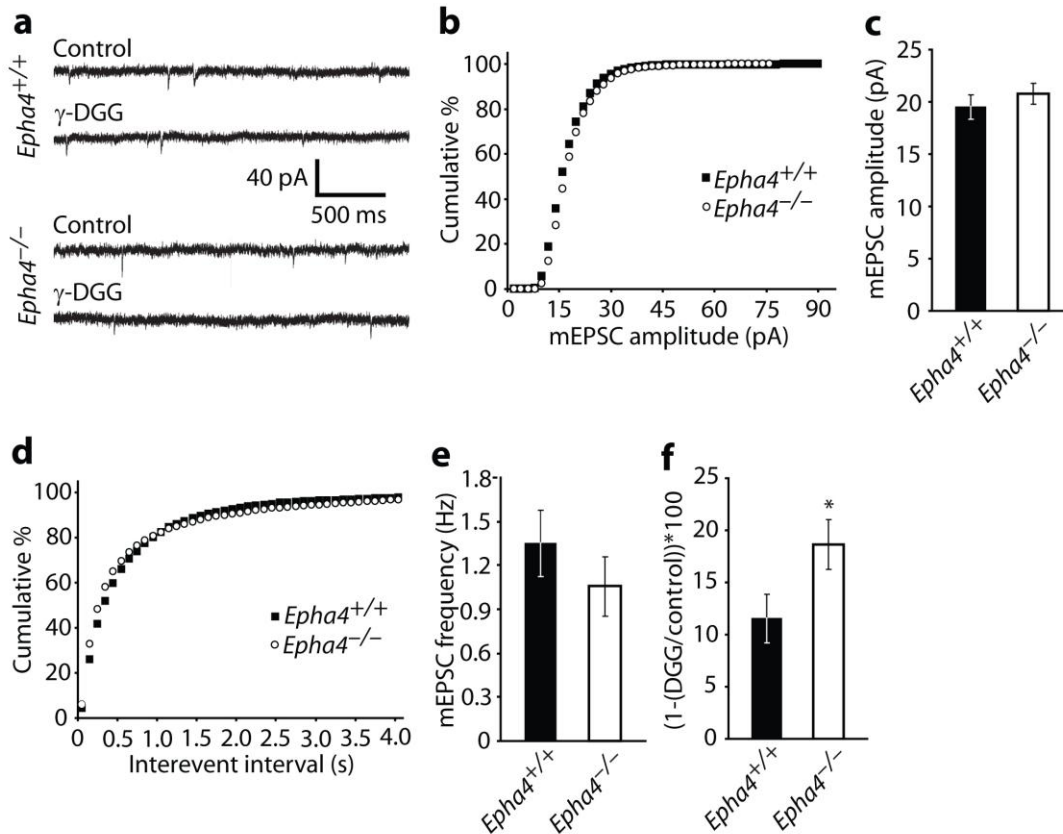


Figure 2.15 Reduced glutamate concentration near synapses in *Epha4*^{-/-} mice. (a) Representative traces of mEPSCs in *Epha4*^{+/+} and *Epha4*^{-/-} mice in absence and presence of 1 mM γ -DGG. (b,c) Graphs depicting cumulative distribution (b) or average (c) of mEPSC amplitudes show no alterations in *Epha4*^{-/-} mice compared to controls (b: $P = 0.6$, two sample KS test; c: $P = 0.4$, t -test; $n=13$ mice per group). (d,e) Graphs showing cumulative distribution of interevent intervals (d) or average frequency (e) of mEPSCs reveal no alterations in *Epha4*^{-/-} mice compared to controls (d: $P = 0.4$, two sample KS test; e: $P = 0.3$, t -test; $n=13$ mice per group). 97% of the total events are represented in (d). (f) Inhibitory effect of γ -DGG on mean mEPSCs amplitude in *Epha4*^{-/-} mice and controls ($18.6\% \pm 2.4\%$ versus $11.6\% \pm 2.3\%$, * $P = 0.04$, t -test; $n = 13$ mice per group). Error bars, s.e.m.

These results suggested that clearance of glutamate near synapses is more efficient in *Epha4* mutants than in control mice, most likely because of the increased amount of glial glutamate transporters in the hippocampus of these mice.

2.13 Reduced neuronal depolarization during high frequency stimulation in *Epha4* and *Efna3* mutants

I showed that elevated abundance of GLAST and GLT1 in *Epha4* and *Efna3* mutants does not alter basal synaptic transmission. However, the increased glutamate uptake by astrocytes may cause insufficient postsynaptic depolarization during high frequency stimulation protocols used to induce LTP. In this case the abundance and activity of glutamate transporters may be important to control the amount of glutamate that escapes from the synaptic cleft and activates peri- and

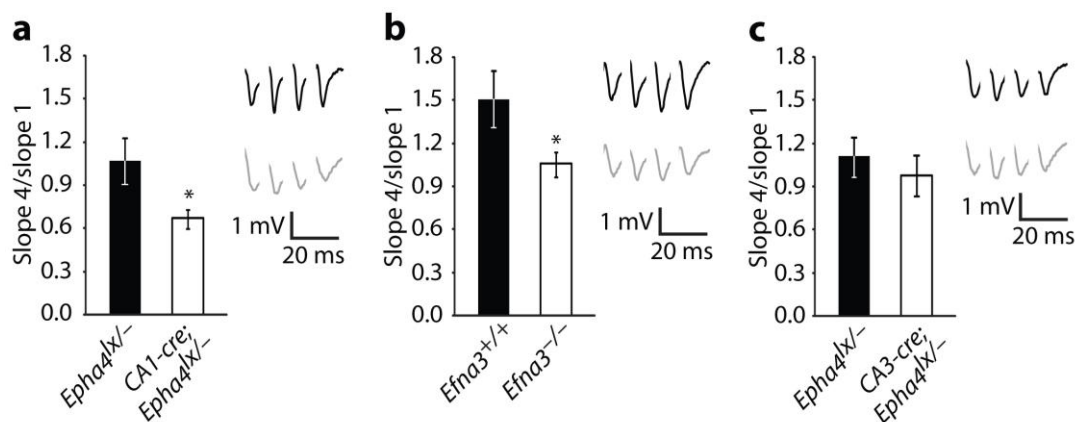


Figure 2.16 Decreased neuronal depolarization during high frequency stimulation in *Epha4* and *Efna3* mutants. (a-c) Bar graphs depicting fEPSP slope 4/slope 1 ratios during a train of four stimuli at 100 Hz (0.67 ± 0.07 in *CA1-cre;Epha4^{lox/-}*, $n = 12$ slices, 7 mice; 1.07 ± 0.16 in *Epha4^{lox/-}*, $n = 14$ slices, 7 mice; * $P = 0.03$; 1.06 ± 0.09 in *Efna3^{-/-}*, $n = 14$ slices, 9 mice; 1.51 ± 0.2 in *Efna3^{+/+}*, $n = 13$ slices, 9 mice; * $P = 0.05$; 0.98 ± 0.14 in *CA3-cre;Epha4^{lox/-}*, $n = 9$ slices, 6 mice; 1.12 ± 0.13 in *Epha4^{lox/-}*, $n = 10$ slices, 6 mice; $P = 0.5$, t -test). Insets: traces from one representative train in controls (black) and mutants (gray). Stimulation artifacts were removed. Error bars, s.e.m.

extrasynaptic glutamate receptors involved in modulation of neuronal excitability and LTP (Lu et al., 1997; Mulholland et al., 2008). Therefore, I analyzed fEPSPs during high frequency stimulation in the *stratum radiatum* of CA1 region of *EphA4* and *Efna3* mutants. fEPSP slopes at the end of the first train of each TBS were significantly reduced in *CA1-cre;Epha4^{lox/-}* and *Efna3^{-/-}* mice compared to those in their respective controls (figure 2.16a,b). Postsynaptic depolarization was instead not altered in *CA3-cre;Epha4^{lox/-}* mice (figure 2.16c) that had showed normal TBS-induced LTP (Figure 2.7c).

These results demonstrated that neuronal depolarization during high frequency stimulation is reduced in *CA1-cre;Epha4^{lox/-}* and *Efna3^{-/-}* mice, most likely as a consequence of the upregulation of glial glutamate transporters.

2.14 Blockade of glutamate transport rescues LTP defects in *EphA4* and *Efna3* mutants

Enhanced clearance of synaptic glutamate by astrocytes is possibly the direct cause of the reduced LTP in *Epha4* and *Efna3* mutant mice. To confirm this hypothesis I analyzed the effects of blocking glutamate uptake on LTP by using (2S, 3S)-3-{3-[4-(trifluoromethyl) benzoylamino]benzyloxy} aspartate (TFB-TBOA), a non-transportable inhibitor that has higher affinity for GLT1 and GLAST than for the neuronal transporter EAAC1 (Tsukada et al., 2005). If the LTP impairments were due to glutamate transporter upregulation, TFB-TBOA should rescue the LTP defects and the difference between mutants and control littermates should disappear. Indeed, the application of three TBSs in presence of TFB-TBOA induced similar amounts of synaptic potentiation in *CA1-cre;Epha4^{lox/-}* and *Efna3^{-/-}* mice compared to their respective controls (figure 2.17a,b). Accordingly, the presence of TFB-TBOA also allowed normal postsynaptic depolarization during high frequency stimulation (figure 2.17c,d). Normal TBS-induced LTP in *CA1-cre;Epha4^{lox/-}* and *Efna3^{-/-}* mice was also observed when the broad-spectrum glutamate transporter

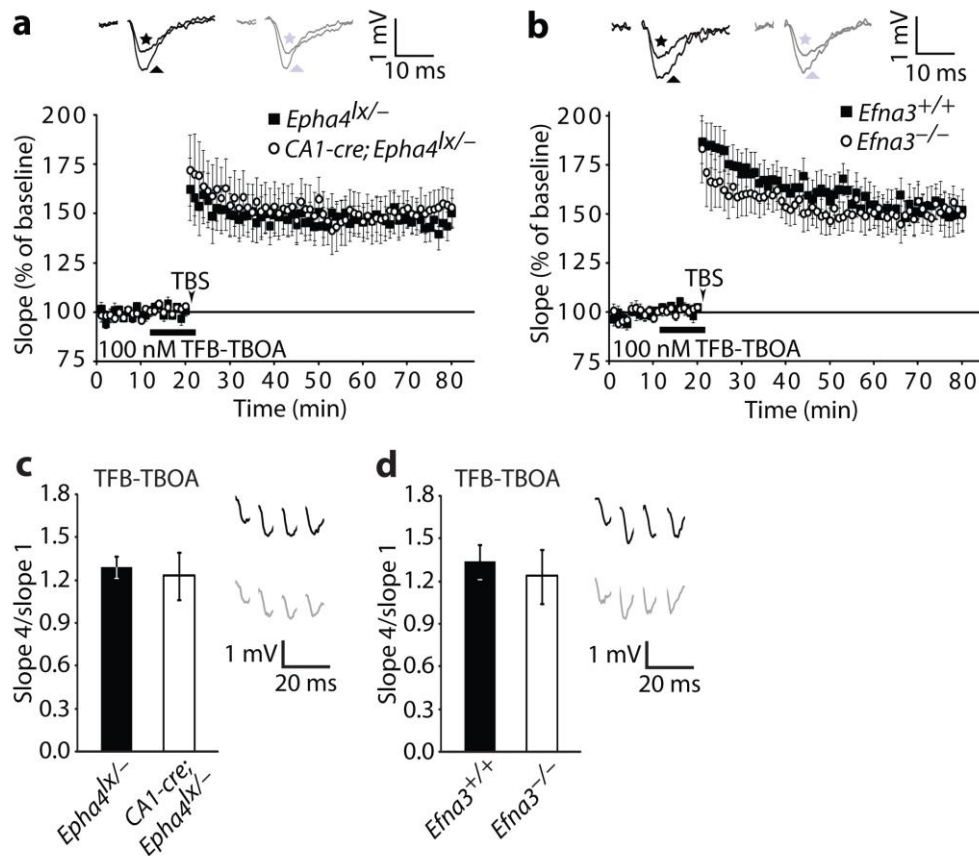


Figure 2.17 Rescue of LTP defects in presence of the glutamate transporter inhibitor TFB-TBOA. (a,b) TBS-induced LTP in presence of TFB-TBOA (black bar; applied 8 min before TBS and washed out 2 min after) in *CA1-cre;Epha4^{lox/-}* (a) and *Efna3^{-/-}* (b) mice and respective controls ($153.5 \pm 9.1\%$ in *CA1-cre;Epha4^{lox/-}*, $n = 9$ slices, 7 mice; $145.2 \pm 6.7\%$ in *Epha4^{lox/-}*, $n = 10$ slices, 7 mice, $P = 0.6$; $152.6 \pm 7.6\%$ in *Efna3^{-/-}*, $n = 11$ slices, 9 mice; $149.9 \pm 10.1\%$ in *Efna3^{+/+}*, $n = 10$ slices, 9 mice, at 55–60 min after stimulus, $P = 0.8$, t -test) Insets: representative traces from controls (black) and mutants (gray) recorded before (stars) and 55–60 min after (triangles) LTP induction. (c,d) Histograms depicting fEPSP slope 4/slope 1 ratios during a train of four stimuli at 100 Hz (slope 4/slope 1: 1.23 ± 0.16 in *CA1-cre;Epha4^{lox/-}*, $n = 9$ slices, 7 mice versus 1.30 ± 0.08 in *Epha4^{lox/-}*, $n = 13$ slices, 7 mice, t -test, $P = 0.7$; 1.24 ± 0.19 in *Efna3^{-/-}*, $n = 12$ slices, 8 mice versus 1.34 ± 0.12 in *Efna3^{+/+}*, $n = 11$ slices, 8 mice, t -test, $P = 0.7$). Insets: traces from one representative train in controls (black) and mutants (gray). Stimulation artifacts were removed. Error bars, s.e.m.

inhibitor L-trans-pyrrolidine-2,4-dicarboxylic acid (tPDC) (Beart and O'Shea, 2007) was used instead of TFB-TBOA (figure 2.18).

These results suggested that the impaired LTP observed in *CA1-cre;Epha4^{lx/-}* and *Efna3^{-/-}* mice is largely due to the reduced levels of glutamate near synapses during high frequency stimulation, caused by increased glutamate uptake by astrocytes.

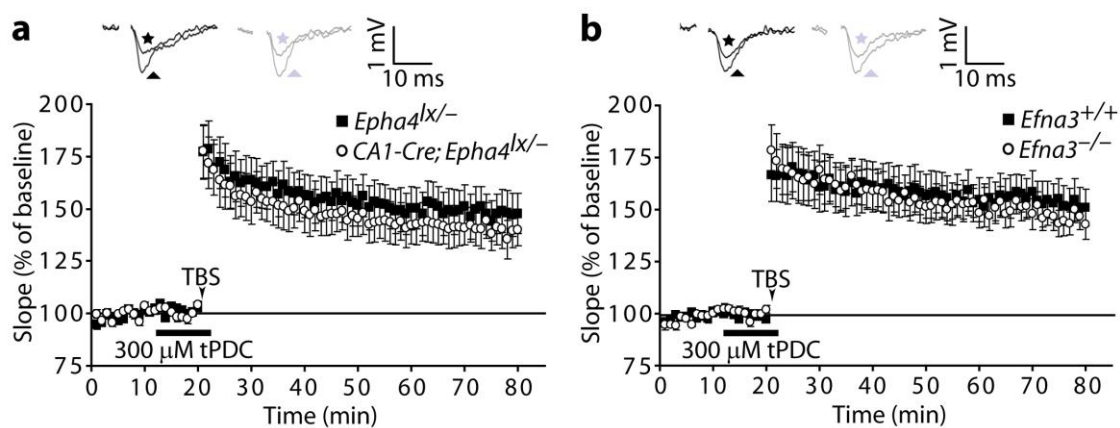


Figure 2.18 Rescue of LTP defects in presence of the broad spectrum glutamate transporter inhibitor tPDC. **(a,b)** TBS-induced LTP in presence of tPDC (black bar; applied 8 min before TBS and washed out 2 min after) in *CA1-cre;Epha4^{lx/-}* **(a)** and *Efna3^{-/-}* **(b)** mice and respective controls (139.3 ± 8.4 % in *CA1-Cre; Epha4^{lx/-}*, $n=13$ slices, 9 mice versus 147.9 ± 9.9 % in *Epha4^{lx/-}*, $n=12$ slices, 9 mice, t -test, $P = 0.5$, t -test; 147.5 ± 6.3 % in *Efna3^{-/-}*, $n=12$ slices, 9 mice versus 154.0 ± 9.6 % in *Efna3^{+/+}*, $n=13$ slices, 9 mice, t -test, $P = 0.6$, at 55-60 minutes after TBS). Insets: representative traces from controls (black) and mutants (gray) recorded before (stars) and 55-60 min after (triangles) LTP induction. Error bars, s.e.m.

2.15 Transgenic mice overexpressing ephrinA3 in astrocytes

To obtain further support for ephrinA3 directly regulating the levels of glial glutamate transporters, two independent transgenic lines (Tg181 and Tg7047) overexpressing ephrinA3 (fused to an hemagglutinin (HA) epitope tag) in glial cells

using the glial specific *Gfap* promoter (Nolte et al., 2001) were generated. Immunostaining of P30-60 brain sections from Tg181 mice with an anti-HA antibody revealed the typical scattered distribution expected for astrocytes (figure 2.19a,b). Similar results were obtained with Tg7047 mice (Filosa et al., 2009). HA-ephrinA3 localization in fine processes of astrocytes was confirmed by colocalization of HA-ephrinA3 with GFP in hippocampi of TG181;*Gfap-GFP* mice (Nolte et al., 2001) (figure 2.19c-f).

These results demonstrated that specific overexpression of ephrinA3 in astrocytes could be achieved with the transgenic lines Tg181 and Tg7047.

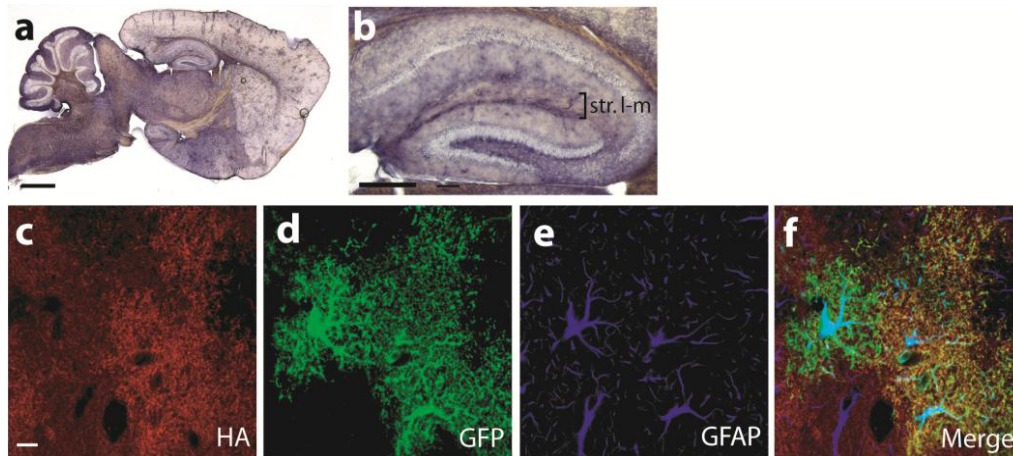


Figure 2.19 Transgenic mice overexpressing ephrinA3 in astrocytes. **(a,b)** Anti-HA immunohistochemistry on brain slices from Tg181 mice. **b** is a high magnification picture of the hippocampus displayed in **a**. **(c-f)** Confocal images of hippocampal sections from adult Tg181 mice crossed to a *Gfap-GFP* reporter line. Triple labeling for the indicated proteins revealed colocalization of HA with GFP but not with the cytoplasmic marker GFAP **(f)**, indicating that the transgenic protein is expressed in fine processes of astrocytes. Scale bars: **a**, 1 mm; **b**, 300 μ m; **c-f**, 10 μ m. Data were generated by S. Paixao.

2.16 EphrinA3 overexpression in astrocytes reduces glial glutamate transporter abundance

To investigate the effects of overexpression of ephrinA3 in astrocytes on GLAST and GLT1 abundance, hippocampal sections from Tg181 mice were co-stained with anti-HA and anti-GLAST or anti-GLT1 antibodies (figure 2.20a-c, e-g). Areas of high, medium and low HA immunoreactivities were selected and average pixel intensities were compared to glial glutamate transporter immunostaining intensities. A clear inverse correlation was observed between HA and GLAST or GLT1 abundance (figure 2.20d,h). Indeed, areas expressing the highest levels of HA-ephrinA3 had significantly lower amounts of GLAST and GLT1. Similar reductions of glial glutamate transporter abundance were also observed in line Tg7047 which expressed lower levels of transgenic ephrinA3 than line Tg181 (Filosa et al., 2009), indicating that the phenotypes observed in Tg181 mice were not due to positional effects of the transgene and suggesting that modest overexpression of ephrinA3 is sufficient to reduce glial glutamate transporter expression.

These results clearly indicated that ephrinA3 in astrocytes negatively controls glial glutamate transporter abundance.

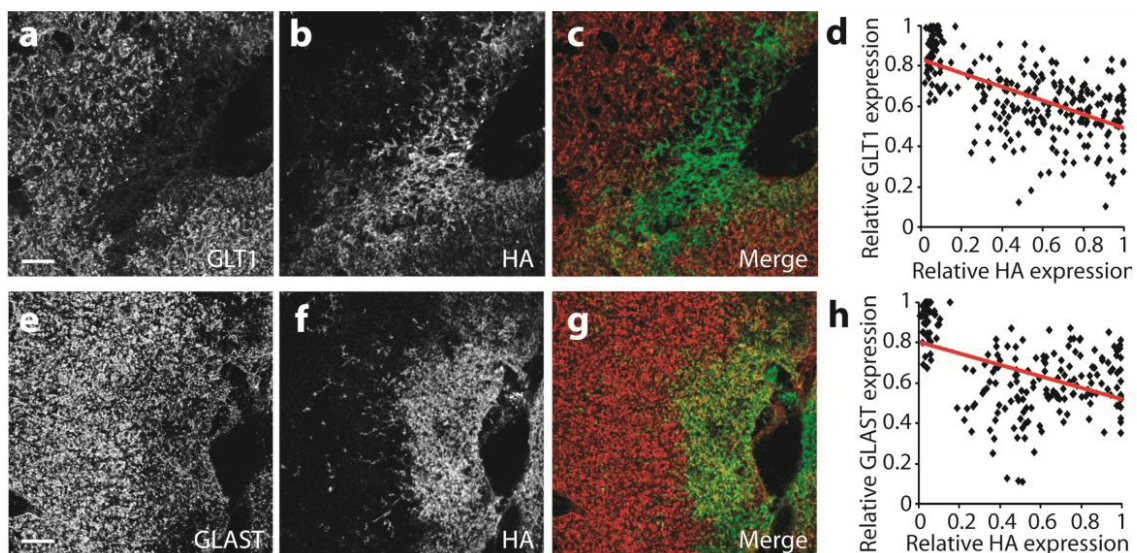


Figure 2.20 (previous page) EphrinA3 overexpression in astrocytes reduces abundance of glial glutamate transporters. **(a-c, e-g)** Single plane confocal images showing double immunofluorescence labeling for GLT1 and HA **(a-c)** and GLAST and HA **(e-g)** in the *stratum lacunosum-moleculare* of hippocampal sections obtained from Tg181 mice. Expression of GLT1 and GLAST (red) are reduced in areas where the levels of transgenic HA-ephrinA3 (HA, green) are high. Scale bars, 10 μm . **(d,h)** Scatter plots showing the negative correlation between GLT1 and HA **(d)** and GLAST and HA **(h)** relative pixel intensities (GLT1 and HA correlation factor = -0.58 , $n = 280$ regions, 3 mice; GLAST and HA correlation factor = -0.46 , $n = 198$ regions, 3 mice, t -test, $P < 0.0001$). Red lines in the scatter plots represent linear regression. Data were generated by S. Paixao.

2.17 EphrinA3 overexpression in astrocytes causes excitotoxicity and increases seizure susceptibility

Reduction of glial glutamate transporters has previously been shown to increase synaptic glutamate concentrations and to cause neurodegeneration (Rothstein et al., 1996; Tanaka et al., 1997). Indeed, excessive amount of extracellular glutamate causes excitotoxicity, manifested as formation of dendritic focal swellings and spine loss, followed by neuronal death (Greenwood and Connolly, 2007). Therefore, mice overexpressing ephrinA3 in astrocytes may have signs of excitotoxicity. To analyze neuronal morphology in ephrinA3 transgenic mice, intercrosses of Tg181 with a transgenic line (GFP-M) which expresses GFP in small neuronal subsets (Feng et al., 2000) were performed. CA1 pyramidal cells from P29-31 Tg181 mice showed focal dendritic swellings that were not present in neurons of wild type controls (figure 2.21a,b), with variable penetrance possibly due to variable expression of the transgene.

Deficiency in glial glutamate transporters has been associated also with epilepsy (Beart and O'Shea, 2007; Maragakis and Rothstein, 2004). For example, elimination of GLT1 or GLAST in mice results in increased sensitivity to pentylenetetrazole (PTZ)-induced seizures (Tanaka et al., 1997; Watase et al.,

1998). To verify whether ephrinA3 transgenic mice were more prone to seizures, PTZ (45 mg per kg body weight) was injected intraperitoneally and the behavior of the mice was monitored. Seizure severity was categorized in four phases, according to (Weiergraber et al., 2006). Phase 1 represents a non-convulsive state

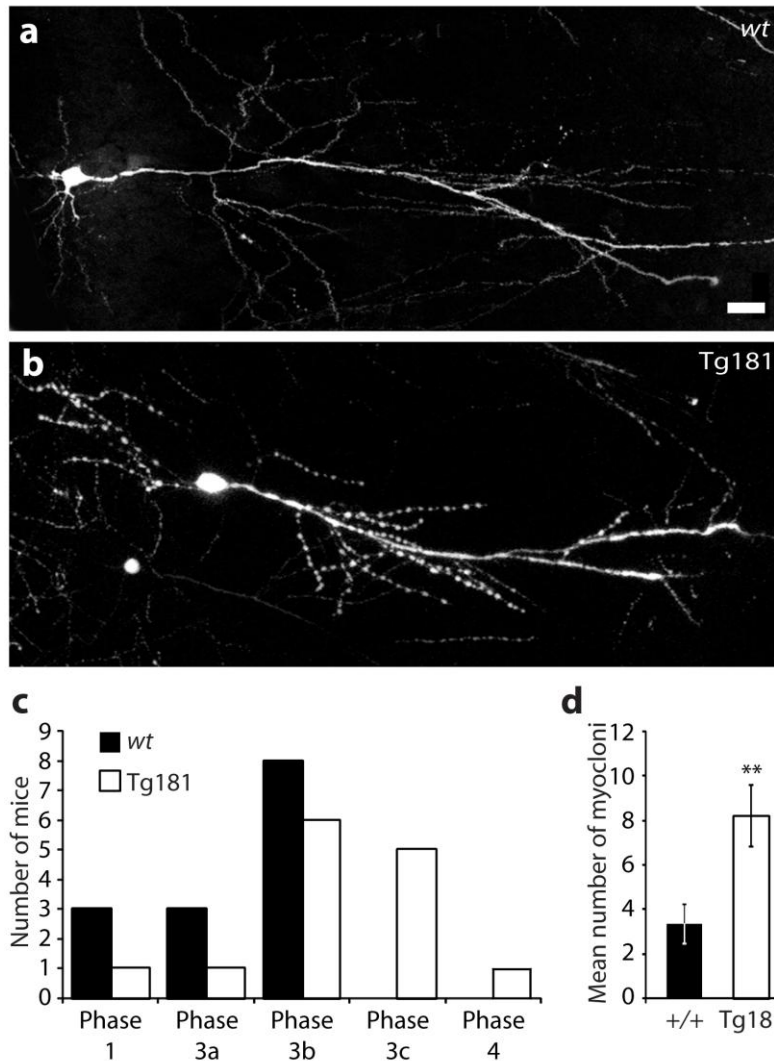


Figure 2.21 EphrinA3 overexpression in astrocytes causes excitotoxicity and increases susceptibility to seizures. (a,b) Confocal images of CA1 pyramidal neurons from wild type (wt, a) and Tg181 (b) mice crossed to GFP-M mice. Focal dendritic swellings are clearly visible in b. Scale bar, 50 μ m. (c) Bar graph showing PTZ-induced seizure severity distribution, depicted as maximal phase reached after intraperitoneal injection of PTZ, in Tg181 and wt mice. Seizure severity was higher in Tg181 mice than in wt controls ($n = 14$ mice per group, $P = 0.01$, Mann-Whitney U -test). (d) Bar graph showing mean number of whole body myocloni in phase 3 after injection of PTZ (3.4 ± 0.8 in wt mice; 8.3 ± 1.4 in Tg181 mice, $n = 12$ mice per group; t -test, $** P = 0.009$). Error bars, s.e.m. Data showed in a,b were generated by S. Paixao. Data depicted in c,d were generated by Lore Becker and Berend Feddersen under the supervision of Thomas Klopstock.

graph showing mean number of whole body myocloni in phase 3 after injection of PTZ (3.4 ± 0.8 in wt mice; 8.3 ± 1.4 in Tg181 mice, $n = 12$ mice per group; t -test, $** P = 0.009$). Error bars, s.e.m. Data showed in a,b were generated by S. Paixao. Data depicted in c,d were generated by Lore Becker and Berend Feddersen under the supervision of Thomas Klopstock.

with reduced motor activity and flat position of the body; phase 3b is characterized by whole body myocloni with loss of upright position; phase 3c involves complete loss of motor control with wild jumping; phase 4 is characterized by generalized tonic-clonic seizures often associated with death due to respiratory insufficiency. Interestingly, Tg181 mice displayed increased seizure severity (figure 2.21c) and more whole-body myocloni (figure 2.21d) after application of PTZ compared to controls.

Taken together, these results suggested that overexpression of ephrinA3 in astrocytes causes excitotoxicity and exacerbation of PTZ-induced seizures, most likely due to downregulation of glial glutamate transporters.

3

Discussion

In the last two decades astrocytes have emerged as key regulators of synaptic function. Presynaptic bouton, postsynaptic spine and astrocytic process constitute a functional unit and the three elements constantly communicate with each other. The molecular mechanisms underlying this crosstalk are only partially known. Astrocytes can detect the release of neurotransmitters from the presynaptic bouton through receptors present on their surface and, in turn, can alter presynaptic and postsynaptic activity by releasing gliotransmitters. While there is good knowledge of the mechanisms used by the presynaptic bouton to influence astrocyte physiology and the signaling systems used by astrocytes to control pre- and postsynaptic functions, communication between dendritic spines and astrocytes is poorly understood.

The results presented here show a new mechanism by which the postsynaptic spine influences physiology of astrocytes and how these changes, in turn, modulate neuronal plasticity. EphA4 in pyramidal cells in CA1 region of the hippocampus binds astrocytic ephrinA3 and triggers a signaling cascade into the astrocyte that negatively controls the abundance of glial glutamate transporters (figure 3.1). Mice lacking EphA4 in CA1 pyramidal cells or ephrinA3 have increased abundance of glial glutamate transporters (this study and Carmona et al., 2009), glutamate is more efficiently removed during high frequency stimulation and the concentration of glutamate near the synapse is reduced (figure 3.1). As a consequence postsynaptic depolarization is attenuated and LTP is partially impaired, most likely because of limited activation of peri- and/or extrasynaptic glutamate receptors. Acute pharmacological inhibition of glutamate uptake allows normal postsynaptic depolarization and rescues the LTP defect present in *Epha4* and *EfnA3* mutant mice. These results agree with previous reports showing that the neuronal glutamate transporter EAAT4 controls long term synaptic plasticity in the cerebellum by regulating the activation of perisynaptic mGluRs (Brasnjo and Otis, 2001; Wadiche and Jahr, 2005). On the other hand, overexpression of ephrinA3 in astrocytes causes excitotoxicity and increases susceptibility to seizures, because of reduced

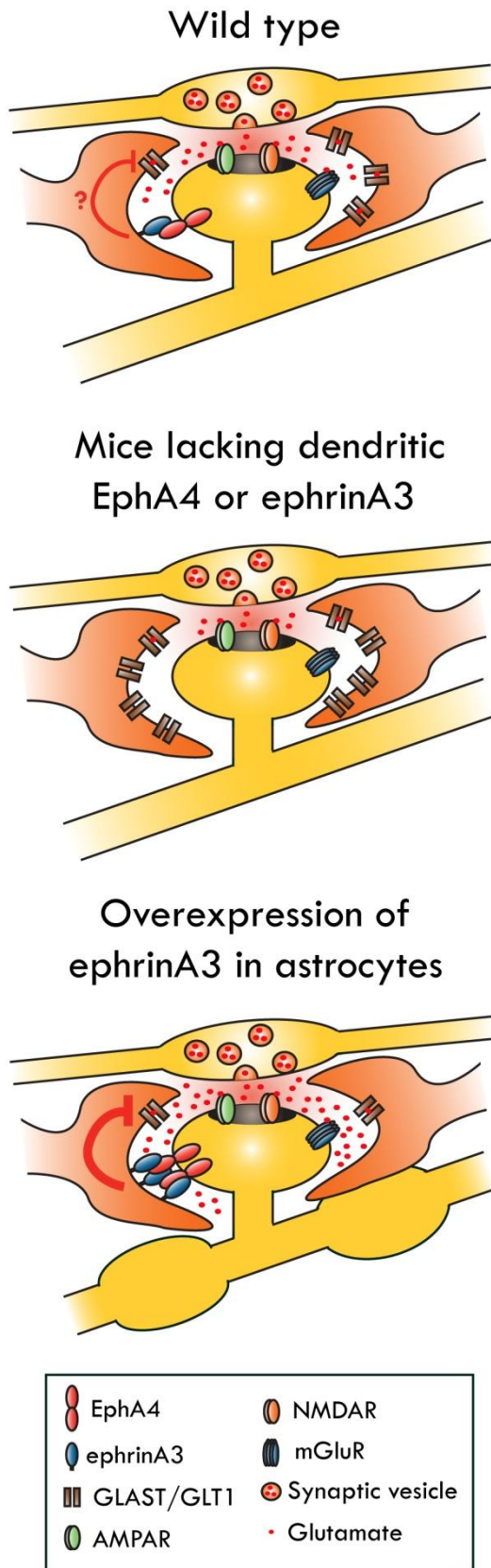


Figure 3.1 Model describing the function of EphA4-ephrinA3 interaction at the neuro-glia interface. Top: the binding between EphA4 in the dendritic spine (yellow) and ephrinA3 on the astrocytic process (orange) triggers a negative signal into the astrocyte that reduces abundance of GLAST and GLT1. The signaling pathway does not converge on transcriptional regulation systems and its specific nature is still unknown. Center: in absence of dendritic EphA4 or ephrinA3 the negative pathway controlling GLAST and GLT1 abundance is not present and glial glutamate transporters are upregulated. This causes enhanced glutamate uptake by astrocytes that leads to lower concentration of glutamate near the synapse, reduced postsynaptic depolarization during high frequency stimulation and impaired LTP. Bottom: Overexpression of ephrinA3 in astrocytes reduces the abundance of GLAST and GLT1, causing neurodegeneration (focal dendritic swellings) and increasing seizure susceptibility, possibly because of elevated concentration of extracellular glutamate.

abundance of glial glutamate transporters and, most likely, increased concentration of extracellular glutamate (figure 3.1).

Considering all the data together a general model emerges in which EphA4-ephrinA3 interaction at the neuro-glia interface controls a wide spectrum of events: physiological regulation of EphA4-ephrinA3 signaling modulates induction and/or expression of long term synaptic plasticity; shifting the balance toward unphysiological activation of this signaling pathway causes pathological damage to the CNS.

3.1 Postsynaptic EphA4 modulates LTP at the CA3-CA1 synapse

EphA4 is present in both pre- and postsynaptic compartments at the CA3-CA1 synapse (Tremblay et al., 2007). However, I found that only postsynaptic EphA4 modulates LTP. The processes of astrocytes can contact both the presynaptic bouton and the postsynaptic spine (Ventura and Harris, 1999). Therefore, in principle, also presynaptic EphA4 should be able to bind to astrocytic ephrinA3. However, glial coverage at hippocampal synapses is asymmetric, with three to four fold more glial contact with spines compared to presynaptic boutons (Lehre and Rusakov, 2002). It follows that postsynaptic EphA4 is potentially more effective in interacting with ephrinA3 present on astrocytes. Moreover, EphA4 is usually localized only in the presynaptic bouton or only in the dendritic spine and rarely in both compartments at the same synapse (Tremblay et al., 2007). Since a significant fraction of synapses in CA1 are not contacted by astrocytic processes (Ventura and Harris, 1999), EphA4 pre- or postsynaptic localization could be correlated with the astrocyte coverage of the synapse, with presynaptic EphA4 enriched at synapses without astrocyte coverage where it could be involved in other functions.

3.2 EphA4 and ephrinBs promotes LTP through different mechanisms

The finding that postsynaptic EphA4 modulates LTP at the CA3-CA1 synapse argues against the previously proposed model in which presynaptic EphA4 activates ephrinB reverse signaling in the postsynaptic spine (Grunwald et al., 2004). Therefore, the modulation of LTP by ephrinB reverse signaling is most likely independent of EphA4 action. Presynaptic EphB receptors could be responsible for activating ephrinBs in the postsynaptic spine (Grunwald et al., 2001).

Alternatively, ephrinBs and EphA4 could modulate synaptic plasticity by interacting in cis in the postsynaptic membrane. However, this is an unlikely scenario for two reasons. First, the only cis interaction between an Eph receptor and an ephrin that has been described so far leads to inhibition of the receptor forward signaling (Carvalho et al., 2006). Instead, in the situation described here the cis interaction should activate ephrinB reverse signaling since *Efnb2* and *Efnb3* mutant mice display impaired LTP at the CA3-CA1 synapse (Bouzioukh et al., 2007; Grunwald et al., 2004). Second, *Efnb2* mutants display LTP defects following application of both TBS and tetanus (Bouzioukh et al., 2007), while here I showed that only TBS-induced LTP is impaired in *Epha4* mutant mice.

EphA4 promotes also LTD in a forward signaling independent manner (Grunwald et al., 2004). It is possible that EphA4 regulates LTP and LTD with different mechanisms and presynaptic EphA4 could be important for promoting LTD by activating postsynaptic ephrinB reverse signaling. It will be crucial to analyze LTD in *Efna3* null mutants to verify this hypothesis. If *Efna3* mutants will show normal LTD, EphA4 must regulate LTP and LTD through divergent mechanisms.

3.3 LTP induced by diverse stimulation patterns is differently affected by EphA4-ephrinA3 signaling

Epha4 and *Efna3* mutant mice display defective LTP when induced with TBS but not with tetanus. This difference could be explained by the kinetic properties of glutamate uptake. The tetanic stimulation utilized in the experiments described here consists of 100 stimuli given at a frequency of 100 Hz. TBS is characterized by short bursts (four stimuli) of high frequency stimulation separated by 160 ms intervals. The increased abundance of glial glutamate transporters in *Epha4* and *Efna3* mutants could affect clearance of glutamate released in response to short bursts of stimuli applied during TBS, but could not be sufficient to significantly alter the dynamics of glutamate released during longer trains of stimuli, such as in case of a tetanus (Diamond and Jahr, 2000). The finding that glutamate uptake during TBS is more efficient in astrocytes lacking ephrinA3 than in controls supports this hypothesis.

3.4 Does EphA4-ephrinA3 interaction control metaplasticity?

The increased glutamate uptake from astrocytes and the potentially reduced activation of perisynaptic glutamate receptors in *Epha4* and *Efna3* mutants could have more profound effects on modulation of long term synaptic plasticity. EphA4-ephrinA3 interaction could contribute to metaplastic control of the system by regulating intrinsic neuronal excitability and thereby changing the threshold for LTP induction. It has been shown that activation of perisynaptic mGluRs controls metaplasticity at the CA3-CA1 synapse (Ireland and Abraham, 2002; van Dam et al., 2004), possibly by affecting phosphorylation and surface expression of voltage-gated potassium channels (Hu et al., 2007; Kim et al., 2007). This type of regulation could affect the overall excitability of the neuron or could be limited to specific dendritic branches. Experiments are under way to investigate a possible

link between regulation of glial glutamate transporter abundance, activation of mGluRs and regulation of intrinsic neuronal excitability in *Epha4* and *Efna3* mutant mice.

3.5 Does EphA4-ephrinA3 interaction regulate plasticity of glutamate uptake?

The data presented here demonstrate that neuronal control of glial glutamate uptake can modulate long term synaptic plasticity at the CA3-CA1 synapse. These findings are consistent with previous observations showing that changes in glutamate uptake parallel changes in synaptic strength in both vertebrates and invertebrates (Genoud et al., 2006; Levenson et al., 2002; Pita-Almenar et al., 2006). For example, LTP induction at the CA3-CA1 synapse has been shown to trigger long term enhancement of glial glutamate uptake through increased expression of GLT1 via a PKA-dependent mechanism (Pita-Almenar et al., 2006). EphA4-ephrinA3 signaling is an excellent candidate for mediating regulation of glial glutamate uptake by neuronal activity. EphA4 in the dendritic spine, by binding ephrinA3 on astrocytes, possibly keeps the abundance of glial glutamate transporters at a relatively low level. Induction of LTP could induce a reduction of binding between EphA4 and ephrinA3, for example by triggering internalization of the receptor or by promoting the binding of antagonists to EphA4. This mechanism could potentially lead to synaptic-specific enhancement of glial glutamate uptake.

3.6 Possible molecular mechanisms mediating ephrinA3 control of glial glutamate transporter abundance

Activation of ephrinA3 reverse signaling in the astrocyte negatively controls abundance of glial glutamate transporters through a posttranscriptional mechanism

(data presented in this thesis and in Filosa et al., 2009). There are several other mechanisms by which ephrinA3 could control the abundance of glial glutamate transporters. EphrinA3 activation could repress translation of the mRNAs coding for GLAST and GLT1. However, Carmona et al. found that stimulation of ephrinA3 with preclustered EphA receptor fusion proteins in acute hippocampal slices decreases the amount of glial glutamate uptake in only two hours (Carmona et al., 2009). If ephrinA3 controlled translation of glial glutamate transporters, the half life of GLAST and GLT1 must be very short to account for the rapid downregulation of glutamate uptake from astrocytes observed in those experiments. Alternatively, ephrinA3 could control internalization and degradation of the two proteins. It has been shown that activation of different kinases, including PKA, PKC and PI3K can regulate internalization and degradation of glial glutamate transporters (Adolph et al., 2007; Gonzalez and Robinson, 2004; Guillet et al., 2005). EphrinA3 activation by neuronal EphA4 is a potential trigger for these molecular pathways. The involvement of different kinases downstream of ephrinA3 could in the future be demonstrated by analyzing GLAST and GLT1 abundance in acute hippocampal slices after stimulation of ephrinA3 reverse signaling in presence of specific kinase inhibitors.

Another important question to address in the future is how ephrinA3 can induce intracellular signaling into the astrocyte without having a cytoplasmic domain. Two mechanisms have been proposed to be used by GPI-anchored ephrinAs to initiate intracellular signaling cascades: interaction with a transmembrane protein (coreceptor) (Lim et al., 2008b; Marler et al., 2008), similarly to GDNF receptors (Airaksinen and Saarma, 2002); modification of the local physical properties of the plasma membrane that triggers recruitment and activation of Src family kinases (Davy et al., 1999). The first hypothesis could be tested by using a candidate approach analyzing interactions between ephrinA3 and known coreceptors of ephrinAs, or by using unbiased proteomic or cell screening methods. The second hypothesis could be more easily tested by

analyzing abundance of glial glutamate transporters after ephrinA3 activation in presence of Src family kinases inhibitors.

3.7 Could there be a link between synaptic plasticity and dendritic spine morphology defects in *Epha4* and *Efn3* mutant mice?

Activation of EphA4 forward signaling has been shown to regulate dendritic spine morphogenesis (Bourgin et al., 2007; Carmona et al., 2009; Fu et al., 2007; Murai et al., 2003). Since changes of spine morphology are correlated to changes of synaptic strength (Alvarez and Sabatini, 2007), the possibility exists that the LTP defect observed in *Epha4* and *Efn3* mutant mice could be a secondary effect caused by alterations of spine shape. However, the role of EphA4 in LTP is independent of forward signaling (Grunwald et al., 2004) and distinct from its role in spine morphogenesis. Moreover, the *Epha4* conditional knock out described here did not show alterations in spine length, width and density (Sonia Paixao, personal communication), possibly due to the late onset of Cre activity [second postnatal week in the CA1-Cre line (Tsien et al., 1996)]. Therefore, the LTP defect and the alteration of spine morphology are distinct phenotypes and the latter does not influence the former. On the other hand, dendritic spine shape and size are strongly dependent on the strength of synaptic connections (Alvarez and Sabatini, 2007). Thus, defects in long term synaptic plasticity may influence the morphology of dendritic spines in *Epha4* and *Efn3* mutants.

3.8 Does EphA4-ephrinA3 interaction control morphology and/or motility of astrocytic processes?

The small processes of astrocytes that contact synapses are highly motile and the astrocyte coverage of the synapse can vary depending on the activity of neuronal connections and the physiological status of the entire organism (Genoud et al., 2006; Oliet and Piet, 2004). For example, increased synaptic activity in the

barrel cortex of mice produced by sensory stimulation induces an increase of astrocytic envelopment of excitatory synapses (Genoud et al., 2006). In the supraoptic nucleus of the hypothalamus astrocytic processes undergo dramatic morphological changes depending on the physiological status of the organism (Oliet and Piet, 2004). These changes alter glial coverage of synapses and consequently impact on synaptic physiology through alterations of glial glutamate uptake and modulation of synaptic NMDARs by astrocyte-released D-serine (Oliet et al., 2001; Panatier et al., 2006).

It has been recently suggested that EphA-ephrinA interaction at the neuro-glia interface regulates motility of small astrocytic protrusions (Nestor et al., 2007). This process can possibly occur in parallel with the regulation of glial glutamate transporter abundance. The two events could act synergistically to modulate synaptic function by regulating glutamate uptake. In accord with this model, it has been shown that sensory stimulation induces changes in both expression of glial glutamate transporters and glial coverage of synapses in the barrel cortex of mice (Genoud et al., 2006). In vivo imaging of astrocytic processes during sensory stimulation in *Epha4* and *Efn3* mutant mice could confirm this hypothesis.

3.9 Potential pathological consequence of EphA4-ephrinA3 signaling malfunction

Alterations of astrocyte physiology, including dysfunction of astrocyte glutamate uptake, have been implicated in many pathological conditions affecting the CNS (Beart and O'Shea, 2007; Seifert et al., 2006). For example, several studies have suggested a link between glutamate uptake malfunction and epilepsy. Mice lacking GLT1 display spontaneous seizures and lower threshold for PTZ-induced seizures (Tanaka et al., 1997). Similarly, pharmacological inhibition of GLT1 reduces the threshold for evoking epileptiform activity in rats (Campbell and Hablitz, 2004; Demarque et al., 2004). Reduced or dysfunctional glial glutamate transporters may also be involved in seizure initiation and/or propagation in patients affected by

epilepsy (During and Spencer, 1993; Mathern et al., 1999; Proper et al., 2002). Moreover, reduced glutamate uptake can lead to neurodegeneration caused by excitotoxicity (Rothstein et al., 1996). In agreement with these evidences, the data presented here show that overexpression of ephrinA3 in astrocytes *in vivo* causes excitotoxicity and increased susceptibility to seizures by reducing abundance of glial glutamate transporters and possibly by increasing the concentration of extracellular glutamate. Pyramidal neurons in ephrinA3 overexpressing mice have dystrophic dendrites with focal swellings and loss of dendritic spines typically present in neural tissue exposed to excitotoxic conditions *in vitro* (Hasbani et al., 2001; Oliva et al., 2002; Swann et al., 2000) and possibly in humans affected by epilepsy (Swann et al., 2000). Furthermore, administration of the convulsive drug PTZ induces more easily seizures in ephrinA3 overexpressing mice than in control animals. It would be interesting to screen for mutations in loci coding for Eph receptors and ephrins in patients affected by epilepsy to investigate a possible direct involvement of Eph-ephrin signaling in this pathological condition.

Reduced expression of glial glutamate transporters has been linked also to ALS. Patients affected by ALS present impaired glutamate uptake and reduced amounts of GLT1 (Rothstein et al., 1992; Rothstein et al., 1995; Sasaki et al., 2000). Rodents carrying a mutant form of the Cu/Zn superoxide dismutase (SOD1) found in some patients with familial ALS reproduce many of the aspects of the disease, including loss of GLT1 (Howland et al., 2002; Trotti et al., 1999). Interestingly, it was recently found that the VAMP-associated membrane protein B (VAPB), one of the proteins mutated in some forms of familial ALS, binds to Eph receptors and modulates their signaling (Tsuda et al., 2008). It would be interesting in the future to investigate a possible link between VAPB-mediated regulation of Eph-ephrin signaling and expression of glial glutamate transporters. Moreover, assessment of motor neuron loss in ephrinA3 overexpressing mice could reveal a more direct link between EphA4-ephrinA3 signaling dysfunction and ALS.

4

Materials and methods

4.1 Materials

4.1.1 Chemicals and drugs

Chemicals were purchased from Biomol, Merck, Roth and Sigma. Enzymes and relative buffers were purchased from New England Biolabs (NEB) or Roche. Kits for plasmid purifications and gel-extractions were purchased from Qiagen. Drugs for electrophysiology experiments were purchased from Tocris. All water used to prepare solutions was filtered with the Milli-Q-Water System (Millipore).

4.1.2 Genotyping oligonucleotides

All oligonucleotides were synthesized by Metabion.

EphA4wtF	5'–CAATCCGCTGGATCTAAGTGCCTGTTAGC–3'
EphA4wtR	5'–ACCGTTCGAAATCTAGCCCAGT–3'
EphA4koF	5'–GACTCTAGAGGATCCACTAGTGTCGA–3'
EphA4koR	5'–TTTTCTCCCTCTTTAAGCAAGGATCAAGC–3'
Cre1	5'–GCCTGCATTACCGGTCGATGCAACGA–3'
Cre2	5'–GTGGCAGATGGCGCGGCAACACCATT–3'
Thy1F	5'–TCTGAGTGGCAAAGGACCTTAGG–3'
Thy1R	5'–CGCTGAACTTGTGGCCGTTTACG–3'
EphrinA3wtF	5'–GGGGTGTCTGAGAGAAGCTG–3'
EphrinA3wtR	5'–CGACATCTCTGCCTTCTTCC–3'
EphrinA3koF	5'–GATGGCGTCGACGATAACTT–3'
EphrinA3koR	5'–AAGTCGTGCTGCTTCATGTG–3'
LacZF	5'–CCAGCTGGCGTAATAGCGAA–3'
LacZR	5'–CGCCCGTTGCACCACAGATG–3'
GFAPF	5'–CAGAGCAGGTTGGAGAGGAG–3'
GFAP-GFPR	5'–GGTCTTGTAGTTGCCGTCGT–3'
GFAP-A3R	5'–GCGGGCAGTAAATATCCAGA–3'

4.1.3 Primary antibodies

Antibody	Species	Source	Dilution	Application
α -digoxigenin (AP conjugated)	Sheep	Roche	1:2000	ISH
α -EAAC1	Mouse monoclonal	Chemicon	1:500	WB
α -EphA4 (α -Sek)	Mouse monoclonal	Becton Dickinson	1:1000	WB
α -EphA4 (intracellular domain)	Rabbit polyclonal, serum 1383	In house	1:1000	WB
α -EphA4 (globular domain)	Rabbit polyclonal, serum 1078	(Egea et al., 2005)	1:1000	WB
α -GFAP	Rabbit polyclonal	DAKO	1:1000	IF, IHC, WB
α -GFAP	Mouse monoclonal	Sigma	1:1000	WB
α -GFP	Rabbit polyclonal	RDI	1:1000	IF
α -GFP	Mouse monoclonal	Molecular Probes	1:2000	IF
α -GLAST	Rabbit polyclonal	Frontier Science	1:5000	IF
α -GLAST	Guinea pig polyclonal	Chemicon	1:5000	WB
α -GLT1	Guinea pig polyclonal	Chemicon	1:2000-1:5000	IF, WB
α -hemagglutinin	Rat monoclonal, clone 3F10	Sigma	1:1000-1:2000	IF, WB
α -tubulin	Mouse monoclonal, clone DM 1A	Sigma	1:50000	WB

Table 4.1 Summary of the primary antibodies used for the experiments described in this thesis. Abbreviations: AP, alkaline phosphatase; IF, immunofluorescence; IHC immunohistochemistry; WB, western blot; α , anti.

4.1.4 Buffers and solutions

General purpose buffers and solutions

PBS (phosphate-buffered saline)

10× stock solution, 1 liter:

80 g NaCl

2 g KCl

11.5 g Na₂HPO₄·7H₂O

2 g KH₂PO₄

Working solution, pH 7.3:

137 mM NaCl

2.7 mM KCl

4.3 mM Na₂HPO₄·7H₂O

1.4 mM KH₂PO₄

4% PFA (Paraformaldehyde)

For 50 ml:

PFA 2 g

5M NaOH 10 µl

H₂O 45 ml at 70 °C

As soon the solution was clear 5 ml of 10X PBS were added. After 2-3 minutes at 70 °C the solution was cooled down on ice.

Solutions for molecular biology

Gel loading buffer

Glycerol 25 ml

50X TAE 1 ml

Orange G 0.1 g

H₂O 24 ml

TE (Tris/EDTA) buffer

10 mM Tris·Cl, pH 8.0

1 mM EDTA, pH 8.0

TAE (Tris/acetate/EDTA) buffer

50× stock solution:

242 g Tris base

57.1 ml glacial acetic acid

37.2 g Na₂EDTA·2H₂O

H₂O up to 1 liter

Working solution, pH 8.5:

40 mM Tris·acetate

2 mM Na₂EDTA·2H₂O

Embedding solutions for vibratome sectioning

0.1 M Acetate buffer, pH 6.5

1 M Sodium acetate 99 ml

1 M Acetic Acid 960 μl

H₂O up to 1 liter

Embedding solution

a) Ovalbumin (Sigma, Cat.# A-S253) 90 g

0.1 M Acetate buffer 200 ml

Ovalbumin was dissolved in acetate buffer (stirring overnight) at room temperature. The solution was then filtered through a gaze in order to remove undissolved albumin and air bubbles.

b) Gelatin 15 g

0.1 M Acetate buffer 100 ml

Gelatin was dissolved in warm acetate buffer. The solution was cooled down to room temperature and (a) and (b) were mixed. Aliquots of the final solution were stored at -20 °C.

Solutions for *in situ* hybridization**Blocking solution**

For 10 ml:

5X MAB, pH 7.5	2 ml
Blocking reagent (Roche, Cat.# 1096 176)	200 µg
Sheep serum	2 ml
H ₂ O	up to 10 ml

Deionized formamide

Ion-exchange resin (Biorad, Cat.# 142-6425)	25 g
Formamide	500 ml

Stirred for 45 minutes, filtered and stored (50 ml aliquots) at -20 °C.

Developing solution

For 10 ml:

BCIP (5-Bromo-4-chloro-3-indolyl phosphate, Sigma)	11 µl
NBT (4-nitroblue tetrazolium chloride, Sigma)	14 µl
NTMT	10 ml

Hybridization solution

For 50 ml:

Deionized Formamide	25 ml
20X SSC, pH 4.5	12.5 ml
Tween-20	100 µl
5% Chaps	5 ml
Blocking reagent (Roche, Cat.# 1096 176)	1 g
10 mg/ml tRNA	250 µl

50 mg/ml Heparin	50 μ l
0.5 M EDTA, pH8.1	500 μ l
H ₂ O	up to 50 ml

5X MAB (maleic acid buffer), pH 7.5

For 1 liter:

Maleic acid	58 g
NaCl	44 g
H ₂ O	up to 800 ml
NaOH pellets	35 g
H ₂ O	up to 1 liter

MABT

1X MAB

0.2% Tween-20

NTMT

For 200 ml:

5 M NaCl	4 ml
1 M Tris, pH 9.5	20 ml
1 M MgCl ₂	10 ml
Tween-20	200 μ l (0.1%)
H ₂ O	up to 200 ml

PBT (PBS Tween)

0.1% Tween-20 in PBS

Solution 1

For 10 ml:

Deionized formamide	5 ml
20X SSC, pH4.5	2.5 ml
20% Tween-20	100 µl
5% Chaps	1 ml
H ₂ O	up to 10 ml

Solution 2

For 10 ml:

Deionized formamide	5 ml
20X SSC, pH4.5	1 ml
20% Tween-20	100 µl
5% Chaps	200 µl
H ₂ O	up to 10 ml

Solution 3

For 10 ml:

20X SSC, pH4.5	1 ml
20% Tween-20	100 µl
5% Chaps	200 µl
H ₂ O	up to 10 ml

20X SSC (sodium chloride/sodium citrate), pH 4.5

For 1 liter:

Sodium citrate	69.2 g
Citric Acid	13.7 g
NaCl	175 g
H ₂ O	up to 1 liter

Solutions for electrophysiology recordings

ACSF1 (artificial cerebrospinal fluid for extracellular field recordings and neuron patch-clamping) 305-315 mosm/Kg, pH 7.4

For 1 liter:

NaCl	7.25 g (124 mM)
KCl	0.22 g (3 mM)
NaH ₂ PO ₄	0.17 g (1.25 mM)
CaCl ₂	0.37 g (2.5 mM)
MgSO ₄	0.50 g (2 mM)
NaHCO ₃	2.18 g (26 mM)
Glucose	1.98 g (10 mM)
H ₂ O	up to 1 liter

The solution was saturated with 95% O₂ and 5% CO₂.

ACSF2 (artificial cerebrospinal fluid for astrocyte patch-clamping)

For 1 liter:

NaCl	7.31 g (125 mM)
KCl	0.18 g (2.5 mM)
NaH ₂ PO ₄	0.17 g (1.25 mM)
CaCl ₂	0.30 g (2 mM)
MgCl ₂	0.095 g (1 mM)
NaHCO ₃	2.18 g (26 mM)
Glucose	3.96 g (20 mM)
H ₂ O	up to 1 liter

The solution was saturated with 95% O₂ and 5% CO₂.

Internal solution 1 (internal solution for neuron patch-clamping) 280 mosm/Kg, pH 7.2

For 50 ml:

CsGluconate	(2.94 ml gluconic acid + 1.8 ml CsOH) (150 mM)
HEPES	119 mg (10 mM)
MgATP	51 mg (2 mM)
EGTA	3.8 mg (0.2 mM)
NaCl	23 mg (8 mM)
H ₂ O	up to 50 ml

Aliquots were stored at -20 °C.

Internal solution 2 (internal solution for astrocyte patch-clamping, pH 7.30)

For 50 ml:

KCH ₃ SO ₃	805 mg (120 mM)
KCl	0.141 mg (32 mM)
HEPES	119 mg (10 mM)
NaCl	11.5 mg (4 mM)
MgATP	102 mg (4 mM)
NaGTP	11 mg (0.4 mM)
H ₂ O	up to 50 ml

4.1.5 Mouse lines

Camk2a-cre transgenic mice were generated by Liliana Minichiello in our research group (Minichiello et al., 1999)

Efn3^{-/-} mice were generated by the company Ozgene for Elena B. Pasquale's laboratory (Carmona et al., 2009).

***Epha4*^{-/-}** mice were generated in Andrew W. Boyd laboratory (Dottori et al., 1998) and maintained on a mixed 129xC57Bl/6 background.

***Epha4*^{lx/lx}** mice were generated by Klas Kullander in collaboration with the transgenic service of the Max Planck Institute for Neurobiology (Klas Kullander, unpublished results and (Filosa et al., 2009)). Briefly, *EphA4* cDNA flanked with loxP sites was inserted into exon 3 of the *EphA4* gene by homologous recombination in embryonic stem cells. Recombinant clones were injected into mouse blastocysts to obtain chimaeric mice transmitting the mutated allele through the germ line. The neomycin resistance gene was removed by crossing heterozygous *Epha4*^{lx/+} mice with deleter-FlpE mice (Rodriguez et al., 2000). Mice were maintained in a mixed 129xC57Bl/6 background.

Gfap-Efna3 transgenic mice were generated by Sonia Paixao (Filosa et al., 2009). Briefly, *Efnb2* cDNA in the pJK38 vector (Lauterbach and Klein, 2006) was replaced by the human *Efna3* cDNA (from nucleotide 137 to 787, GenBank accession number NM_004952.4), EYFP was then removed and the pCMV promoter was replaced by the human glial specific *Gfap* promoter (Nolte et al., 2001). The *ApalI/DrallI* fragment containing the *Efna3* transgene was isolated by electroelution and purified with Elutip-D minicolumns (Schleicher & Schüll). Oocytes from FVB mice were injected using conventional microinjection technology. Founder lines were mated with C57Bl/6 mice and maintained on a mixed FVBxC57Bl/6 background.

Gfap-GFP transgenic mice were generated in Frank Kirchhoff laboratory (Nolte et al., 2001).

Grik4-cre (CA3-cre) knock-in mice were generated by York Rudhard in Ralf Schoepfer's laboratory (Filosa et al., 2009). Briefly, a YAC containing the *Grik4* gene modified to carry a targeting cassette in the 3' untranslated region of *Grik4*

was used for homologous recombination in embryonic stem cells. The targeting cassette consisted of an IRES element, EGFP-Cre and *frt*-flanked selection markers *neo* and *his3* which were removed by crossing CA3-cre mice with Flp deleter mice (Rodriguez et al., 2000).

PGK-cre transgenic mice were generated in Peter Lonai's laboratory (Lallemant et al., 1998).

R4Ag11CaMKII-cre (CA1-cre) transgenic mice were generated in Susumu Tonegawa's laboratory (Tsien et al., 1996).

Thy1-GFP transgenic mice were generated in Joshua R. Sanes's laboratory (Feng et al., 2000).

4.2 Methods

4.2.1 Molecular biology

Tail DNA preparation and genotyping

Tail biopsies (1-3 mm) were taken from mice and incubated at 95 °C three times for 15 min in 100 µl of 50 mM NaOH and vortexed thoroughly between heating steps. Samples were then centrifuged to precipitate the remaining debris and the mix was neutralized with the addition of 10 µl 1.5 M Tris-HCl, pH 8.8 and stored at 4 °C. 1-2 µl of DNA were used as template for polymerase chain reaction (PCR). PCR was carried out in a total volume of 50 µl and contained 2.5 mM dNTPs, 50mM specific primers, 1X PCR buffer (NEB) and 0.5 µl of Taq polymerase (NEB). The primers and the PCR programs used for the amplification of specific alleles are summarized in table 4.2.

Allele	Primers	Step 1	Step 2	Step 3	Step 4	Step 5	Step 6
<i>Epha4 wt</i>	EphA4wtF + EphA4wtR	2 min @ 95°C	30 s @ 95°C	1 min 30 s @ 68°C	1 min 15 s @ 72°C	30X step 2 - 4	6 min @ 72°C
<i>Epha4 ko</i>	EphA4koF + EphA4koR	3 min @ 94°C	1 min @ 94°C	1 min @ 65°C	1 min @ 72°C	37X step 2 - 4	20 min @ 72°C
<i>Epha4 lx</i>	LacZF + LacZR	5 min @ 95°C	30 s @ 95°C	30 s @ 58°C	30 s @ 72°C	35X step 2 - 4	5 min @ 72°C
<i>Efna3 wt</i>	EphrinA3wt F + EphrinA3wt R	5 min @ 95°C	30 s @ 95°C	30 s @ 63°C	30 s @ 72°C	35X step 2 - 4	5 min @ 72°C
<i>Efna3 ko</i>	EphrinA3ko F + EphrinA3ko R	2 min @ 95°C	1 min @ 95°C	1 min @ 64°C	1 min @ 72°C	35X step 2 - 4	2 min @ 72°C
<i>Cre</i>	Cre1 + Cre2	3 min @ 94°C	1 min @ 94°C	1 min @ 67°C	1 min @ 72°C	35X step 2 - 4	5 min @ 72°C
<i>GFAP-HA-A3</i>	GFAPF + GFAP-A3R	5 min @ 95°C	30 s @ 95°C	30 s @ 61°C	45 s @ 72°C	40X step 2 - 4	X
<i>GFAP-eGFP</i>	GFAPF + GFAP-GFPR	5 min @ 95°C	30 s @ 95°C	30 s @ 59°C	30 s @ 72°C	35X step 2 - 4	X
<i>Thy1-GFP</i>	Thy1F + Thy1R	5 min @ 95°C	30 s @ 95°C	30 s @ 60°C	1 min @ 72°C	35X step 2 - 4	3 min @ 72°C

Table 4.2 Summary of the primers and PCR programs used to amplify the indicated alleles.

Agarose gel electrophoresis

Gels with 1% agarose in TAE with 3 μ l ethidium bromide/100 ml TAE were used. Warm gels were poured into a chamber containing combs. Once the gel had solidified the combs were removed and the gel submerged in 1X TAE in an electrophoresis chamber. PCR products, RNA probes or products of enzymatic digestions were loaded into the wells together with gel loading buffer (10:1) and separated according to their size for 20-30 min at ~200V. DNA or RNA was visualized under UV light using a gel documenting system (BioRad).

Transformation of competent *E.coli* by electroporation

50 μ l of competent bacteria (DH5 α , Invitrogen) were thawed on ice and 0.2-2 μ l of plasmid DNA were added. The mix was transferred into a sterile, pre-chilled 0.2 cm electroporation cuvette. One electric pulse was applied to the cuvette with the pulser apparatus set to 25 μ F and 2.5 kV; the pulse controller to 200 Ω . 1 ml of LB medium was immediately added to the cells, which were then transferred to a plastic tube and shaken for 60 min. The bacteria were then plated on LB plates containing ampicillin and grown over night at 37 °C.

Preparation of plasmid DNA

Plasmid DNA was purified from large scale (500ml, maxipreparation) bacterial cultures. Single colonies of transformed bacteria were picked from LB plates containing ampicillin and inoculated into flasks containing LB medium with 100 μ g/ml ampicillin and grown overnight shaking at 37 °C. Harvesting and purification of maxipreparation was carried out according to Qiagen protocol using Qiagen buffers. The DNA concentration was measured in a UV spectrometer at 260 nm.

Molecular Cloning

A pcDNA3 vector containing *Epha4* cDNA was modified in order to obtain a vector containing an *Epha4* cDNA fragment extending from nucleotide 880 to 1551 (GenBank accession number NM_007936). The original vector was digested with the restriction enzymes BamHI and HindIII. The digested products were separated by agarose gel electrophoresis and the band corresponding to the fragment containing the backbone vector together with the cDNA portion of interest was cut out from the gel. The DNA was purified by using the QIAquick gel extraction kit (Qiagen). 50 ng of the purified DNA were incubated over night in 10 μ l of 1X T4 ligase buffer solution with 1 μ l of T4 ligase and 1 mM ATP. The circularized DNA was precipitated by adding 1 μ l of 3M NaAcetate, 1 μ l of glycogen and 30 μ l of

ethanol to the ligase solution (cooled on dry ice) and by centrifuging the solution at 13000 rounds per minute (rpm) for 10 min. The pellet was washed twice with 100 μ l of ethanol, centrifuged at 13000 rpm for 2 min, then dried and finally dissolved in 10 μ l of water.

Generation and labeling of antisense RNA probes

10 μ g of plasmid DNA were linearized by digesting it for 3 h at 37 °C with the restriction enzyme XhoI. After purification with phenol/chloroform extraction, 2 μ l of the linearized DNA were incubated with 2 μ l transcription buffer (Roche, *in situ* probe labeling kit), 2 μ l of 0.1M DTT, 2 μ l digoxigenin-conjugated dNTPs, 1 μ l RNase inhibitor and 1 μ l of the specific RNA polymerase in a total volume of 20 μ l for 3 h at 37 °C. Then, 10 μ l of 4 M LiCl, 100 μ l TE and 300 μ l of ethanol were added to the mix and incubated for 30 min at -20 °C. Subsequently, the mix was centrifuged for 20 min at 4 °C. The pellet was washed with 70% ethanol, dried on ice and then dissolved in 100 μ l TE. Aliquots were stored at -20 °C. For *in situ* hybridization 20-30 μ l of RNA probe solution were used per ml of hybridization buffer.

4.2.2 Biochemistry

Tissues were homogenized in ice-cold buffer (50 mM Tris-HCl, pH 7.4, 150 mM NaCl, 1% Triton X-100) containing protease and phosphatase inhibitor cocktail tablets (Roche). The protein extracts were separated by SDS-PAGE and probed by immunoblotting with primary antibodies and horseradish peroxidase (HRP)-conjugated secondary antibodies (Amersham Biosciences), 1:5000. Detection was performed with luminol (Santa Cruz). For immunoprecipitations, hippocampal lysates were incubated with Protein A-Sepharose beads (Amersham) pre-conjugated with an anti-EphA4 antibody (serum 1383). Western blots were

quantified using ImageJ software. Optical density values were normalized to tubulin signal. Glutamate transporter proteins tend to form homomultimers (Haugeto et al., 1996). For GLAST a more prominent band of 120 kDa was quantified, probably corresponding to the dimeric form. For GLT1 a band of 70 kDa was quantified, corresponding to the monomeric form.

4.2.3 Histology and image analysis

Cardiac perfusion

Mice were anaesthetised with an intraperitoneal injection of chloralhydrate (8% chloralhydrate, 0.9% NaCl in H₂O). Skin and ribcage were cut open and the diaphragm was removed. A small incision was made into the right auriculum and a needle connected to a peristaltic pump was inserted into the left ventricle to replace the animal's blood by cold PBS. This was followed by approximately 25 ml of cold 4% PFA solution for fixation. Brains or hippocampi were dissected out and postfixed overnight at 4 °C in 4% PFA.

Vibratome sections

A layer of 2 ml embedding solution was poured into a small plastic mould and crosslinking was allowed by adding 100 µl of 25% glutaraldehyde solution. The perfused and postfixed brains or hippocampi were placed on top and other 3.5 ml embedding solution with 175 µl of glutaraldehyde was poured over them. The mould was left to set for 5 min at room temperature before cutting 40-60 µm coronal sections with a vibratome.

In situ hybridization analysis

Vibratome sections were dehydrated in increasing concentrations of methanol in PBS and stored at -20 °C. After rehydration in decreasing concentrations of methanol in PBS, the slices were treated with proteinase K (20 µg/ml) in PBT and

postfixed for 20 min in 4% PFA, 0.2% glutaraldehyde. The sections were then prehybridized at 70 °C for 1 h in hybridization solution. Hybridization was carried out overnight at 60 °C in hybridization solution containing the digoxigenin-labeled riboprobe. The slices were then washed at 60 °C three times in solution 1, three times in solution 2 and three times in solution 3. After two washes at 70 °C in MABT, slices were incubated in blocking solution for 1.5 h at room temperature and then incubated overnight at 4 °C with an alkaline phosphatase-conjugated anti-digoxigenin antibody (Roche) diluted 1:2000 in blocking solution. Slices were then washed 8-10 times with MABT and once in NTMT at room temperature. The signal was visualized by a color reaction using 500 µl of developing solution. The reaction was allowed to develop in the dark at 4 °C and was stopped with PBT. The slices were postfixed with 4% PFA.

Quantification of recombination efficiency

Densitometric measurements of mRNA expression levels were performed using ImageJ software. Three equally sized areas were selected in CA1 and CA3 pyramidal layer (red and blue squares in figure 2.3a, respectively) in every digital picture of *Epha4* in situ hybridizations. The signal intensity values were corrected for background, determined as signal intensity in the stratum radiatum of CA1 (yellow squares in figure 2.3a). The relative abundance of *Epha4* mRNA was expressed as CA3/CA1 or CA1/CA3 ratios. The recombination efficiency was calculated as a ratio of CA1/CA3 values in CA1-cre;*Epha4*^{lx/-} slices and CA1/CA3 values in *Epha4*^{lx/-} slices for CA1-cre;*Epha4*^{lx/-} mice and as a ratio of CA3/CA1 values in CA3-cre;*Epha4*^{lx/-} and CA3/CA1 values in *Epha4*^{lx/-} slices for CA3-cre;*Epha4*^{lx/-} mice.

Immunofluorescence and immunohistochemistry

For immunofluorescence, vibratome free-floating sections (50 µm thick) were permeabilized with 0.5% TritonX-100 in PBS, blocked in 0.1% TritonX-100, 5%

BSA and 5% donkey serum in PBS for 1 h at room temperature and incubated with primary antibodies overnight at 4 °C in blocking solution. The sections were washed three times for 30 min in PBS containing 0.1% Triton X-100 and incubated for 1 h at room temperature with donkey Cy2, Cy3 and Cy5-conjugated secondary antibodies (Jackson ImmunoResearch), diluted 1:800 in blocking solution. The sections were then mounted using aqueous mounting medium with antifading reagent (Biomedica). The Vectastain ABC kit (Vector Laboratories) was used for immunohistochemistry following provider's instructions.

4.2.4 Assessment of seizure susceptibility

Mice were injected intraperitoneally with 45 mg per kg body weight PTZ, diluted in saline solution. After injection, mice were carefully monitored and videotaped.

4.2.5 Electrophysiology

Acute hippocampal slices preparation

Mice (P40-80 for extracellular field recordings (EFRs), P12-24 for neuron patch-clamp recordings and P18-24 for astrocyte patch-clamp recordings) were decapitated under diethylether anesthesia. Hippocampi were dissected in cold ACSF1 for EFRs and neuron patch-clamping and in ACSF2 for astrocyte patch-clamping. Slices (400 µm thick for EFRs and neuron patch-clamping and 300 µm thick for astrocyte patch-clamping) were prepared using a custom made tissue slicer for EFRs or a vibratome for neuron and astrocyte patch-clamp recordings and maintained in ACSF1 or ACSF2 at room temperature for 1-2 h before recording.

Extracellular field recordings

Acute hippocampal slices were perfused with ACSF1 during recordings. Input-output relations were measured at 25 °C. All the other experiments were

performed at 33 °C. Synaptic responses were evoked by stimulating Schaffer collaterals with 0.2 ms pulses using monopolar tungsten electrodes. Field excitatory postsynaptic potentials (fEPSPs) were recorded in the stratum radiatum of CA1 region using glass microelectrodes filled with 3 M NaCl (resistance 5-15 M Ω). For baseline recordings, slices were stimulated at 0.1 Hz for 20 min at stimulation intensities of 40-50 % of the highest measured fEPSP size. LTP was induced by applying one tetanus (100 Hz for 1 s) or a theta-burst stimulation (TBS) consisting of three bursts (10 s interval), each composed of ten trains (5 Hz) with four pulses (100 Hz). Paired pulse facilitation (PPF) was tested by applying two pulses with inter-stimulus intervals (ISI) ranging from 10 ms to 160 ms. An Axoclamp 2B amplifier (Axon Instruments) was used for the experiments. Data were sampled at 5 kHz and analyzed using a program written in LabView (National Instruments). All measurements were carried out and analyzed by an investigator blind to the genotype.

Neuron patch-clamp recordings

Recordings were performed at 33 °C. Borosilicate patch pipettes (resistance 2-7 M Ω) were filled with internal solution 1. Pyramidal cells were visually identified by using a microscope with transmitted infrared light (Olympus BX51WI) connected to an infrared camera (Till Photonics). Spontaneous miniature excitatory post synaptic currents (mEPSCs) were recorded in whole-cell configuration at -70 mV. mEPSCs were recorded first in ACSF1 containing 100 μ M picrotoxin (PTX) and 200 nM tetrodotoxin (TTX) and then in ACSF1 containing PTX, TTX and 1 mM γ -DGG. AMPAR and NMDAR currents in CA1 pyramidal cells were evoked by stimulating Schaffer collaterals with a monopolar tungsten electrode. The experiments were performed in ACSF1 containing 100 μ M PTX. AMPAR currents were recorded in voltage-clamp mode at a membrane potential of -70 mV and peak amplitudes of the currents were measured. NMDAR currents were recorded at +40 mV and measured 70 ms after stimulus to avoid the initial mixed AMPAR/NMDAR

component. A Digidata 1440A digitizer and a Multiclamp 700B (both from Axon Instruments) were used for the experiments. Data were collected and analyzed using pCLAMP 10 Software (Axon Instruments). All measurements were carried out and analyzed by an investigator blind to the genotype.

Astrocyte patch-clamp recordings

Astrocyte patch-clamp recordings were performed at 24-26 °C with an EPC10 Double amplifier (HEKA Electronics). Glass pipettes (resistance 2-4 M Ω) were filled with intracellular solution 2. During experiments, slices were perfused with ACSF2 containing 20 μ M bicuculline and 2.5 mM kynurenic acid to suppress activation of ionotropic glutamate as well as GABA_A receptors. Astrocytes were held in voltage-clamp mode at a membrane potential of -85 mV. Recordings were discarded when the series resistance exceeded 17 M Ω . Astrocytes were identified based on their membrane potential close to -85 mV, their high capacitance, low membrane resistance and passive current-voltage relationship upon application of depolarizing current pulses. Schaffer collaterals were stimulated with a tungsten concentric bipolar electrode (pulse duration 0.1 ms). Currents were corrected for the slow current insensitive to the glutamate transporter blockers L-trans-pyrrolidine-2,4-dicarboxylic acid (PDC, 300 μ M) and dihydrokainic acid (DHK, 300 μ M), likely reflecting accumulation of extracellular potassium. Extracellular field potentials for fiber volley detection were recorded with ACSF2-filled glass microelectrodes at a maximal distance of 50 μ m from the recorded astrocyte. The stimulation intensity was adjusted such that fiber volley amplitudes were between -0.15 and -0.4 mV. For each stimulation intensity, 5-10 (single pulse experiments) or 3 (TBS) recordings were averaged. Data were collected at 10 KHz and were analyzed with IgorPro (Wavemetrics). All measurements were carried out and analyzed by an investigator blind to the genotype.

4.2.6 Statistical analysis

Statistical significance was determined using two-tailed Student's *t*-tests in Microsoft Excel, two-way analysis of variance (ANOVA) with repetitions using the software Statistics (Blackwell Scientific Publications), analysis of covariance (ANCOVA) from the VassarStats statistical computations website (<http://faculty.vassar.edu/lowry/VassarStats.html>) and two-sample Kolmogorov-Smirnov tests using the Statistics to Use website (<http://www.physics.csbsju.edu/stats/KS-test.html>; T.W. Kirkman, 1996). The Mann-Whitney U-test was performed using SPSS software (release 11.0; SPSS Inc.). All values in the text and in the figure legends indicate mean \pm s.e.m. All error bars in the graphs represent s.e.m.

5

Bibliography

- Abbott, L.F., and Nelson, S.B. (2000). Synaptic plasticity: taming the beast. *Nat Neurosci* 3 *Suppl*, 1178-1183.
- Abraham, W.C. (2008). Metaplasticity: tuning synapses and networks for plasticity. *Nat Rev Neurosci* 9, 387.
- Abraham, W.C., and Bear, M.F. (1996). Metaplasticity: the plasticity of synaptic plasticity. *Trends Neurosci* 19, 126-130.
- Adams, J.P., and Dudek, S.M. (2005). Late-phase long-term potentiation: getting to the nucleus. *Nat Rev Neurosci* 6, 737-743.
- Adolph, O., Koster, S., Rath, M., Georgieff, M., Weigt, H.U., Engele, J., Senftleben, U., and Fohr, K.J. (2007). Rapid increase of glial glutamate uptake via blockade of the protein kinase A pathway. *Glia* 55, 1699-1707.
- Airaksinen, M.S., and Saarma, M. (2002). The GDNF family: signalling, biological functions and therapeutic value. *Nat Rev Neurosci* 3, 383-394.
- Albensi, B.C., Oliver, D.R., Toupin, J., and Odero, G. (2007). Electrical stimulation protocols for hippocampal synaptic plasticity and neuronal hyper-excitability: are they effective or relevant? *Exp Neurol* 204, 1-13.
- Alvarez, V.A., and Sabatini, B.L. (2007). Anatomical and physiological plasticity of dendritic spines. *Annu Rev Neurosci* 30, 79-97.
- Andersen, P. (2007). *The hippocampus book* (Oxford ; New York: Oxford University Press).
- Anwyl, R. (1999). Metabotropic glutamate receptors: electrophysiological properties and role in plasticity. *Brain Res Brain Res Rev* 29, 83-120.
- Armstrong, J.N., Saganich, M.J., Xu, N.J., Henkemeyer, M., Heinemann, S.F., and Contractor, A. (2006). B-ephrin reverse signaling is required for NMDA-independent long-term potentiation of mossy fibers in the hippocampus. *J Neurosci* 26, 3474-3481.
- Arnth-Jensen, N., Jabaudon, D., and Scanziani, M. (2002). Cooperation between independent hippocampal synapses is controlled by glutamate uptake. *Nat Neurosci* 5, 325-331.
- Barres, B.A. (2008). The mystery and magic of glia: a perspective on their roles in health and disease. *Neuron* 60, 430-440.
- Baude, A., Nusser, Z., Roberts, J.D., Mulvihill, E., McIlhinney, R.A., and Somogyi, P. (1993). The metabotropic glutamate receptor (mGluR1 alpha) is concentrated at perisynaptic membrane of neuronal subpopulations as detected by immunogold reaction. *Neuron* 11, 771-787.

- Beart, P.M., and O'Shea, R.D. (2007). Transporters for L-glutamate: an update on their molecular pharmacology and pathological involvement. *Br J Pharmacol* 150, 5-17.
- Beattie, E.C., Stellwagen, D., Morishita, W., Bresnahan, J.C., Ha, B.K., Von Zastrow, M., Beattie, M.S., and Malenka, R.C. (2002). Control of synaptic strength by glial TNF α . *Science* 295, 2282-2285.
- Beg, A.A., Sommer, J.E., Martin, J.H., and Scheiffele, P. (2007). α 2-Chimaerin is an essential EphA4 effector in the assembly of neuronal locomotor circuits. *Neuron* 55, 768-778.
- Bergles, D.E., and Jahr, C.E. (1998). Glial contribution to glutamate uptake at Schaffer collateral-commissural synapses in the hippocampus. *J Neurosci* 18, 7709-7716.
- Bi, G., and Poo, M. (2001). Synaptic modification by correlated activity: Hebb's postulate revisited. *Annu Rev Neurosci* 24, 139-166.
- Binns, K.L., Taylor, P.P., Sicheri, F., Pawson, T., and Holland, S.J. (2000). Phosphorylation of tyrosine residues in the kinase domain and juxtamembrane region regulates the biological and catalytic activities of Eph receptors. *Mol Cell Biol* 20, 4791-4805.
- Bourgin, C., Murai, K.K., Richter, M., and Pasquale, E.B. (2007). The EphA4 receptor regulates dendritic spine remodeling by affecting β 1-integrin signaling pathways. *J Cell Biol* 178, 1295-1307.
- Bourne, J.N., and Harris, K.M. (2008). Balancing structure and function at hippocampal dendritic spines. *Annu Rev Neurosci* 31, 47-67.
- Bouzioukh, F., Wilkinson, G.A., Adelman, G., Frotscher, M., Stein, V., and Klein, R. (2007). Tyrosine phosphorylation sites in ephrinB2 are required for hippocampal long-term potentiation but not long-term depression. *J Neurosci* 27, 11279-11288.
- Brager, D.H., Cai, X., and Thompson, S.M. (2003). Activity-dependent activation of presynaptic protein kinase C mediates post-tetanic potentiation. *Nat Neurosci* 6, 551-552.
- Brasnjo, G., and Otis, T.S. (2001). Neuronal glutamate transporters control activation of postsynaptic metabotropic glutamate receptors and influence cerebellar long-term depression. *Neuron* 31, 607-616.
- Brown, D.A., and London, E. (1998). Functions of lipid rafts in biological membranes. *Annu Rev Cell Dev Biol* 14, 111-136.
- Bruckner, K., Pablo Labrador, J., Scheiffele, P., Herb, A., Seeburg, P.H., and Klein, R. (1999). EphrinB ligands recruit GRIP family PDZ adaptor proteins into raft membrane microdomains. *Neuron* 22, 511-524.

- Caceres, M., Suwyn, C., Maddox, M., Thomas, J.W., and Preuss, T.M. (2007). Increased cortical expression of two synaptogenic thrombospondins in human brain evolution. *Cereb Cortex* 17, 2312-2321.
- Campbell, S.L., and Hablitz, J.J. (2004). Glutamate transporters regulate excitability in local networks in rat neocortex. *Neuroscience* 127, 625-635.
- Carmona, M.A., Murai, K.K., Wang, L., Roberts, A.J., and Pasquale, E.B. (2009). Glial ephrin-A3 regulates hippocampal dendritic spine morphology and glutamate transport. *Proc Natl Acad Sci U S A* 106, 12524-12529.
- Carvalho, R.F., Beutler, M., Marler, K.J., Knoll, B., Becker-Barroso, E., Heintzmann, R., Ng, T., and Drescher, U. (2006). Silencing of EphA3 through a cis interaction with ephrinA5. *Nat Neurosci* 9, 322-330.
- Chen, X., Yuan, L.L., Zhao, C., Birnbaum, S.G., Frick, A., Jung, W.E., Schwarz, T.L., Sweatt, J.D., and Johnston, D. (2006). Deletion of Kv4.2 gene eliminates dendritic A-type K⁺ current and enhances induction of long-term potentiation in hippocampal CA1 pyramidal neurons. *J Neurosci* 26, 12143-12151.
- Christopherson, K.S., Ullian, E.M., Stokes, C.C., Mullowney, C.E., Hell, J.W., Agah, A., Lawler, J., Mosher, D.F., Bornstein, P., and Barres, B.A. (2005). Thrombospondins are astrocyte-secreted proteins that promote CNS synaptogenesis. *Cell* 120, 421-433.
- Coate, T.M., Swanson, T.L., and Copenhaver, P.F. (2009). Reverse signaling by glycosylphosphatidylinositol-linked Manduca ephrin requires a SRC family kinase to restrict neuronal migration in vivo. *J Neurosci* 29, 3404-3418.
- Contractor, A., Rogers, C., Maron, C., Henkemeyer, M., Swanson, G.T., and Heinemann, S.F. (2002). Trans-synaptic Eph receptor-ephrin signaling in hippocampal mossy fiber LTP. *Science* 296, 1864-1869.
- Cowan, C.A., and Henkemeyer, M. (2001). The SH2/SH3 adaptor Grb4 transduces B-ephrin reverse signals. *Nature* 413, 174-179.
- Cowan, C.A., and Henkemeyer, M. (2002). Ephrins in reverse, park and drive. *Trends Cell Biol* 12, 339-346.
- Cowan, C.W., Shao, Y.R., Sahin, M., Shamah, S.M., Lin, M.Z., Greer, P.L., Gao, S., Griffith, E.C., Brugge, J.S., and Greenberg, M.E. (2005). Vav family GEFs link activated Ephs to endocytosis and axon guidance. *Neuron* 46, 205-217.
- Cowan, W.M., Südhof, T.C., Stevens, C.F., and Howard Hughes Medical Institute. (2001). *Synapses* (Baltimore: Johns Hopkins University Press).
- Cull-Candy, S.G., and Leszkiewicz, D.N. (2004). Role of distinct NMDA receptor subtypes at central synapses. *Sci STKE* 2004, re16.
- Dalva, M.B., McClelland, A.C., and Kayser, M.S. (2007). Cell adhesion molecules: signalling functions at the synapse. *Nat Rev Neurosci* 8, 206-220.

Dalva, M.B., Takasu, M.A., Lin, M.Z., Shamah, S.M., Hu, L., Gale, N.W., and Greenberg, M.E. (2000). EphB receptors interact with NMDA receptors and regulate excitatory synapse formation. *Cell* 103, 945-956.

Davis, S., Gale, N.W., Aldrich, T.H., Maisonpierre, P.C., Lhotak, V., Pawson, T., Goldfarb, M., and Yancopoulos, G.D. (1994). Ligands for EPH-related receptor tyrosine kinases that require membrane attachment or clustering for activity. *Science* 266, 816-819.

Davy, A., Gale, N.W., Murray, E.W., Klinghoffer, R.A., Soriano, P., Feuerstein, C., and Robbins, S.M. (1999). Compartmentalized signaling by GPI-anchored ephrin-A5 requires the Fyn tyrosine kinase to regulate cellular adhesion. *Genes Dev* 13, 3125-3135.

Davy, A., and Robbins, S.M. (2000). Ephrin-A5 modulates cell adhesion and morphology in an integrin-dependent manner. *EMBO J* 19, 5396-5405.

Demarque, M., Villeneuve, N., Manent, J.B., Becq, H., Represa, A., Ben-Ari, Y., and Aniksztejn, L. (2004). Glutamate transporters prevent the generation of seizures in the developing rat neocortex. *J Neurosci* 24, 3289-3294.

Diamond, J.S., and Jahr, C.E. (1997). Transporters buffer synaptically released glutamate on a submillisecond time scale. *J Neurosci* 17, 4672-4687.

Diamond, J.S., and Jahr, C.E. (2000). Synaptically released glutamate does not overwhelm transporters on hippocampal astrocytes during high-frequency stimulation. *J Neurophysiol* 83, 2835-2843.

Dobrunz, L.E., and Stevens, C.F. (1997). Heterogeneity of release probability, facilitation, and depletion at central synapses. *Neuron* 18, 995-1008.

Dottori, M., Hartley, L., Galea, M., Paxinos, G., Polizzotto, M., Kilpatrick, T., Bartlett, P.F., Murphy, M., Kontgen, F., and Boyd, A.W. (1998). EphA4 (Sek1) receptor tyrosine kinase is required for the development of the corticospinal tract. *Proc Natl Acad Sci U S A* 95, 13248-13253.

Drescher, U. (2002). Eph family functions from an evolutionary perspective. *Curr Opin Genet Dev* 12, 397-402.

Dudek, S.M., and Bear, M.F. (1992). Homosynaptic long-term depression in area CA1 of hippocampus and effects of N-methyl-D-aspartate receptor blockade. *Proc Natl Acad Sci U S A* 89, 4363-4367.

During, M.J., and Spencer, D.D. (1993). Extracellular hippocampal glutamate and spontaneous seizure in the conscious human brain. *Lancet* 341, 1607-1610.

Egea, J., and Klein, R. (2007). Bidirectional Eph-ephrin signaling during axon guidance. *Trends Cell Biol* 17, 230-238.

Egea, J., Nissen, U.V., Dufour, A., Sahin, M., Greer, P., Kullander, K., Mrcic-Flogel, T.D., Greenberg, M.E., Kiehn, O., Vanderhaeghen, P., and Klein, R. (2005).

Regulation of EphA 4 kinase activity is required for a subset of axon guidance decisions suggesting a key role for receptor clustering in Eph function. *Neuron* 47, 515-528.

Engert, F., and Bonhoeffer, T. (1999). Dendritic spine changes associated with hippocampal long-term synaptic plasticity. *Nature* 399, 66-70.

Essmann, C.L., Martinez, E., Geiger, J.C., Zimmer, M., Traut, M.H., Stein, V., Klein, R., and Acker-Palmer, A. (2008). Serine phosphorylation of ephrinB2 regulates trafficking of synaptic AMPA receptors. *Nat Neurosci* 11, 1035-1043.

Fagni, L., Chavis, P., Ango, F., and Bockaert, J. (2000). Complex interactions between mGluRs, intracellular Ca²⁺ stores and ion channels in neurons. *Trends Neurosci* 23, 80-88.

Fellin, T., Pascual, O., Gobbo, S., Pozzan, T., Haydon, P.G., and Carmignoto, G. (2004). Neuronal synchrony mediated by astrocytic glutamate through activation of extrasynaptic NMDA receptors. *Neuron* 43, 729-743.

Feng, G., Mellor, R.H., Bernstein, M., Keller-Peck, C., Nguyen, Q.T., Wallace, M., Nerbonne, J.M., Lichtman, J.W., and Sanes, J.R. (2000). Imaging neuronal subsets in transgenic mice expressing multiple spectral variants of GFP. *Neuron* 28, 41-51.

Fiacco, T.A., and McCarthy, K.D. (2004). Intracellular astrocyte calcium waves in situ increase the frequency of spontaneous AMPA receptor currents in CA1 pyramidal neurons. *J Neurosci* 24, 722-732.

Filosa, A., Paixao, S., Honsek, S.D., Carmona, M.A., Becker, L., Feddersen, B., Gaitanos, L., Rudhard, Y., Schoepfer, R., Klopstock, T., *et al.* (2009). Neuron-glia communication via EphA4/ephrin-A3 modulates LTP through glial glutamate transport. *Nat Neurosci* 12, 1285-1292.

Flavell, S.W., and Greenberg, M.E. (2008). Signaling mechanisms linking neuronal activity to gene expression and plasticity of the nervous system. *Annu Rev Neurosci* 31, 563-590.

Fu, W.Y., Chen, Y., Sahin, M., Zhao, X.S., Shi, L., Bikoff, J.B., Lai, K.O., Yung, W.H., Fu, A.K., Greenberg, M.E., and Ip, N.Y. (2007). Cdk5 regulates EphA4-mediated dendritic spine retraction through an ephexin1-dependent mechanism. *Nat Neurosci* 10, 67-76.

Gale, N.W., Holland, S.J., Valenzuela, D.M., Flenniken, A., Pan, L., Ryan, T.E., Henkemeyer, M., Strebhardt, K., Hirai, H., Wilkinson, D.G., *et al.* (1996). Eph receptors and ligands comprise two major specificity subclasses and are reciprocally compartmentalized during embryogenesis. *Neuron* 17, 9-19.

Ge, W.P., and Duan, S. (2007). Persistent enhancement of neuron-glia signaling mediated by increased extracellular K⁺ accompanying long-term synaptic potentiation. *J Neurophysiol* 97, 2564-2569.

- Genoud, C., Quairiaux, C., Steiner, P., Hirling, H., Welker, E., and Knott, G.W. (2006). Plasticity of astrocytic coverage and glutamate transporter expression in adult mouse cortex. *PLoS Biol* 4, e343.
- Goel, A., and Lee, H.K. (2007). Persistence of experience-induced homeostatic synaptic plasticity through adulthood in superficial layers of mouse visual cortex. *J Neurosci* 27, 6692-6700.
- Gonzalez, M.I., and Robinson, M.B. (2004). Protein kinase C-dependent remodeling of glutamate transporter function. *Mol Interv* 4, 48-58.
- Greenwood, S.M., and Connolly, C.N. (2007). Dendritic and mitochondrial changes during glutamate excitotoxicity. *Neuropharmacology* 53, 891-898.
- Grootjans, J.J., Reekmans, G., Ceulemans, H., and David, G. (2000). Syntenin-syndecan binding requires syndecan-synteny and the co-operation of both PDZ domains of syntenin. *J Biol Chem* 275, 19933-19941.
- Grunwald, I.C., Korte, M., Adelmann, G., Plueck, A., Kullander, K., Adams, R.H., Frotscher, M., Bonhoeffer, T., and Klein, R. (2004). Hippocampal plasticity requires postsynaptic ephrinBs. *Nat Neurosci* 7, 33-40.
- Grunwald, I.C., Korte, M., Wolfer, D., Wilkinson, G.A., Unsicker, K., Lipp, H.P., Bonhoeffer, T., and Klein, R. (2001). Kinase-independent requirement of EphB2 receptors in hippocampal synaptic plasticity. *Neuron* 32, 1027-1040.
- Guillet, B.A., Velly, L.J., Canolle, B., Masméjean, F.M., Nieoullon, A.L., and Pisano, P. (2005). Differential regulation by protein kinases of activity and cell surface expression of glutamate transporters in neuron-enriched cultures. *Neurochem Int* 46, 337-346.
- Halassa, M.M., Fellin, T., and Haydon, P.G. (2007). The tripartite synapse: roles for gliotransmission in health and disease. *Trends Mol Med* 13, 54-63.
- Hasbani, M.J., Schlieff, M.L., Fisher, D.A., and Goldberg, M.P. (2001). Dendritic spines lost during glutamate receptor activation reemerge at original sites of synaptic contact. *J Neurosci* 21, 2393-2403.
- Haugeto, O., Ullensvang, K., Levy, L.M., Chaudhry, F.A., Honore, T., Nielsen, M., Lehre, K.P., and Danbolt, N.C. (1996). Brain glutamate transporter proteins form homomultimers. *J Biol Chem* 271, 27715-27722.
- Heasman, S.J., and Ridley, A.J. (2008). Mammalian Rho GTPases: new insights into their functions from in vivo studies. *Nat Rev Mol Cell Biol* 9, 690-701.
- Henderson, J.T., Georgiou, J., Jia, Z., Robertson, J., Elowe, S., Roder, J.C., and Pawson, T. (2001). The receptor tyrosine kinase EphB2 regulates NMDA-dependent synaptic function. *Neuron* 32, 1041-1056.

Henkemeyer, M., Itkis, O.S., Ngo, M., Hickmott, P.W., and Ethell, I.M. (2003). Multiple EphB receptor tyrosine kinases shape dendritic spines in the hippocampus. *J Cell Biol* 163, 1313-1326.

Henkemeyer, M., Orioli, D., Henderson, J.T., Saxton, T.M., Roder, J., Pawson, T., and Klein, R. (1996). Nuk controls pathfinding of commissural axons in the mammalian central nervous system. *Cell* 86, 35-46.

Hertz, L., and Zielke, H.R. (2004). Astrocytic control of glutamatergic activity: astrocytes as stars of the show. *Trends Neurosci* 27, 735-743.

Himanen, J.P., Chumley, M.J., Lackmann, M., Li, C., Barton, W.A., Jeffrey, P.D., Vearing, C., Geleick, D., Feldheim, D.A., Boyd, A.W., et al. (2004). Repelling class discrimination: ephrin-A5 binds to and activates EphB2 receptor signaling. *Nat Neurosci* 7, 501-509.

Hofer, S.B., Mrsic-Flogel, T.D., Bonhoeffer, T., and Hubener, M. (2009). Experience leaves a lasting structural trace in cortical circuits. *Nature* 457, 313-317.

Holmberg, J., Armulik, A., Senti, K.A., Edoff, K., Spalding, K., Momma, S., Cassidy, R., Flanagan, J.G., and Frisen, J. (2005). Ephrin-A2 reverse signaling negatively regulates neural progenitor proliferation and neurogenesis. *Genes Dev* 19, 462-471.

Howland, D.S., Liu, J., She, Y., Goad, B., Maragakis, N.J., Kim, B., Erickson, J., Kulik, J., DeVito, L., Psaltis, G., et al. (2002). Focal loss of the glutamate transporter EAAT2 in a transgenic rat model of SOD1 mutant-mediated amyotrophic lateral sclerosis (ALS). *Proc Natl Acad Sci U S A* 99, 1604-1609.

Hu, H.J., Alter, B.J., Carrasquillo, Y., Qiu, C.S., and Gereau, R.W.t. (2007). Metabotropic glutamate receptor 5 modulates nociceptive plasticity via extracellular signal-regulated kinase-Kv4.2 signaling in spinal cord dorsal horn neurons. *J Neurosci* 27, 13181-13191.

Huai, J., and Drescher, U. (2001). An ephrin-A-dependent signaling pathway controls integrin function and is linked to the tyrosine phosphorylation of a 120-kDa protein. *J Biol Chem* 276, 6689-6694.

Huang, Y.H., Sinha, S.R., Tanaka, K., Rothstein, J.D., and Bergles, D.E. (2004). Astrocyte glutamate transporters regulate metabotropic glutamate receptor-mediated excitation of hippocampal interneurons. *J Neurosci* 24, 4551-4559.

Ireland, D.R., and Abraham, W.C. (2002). Group I mGluRs increase excitability of hippocampal CA1 pyramidal neurons by a PLC-independent mechanism. *J Neurophysiol* 88, 107-116.

Irie, F., and Yamaguchi, Y. (2002). EphB receptors regulate dendritic spine development via intersectin, Cdc42 and N-WASP. *Nat Neurosci* 5, 1117-1118.

- Iwasato, T., Katoh, H., Nishimaru, H., Ishikawa, Y., Inoue, H., Saito, Y.M., Ando, R., Iwama, M., Takahashi, R., Negishi, M., and Itohara, S. (2007). Rac-GAP alpha-chimerin regulates motor-circuit formation as a key mediator of EphrinB3/EphA4 forward signaling. *Cell* 130, 742-753.
- Janssen, W.G., Vissavajhala, P., Andrews, G., Moran, T., Hof, P.R., and Morrison, J.H. (2005). Cellular and synaptic distribution of NR2A and NR2B in macaque monkey and rat hippocampus as visualized with subunit-specific monoclonal antibodies. *Exp Neurol* 191 Suppl 1, S28-44.
- Jourdain, P., Bergersen, L.H., Bhaukaurally, K., Bezzi, P., Santello, M., Domercq, M., Matute, C., Tonello, F., Gundersen, V., and Volterra, A. (2007). Glutamate exocytosis from astrocytes controls synaptic strength. *Nat Neurosci* 10, 331-339.
- Kalo, M.S., and Pasquale, E.B. (1999). Multiple in vivo tyrosine phosphorylation sites in EphB receptors. *Biochemistry* 38, 14396-14408.
- Kandel, E.R. (2001). The molecular biology of memory storage: a dialogue between genes and synapses. *Science* 294, 1030-1038.
- Kelleher, R.J., 3rd, Govindarajan, A., and Tonegawa, S. (2004). Translational regulatory mechanisms in persistent forms of synaptic plasticity. *Neuron* 44, 59-73.
- Kennedy, M.B., Beale, H.C., Carlisle, H.J., and Washburn, L.R. (2005). Integration of biochemical signalling in spines. *Nat Rev Neurosci* 6, 423-434.
- Kettenmann, H., and Verkhratsky, A. (2008). Neuroglia: the 150 years after. *Trends Neurosci* 31, 653-659.
- Kim, E., and Sheng, M. (2004). PDZ domain proteins of synapses. *Nat Rev Neurosci* 5, 771-781.
- Kim, J., Jung, S.C., Clemens, A.M., Petralia, R.S., and Hoffman, D.A. (2007). Regulation of dendritic excitability by activity-dependent trafficking of the A-type K⁺ channel subunit Kv4.2 in hippocampal neurons. *Neuron* 54, 933-947.
- Kim, S.J., and Linden, D.J. (2007). Ubiquitous plasticity and memory storage. *Neuron* 56, 582-592.
- Kirkwood, A., Rioult, M.C., and Bear, M.F. (1996). Experience-dependent modification of synaptic plasticity in visual cortex. *Nature* 381, 526-528.
- Klausberger, T., and Somogyi, P. (2008). Neuronal diversity and temporal dynamics: the unity of hippocampal circuit operations. *Science* 321, 53-57.
- Klein, R. (2009). Bidirectional modulation of synaptic functions by Eph/ephrin signaling. *Nat Neurosci* 12, 15-20.
- Knoll, B., Zarbališ, K., Wurst, W., and Drescher, U. (2001). A role for the EphA family in the topographic targeting of vomeronasal axons. *Development* 128, 895-906.

- Kohr, G. (2006). NMDA receptor function: subunit composition versus spatial distribution. *Cell Tissue Res* 326, 439-446.
- Konstantinova, I., Nikolova, G., Ohara-Imaizumi, M., Meda, P., Kucera, T., Zarbalis, K., Wurst, W., Nagamatsu, S., and Lammert, E. (2007). EphA-Ephrin-A-mediated beta cell communication regulates insulin secretion from pancreatic islets. *Cell* 129, 359-370.
- Kozorovitskiy, Y., Gross, C.G., Kopil, C., Battaglia, L., McBreen, M., Stranahan, A.M., and Gould, E. (2005). Experience induces structural and biochemical changes in the adult primate brain. *Proc Natl Acad Sci U S A* 102, 17478-17482.
- Kullander, K., Croll, S.D., Zimmer, M., Pan, L., McClain, J., Hughes, V., Zabski, S., DeChiara, T.M., Klein, R., Yancopoulos, G.D., and Gale, N.W. (2001a). Ephrin-B3 is the midline barrier that prevents corticospinal tract axons from recrossing, allowing for unilateral motor control. *Genes Dev* 15, 877-888.
- Kullander, K., and Klein, R. (2002). Mechanisms and functions of Eph and ephrin signalling. *Nat Rev Mol Cell Biol* 3, 475-486.
- Kullander, K., Mather, N.K., Diella, F., Dottori, M., Boyd, A.W., and Klein, R. (2001b). Kinase-dependent and kinase-independent functions of EphA4 receptors in major axon tract formation in vivo. *Neuron* 29, 73-84.
- Lallemand, Y., Luria, V., Haffner-Krausz, R., and Lonai, P. (1998). Maternally expressed PGK-Cre transgene as a tool for early and uniform activation of the Cre site-specific recombinase. *Transgenic Res* 7, 105-112.
- Lauterbach, J., and Klein, R. (2006). Release of full-length EphB2 receptors from hippocampal neurons to cocultured glial cells. *J Neurosci* 26, 11575-11581.
- Lehre, K.P., and Rusakov, D.A. (2002). Asymmetry of glia near central synapses favors presynaptically directed glutamate escape. *Biophys J* 83, 125-134.
- Levenson, J., Weeber, E., Selcher, J.C., Kategaya, L.S., Sweatt, J.D., and Eskin, A. (2002). Long-term potentiation and contextual fear conditioning increase neuronal glutamate uptake. *Nat Neurosci* 5, 155-161.
- Liebl, D.J., Morris, C.J., Henkemeyer, M., and Parada, L.F. (2003). mRNA expression of ephrins and Eph receptor tyrosine kinases in the neonatal and adult mouse central nervous system. *J Neurosci Res* 71, 7-22.
- Lim, B.K., Matsuda, N., and Poo, M.M. (2008a). Ephrin-B reverse signaling promotes structural and functional synaptic maturation in vivo. *Nat Neurosci* 11, 160-169.
- Lim, Y.S., McLaughlin, T., Sung, T.C., Santiago, A., Lee, K.F., and O'Leary, D.D. (2008b). p75(NTR) mediates ephrin-A reverse signaling required for axon repulsion and mapping. *Neuron* 59, 746-758.
- Lisman, J., Schulman, H., and Cline, H. (2002). The molecular basis of CaMKII function in synaptic and behavioural memory. *Nat Rev Neurosci* 3, 175-190.

- Liu, G., Choi, S., and Tsien, R.W. (1999). Variability of neurotransmitter concentration and nonsaturation of postsynaptic AMPA receptors at synapses in hippocampal cultures and slices. *Neuron* 22, 395-409.
- Lu, Q., Sun, E.E., Klein, R.S., and Flanagan, J.G. (2001). Ephrin-B reverse signaling is mediated by a novel PDZ-RGS protein and selectively inhibits G protein-coupled chemoattraction. *Cell* 105, 69-79.
- Lu, Y.M., Jia, Z., Janus, C., Henderson, J.T., Gerlai, R., Wojtowicz, J.M., and Roder, J.C. (1997). Mice lacking metabotropic glutamate receptor 5 show impaired learning and reduced CA1 long-term potentiation (LTP) but normal CA3 LTP. *J Neurosci* 17, 5196-5205.
- Lu, Y.M., Roder, J.C., Davidow, J., and Salter, M.W. (1998). Src activation in the induction of long-term potentiation in CA1 hippocampal neurons. *Science* 279, 1363-1367.
- Lujan, R., Nusser, Z., Roberts, J.D., Shigemoto, R., and Somogyi, P. (1996). Perisynaptic location of metabotropic glutamate receptors mGluR1 and mGluR5 on dendrites and dendritic spines in the rat hippocampus. *Eur J Neurosci* 8, 1488-1500.
- Maffei, A., Nelson, S.B., and Turrigiano, G.G. (2004). Selective reconfiguration of layer 4 visual cortical circuitry by visual deprivation. *Nat Neurosci* 7, 1353-1359.
- Majewska, A.K., Newton, J.R., and Sur, M. (2006). Remodeling of synaptic structure in sensory cortical areas in vivo. *J Neurosci* 26, 3021-3029.
- Malenka, R.C., and Bear, M.F. (2004). LTP and LTD: an embarrassment of riches. *Neuron* 44, 5-21.
- Maragakis, N.J., and Rothstein, J.D. (2004). Glutamate transporters: animal models to neurologic disease. *Neurobiol Dis* 15, 461-473.
- Marler, K.J., Becker-Barroso, E., Martinez, A., Llovera, M., Wentzel, C., Poopalasundaram, S., Hindges, R., Soriano, E., Comella, J., and Drescher, U. (2008). A TrkB/EphrinA interaction controls retinal axon branching and synaptogenesis. *J Neurosci* 28, 12700-12712.
- Marquardt, T., Shirasaki, R., Ghosh, S., Andrews, S.E., Carter, N., Hunter, T., and Pfaff, S.L. (2005). Coexpressed EphA receptors and ephrin-A ligands mediate opposing actions on growth cone navigation from distinct membrane domains. *Cell* 121, 127-139.
- Martin, K.C., and Kosik, K.S. (2002). Synaptic tagging -- who's it? *Nat Rev Neurosci* 3, 813-820.
- Martin, S.J., Grimwood, P.D., and Morris, R.G. (2000). Synaptic plasticity and memory: an evaluation of the hypothesis. *Annu Rev Neurosci* 23, 649-711.

Mathern, G.W., Mendoza, D., Lozada, A., Pretorius, J.K., Dehnes, Y., Danbolt, N.C., Nelson, N., Leite, J.P., Chimelli, L., Born, D.E., *et al.* (1999). Hippocampal GABA and glutamate transporter immunoreactivity in patients with temporal lobe epilepsy. *Neurology* 52, 453-472.

Matsuzaki, M., Honkura, N., Ellis-Davies, G.C., and Kasai, H. (2004). Structural basis of long-term potentiation in single dendritic spines. *Nature* 429, 761-766.

Matthias, K., Kirchhoff, F., Seifert, G., Huttmann, K., Matyash, M., Kettenmann, H., and Steinhauser, C. (2003). Segregated expression of AMPA-type glutamate receptors and glutamate transporters defines distinct astrocyte populations in the mouse hippocampus. *J Neurosci* 23, 1750-1758.

Minichiello, L., Korte, M., Wolfer, D., Kuhn, R., Unsicker, K., Cestari, V., Rossi-Arnaud, C., Lipp, H.P., Bonhoeffer, T., and Klein, R. (1999). Essential role for TrkB receptors in hippocampus-mediated learning. *Neuron* 24, 401-414.

Morgan, S.L., and Teyler, T.J. (2001). Electrical stimuli patterned after the theta-rhythm induce multiple forms of LTP. *J Neurophysiol* 86, 1289-1296.

Mothes, J.P., Parent, A.T., Wolosker, H., Brady, R.O., Jr., Linden, D.J., Ferris, C.D., Rogawski, M.A., and Snyder, S.H. (2000). D-serine is an endogenous ligand for the glycine site of the N-methyl-D-aspartate receptor. *Proc Natl Acad Sci U S A* 97, 4926-4931.

Mothes, J.P., Pollegioni, L., Ouanounou, G., Martineau, M., Fossier, P., and Baux, G. (2005). Glutamate receptor activation triggers a calcium-dependent and SNARE protein-dependent release of the gliotransmitter D-serine. *Proc Natl Acad Sci U S A* 102, 5606-5611.

Mulholland, P.J., Carpenter-Hyland, E.P., Hering, M.C., Becker, H.C., Woodward, J.J., and Chandler, L.J. (2008). Glutamate transporters regulate extrasynaptic NMDA receptor modulation of Kv2.1 potassium channels. *J Neurosci* 28, 8801-8809.

Murai, K.K., Nguyen, L.N., Irie, F., Yamaguchi, Y., and Pasquale, E.B. (2003). Control of hippocampal dendritic spine morphology through ephrin-A3/EphA4 signaling. *Nat Neurosci* 6, 153-160.

Murthy, V.N., and De Camilli, P. (2003). Cell biology of the presynaptic terminal. *Annu Rev Neurosci* 26, 701-728.

Nagerl, U.V., Eberhorn, N., Cambridge, S.B., and Bonhoeffer, T. (2004). Bidirectional activity-dependent morphological plasticity in hippocampal neurons. *Neuron* 44, 759-767.

Nave, K.A., and Trapp, B.D. (2008). Axon-glia signaling and the glial support of axon function. *Annu Rev Neurosci* 31, 535-561.

- Nelson, S.B., and Turrigiano, G.G. (2008). Strength through diversity. *Neuron* 60, 477-482.
- Nestor, M.W., Mok, L.P., Tulapurkar, M.E., and Thompson, S.M. (2007). Plasticity of neuron-glia interactions mediated by astrocytic EphARs. *J Neurosci* 27, 12817-12828.
- Nicoll, R.A. (2003). Expression mechanisms underlying long-term potentiation: a postsynaptic view. *Philos Trans R Soc Lond B Biol Sci* 358, 721-726.
- Nicoll, R.A., and Schmitz, D. (2005). Synaptic plasticity at hippocampal mossy fibre synapses. *Nat Rev Neurosci* 6, 863-876.
- Nimchinsky, E.A., Sabatini, B.L., and Svoboda, K. (2002). Structure and function of dendritic spines. *Annu Rev Physiol* 64, 313-353.
- Nishiyama, A., Komitova, M., Suzuki, R., and Zhu, X. (2009). Polydendrocytes (NG2 cells): multifunctional cells with lineage plasticity. *Nat Rev Neurosci* 10, 9-22.
- Nolte, C., Matyash, M., Pivneva, T., Schipke, C.G., Ohlemeyer, C., Hanisch, U.K., Kirchhoff, F., and Kettenmann, H. (2001). GFAP promoter-controlled EGFP-expressing transgenic mice: a tool to visualize astrocytes and astrogliosis in living brain tissue. *Glia* 33, 72-86.
- O'Keefe, J., and Nadel, L. (1978). *The hippocampus as a cognitive map* (Oxford New York: Clarendon Press ; Oxford University Press).
- Oliet, S.H., Malenka, R.C., and Nicoll, R.A. (1997). Two distinct forms of long-term depression coexist in CA1 hippocampal pyramidal cells. *Neuron* 18, 969-982.
- Oliet, S.H., and Piet, R. (2004). Anatomical remodelling of the supraoptic nucleus: changes in synaptic and extrasynaptic transmission. *J Neuroendocrinol* 16, 303-307.
- Oliet, S.H., Piet, R., and Poulain, D.A. (2001). Control of glutamate clearance and synaptic efficacy by glial coverage of neurons. *Science* 292, 923-926.
- Oliva, A.A., Jr., Lam, T.T., and Swann, J.W. (2002). Distally directed dendrotoxicity induced by kainic Acid in hippocampal interneurons of green fluorescent protein-expressing transgenic mice. *J Neurosci* 22, 8052-8062.
- Palmer, A., Zimmer, M., Erdmann, K.S., Eulenburg, V., Porthin, A., Heumann, R., Deutsch, U., and Klein, R. (2002). EphrinB phosphorylation and reverse signaling: regulation by Src kinases and PTP-BL phosphatase. *Mol Cell* 9, 725-737.
- Panatier, A., Theodosis, D.T., Mothet, J.P., Touquet, B., Pollegioni, L., Poulain, D.A., and Oliet, S.H. (2006). Glia-derived D-serine controls NMDA receptor activity and synaptic memory. *Cell* 125, 775-784.

- Pasquale, E.B. (2008). Eph-ephrin bidirectional signaling in physiology and disease. *Cell* 133, 38-52.
- Pastalkova, E., Serrano, P., Pinkhasova, D., Wallace, E., Fenton, A.A., and Sacktor, T.C. (2006). Storage of spatial information by the maintenance mechanism of LTP. *Science* 313, 1141-1144.
- Pawson, T., and Scott, J.D. (1997). Signaling through scaffold, anchoring, and adaptor proteins. *Science* 278, 2075-2080.
- Penzes, P., Beeser, A., Chernoff, J., Schiller, M.R., Eipper, B.A., Mains, R.E., and Huganir, R.L. (2003). Rapid induction of dendritic spine morphogenesis by trans-synaptic ephrinB-EphB receptor activation of the Rho-GEF kalirin. *Neuron* 37, 263-274.
- Perea, G., and Araque, A. (2007). Astrocytes potentiate transmitter release at single hippocampal synapses. *Science* 317, 1083-1086.
- Perea, G., Navarrete, M., and Araque, A. (2009). Tripartite synapses: astrocytes process and control synaptic information. *Trends Neurosci* 32, 421-431.
- Pfrieger, F.W., and Barres, B.A. (1997). Synaptic efficacy enhanced by glial cells in vitro. *Science* 277, 1684-1687.
- Pita-Almenar, J.D., Collado, M.S., Colbert, C.M., and Eskin, A. (2006). Different mechanisms exist for the plasticity of glutamate reuptake during early long-term potentiation (LTP) and late LTP. *J Neurosci* 26, 10461-10471.
- Proper, E.A., Hoogland, G., Kappen, S.M., Jansen, G.H., Rensen, M.G., Schrama, L.H., van Veelen, C.W., van Rijen, P.C., van Nieuwenhuizen, O., Gispen, W.H., and de Graan, P.N. (2002). Distribution of glutamate transporters in the hippocampus of patients with pharmaco-resistant temporal lobe epilepsy. *Brain* 125, 32-43.
- Qin, H., Noberini, R., Huan, X., Shi, J., Pasquale, E.B., and Song, J. (2010). Structural Characterization of the EphA4-Ephrin-B2 Complex Reveals New Features Enabling Eph-Ephrin Binding Promiscuity. *J Biol Chem* 285, 644-654.
- Richter, M., Murai, K.K., Bourgin, C., Pak, D.T., and Pasquale, E.B. (2007). The EphA4 receptor regulates neuronal morphology through SPAR-mediated inactivation of Rap GTPases. *J Neurosci* 27, 14205-14215.
- Rodriguez, C.I., Buchholz, F., Galloway, J., Sequerra, R., Kasper, J., Ayala, R., Stewart, A.F., and Dymecki, S.M. (2000). High-efficiency deleter mice show that FLPe is an alternative to Cre-loxP. *Nat Genet* 25, 139-140.
- Rossman, K.L., Der, C.J., and Sondek, J. (2005). GEF means go: turning on RHO GTPases with guanine nucleotide-exchange factors. *Nat Rev Mol Cell Biol* 6, 167-180.
- Rothstein, J.D., Dykes-Hoberg, M., Pardo, C.A., Bristol, L.A., Jin, L., Kuncl, R.W., Kanai, Y., Hediger, M.A., Wang, Y., Schielke, J.P., and Welty, D.F. (1996).

Knockout of glutamate transporters reveals a major role for astroglial transport in excitotoxicity and clearance of glutamate. *Neuron* 16, 675-686.

Rothstein, J.D., Martin, L.J., and Kuncl, R.W. (1992). Decreased glutamate transport by the brain and spinal cord in amyotrophic lateral sclerosis. *N Engl J Med* 326, 1464-1468.

Rothstein, J.D., Van Kammen, M., Levey, A.I., Martin, L.J., and Kuncl, R.W. (1995). Selective loss of glial glutamate transporter GLT-1 in amyotrophic lateral sclerosis. *Ann Neurol* 38, 73-84.

Sahin, M., Greer, P.L., Lin, M.Z., Poucher, H., Eberhart, J., Schmidt, S., Wright, T.M., Shamah, S.M., O'Connell, S., Cowan, C.W., et al. (2005). Eph-dependent tyrosine phosphorylation of ephexin1 modulates growth cone collapse. *Neuron* 46, 191-204.

Salter, M.W., and Kalia, L.V. (2004). Src kinases: a hub for NMDA receptor regulation. *Nat Rev Neurosci* 5, 317-328.

Sanes, J.R., and Lichtman, J.W. (1999). Can molecules explain long-term potentiation? *Nat Neurosci* 2, 597-604.

Sarantis, M., Ballerini, L., Miller, B., Silver, R.A., Edwards, M., and Attwell, D. (1993). Glutamate uptake from the synaptic cleft does not shape the decay of the non-NMDA component of the synaptic current. *Neuron* 11, 541-549.

Sasaki, S., Komori, T., and Iwata, M. (2000). Excitatory amino acid transporter 1 and 2 immunoreactivity in the spinal cord in amyotrophic lateral sclerosis. *Acta Neuropathol* 100, 138-144.

Segura, I., Essmann, C.L., Weinges, S., and Acker-Palmer, A. (2007). Grb4 and GIT1 transduce ephrinB reverse signals modulating spine morphogenesis and synapse formation. *Nat Neurosci* 10, 301-310.

Seifert, G., Schilling, K., and Steinhauser, C. (2006). Astrocyte dysfunction in neurological disorders: a molecular perspective. *Nat Rev Neurosci* 7, 194-206.

Shalin, S.C., Hernandez, C.M., Dougherty, M.K., Morrison, D.K., and Sweatt, J.D. (2006). Kinase suppressor of Ras1 compartmentalizes hippocampal signal transduction and subserves synaptic plasticity and memory formation. *Neuron* 50, 765-779.

Shamah, S.M., Lin, M.Z., Goldberg, J.L., Estrach, S., Sahin, M., Hu, L., Bazalakova, M., Neve, R.L., Corfas, G., Debant, A., and Greenberg, M.E. (2001). EphA receptors regulate growth cone dynamics through the novel guanine nucleotide exchange factor ephexin. *Cell* 105, 233-244.

Sheng, M., and Hoogenraad, C.C. (2007). The postsynaptic architecture of excitatory synapses: a more quantitative view. *Annu Rev Biochem* 76, 823-847.

- Sheng, M., and Kim, M.J. (2002). Postsynaptic signaling and plasticity mechanisms. *Science* 298, 776-780.
- Shepherd, J.D., and Huganir, R.L. (2007). The cell biology of synaptic plasticity: AMPA receptor trafficking. *Annu Rev Cell Dev Biol* 23, 613-643.
- Sherwood, C.C., Stimpson, C.D., Raghanti, M.A., Wildman, D.E., Uddin, M., Grossman, L.I., Goodman, M., Redmond, J.C., Bonar, C.J., Erwin, J.M., and Hof, P.R. (2006). Evolution of increased glia-neuron ratios in the human frontal cortex. *Proc Natl Acad Sci U S A* 103, 13606-13611.
- Shi, L., Fu, W.Y., Hung, K.W., Porchetta, C., Hall, C., Fu, A.K., and Ip, N.Y. (2007). Alpha2-chimaerin interacts with EphA4 and regulates EphA4-dependent growth cone collapse. *Proc Natl Acad Sci U S A* 104, 16347-16352.
- Silva, A.J., Stevens, C.F., Tonegawa, S., and Wang, Y. (1992). Deficient hippocampal long-term potentiation in alpha-calcium-calmodulin kinase II mutant mice. *Science* 257, 201-206.
- Snyder, E.M., Philpot, B.D., Huber, K.M., Dong, X., Fallon, J.R., and Bear, M.F. (2001). Internalization of ionotropic glutamate receptors in response to mGluR activation. *Nat Neurosci* 4, 1079-1085.
- Soulet, D., and Rivest, S. (2008). Microglia. *Curr Biol* 18, R506-508.
- Squire, L.R., Stark, C.E., and Clark, R.E. (2004). The medial temporal lobe. *Annu Rev Neurosci* 27, 279-306.
- Stein, E., Lane, A.A., Cerretti, D.P., Schoecklmann, H.O., Schroff, A.D., Van Etten, R.L., and Daniel, T.O. (1998). Eph receptors discriminate specific ligand oligomers to determine alternative signaling complexes, attachment, and assembly responses. *Genes Dev* 12, 667-678.
- Stellwagen, D., and Malenka, R.C. (2006). Synaptic scaling mediated by glial TNF-alpha. *Nature* 440, 1054-1059.
- Stoppini, L., Buchs, P.A., and Muller, D. (1991). A simple method for organotypic cultures of nervous tissue. *J Neurosci Methods* 37, 173-182.
- Sudhof, T.C. (2004). The synaptic vesicle cycle. *Annu Rev Neurosci* 27, 509-547.
- Sutton, M.A., and Schuman, E.M. (2006). Dendritic protein synthesis, synaptic plasticity, and memory. *Cell* 127, 49-58.
- Swann, J.W., Al-Noori, S., Jiang, M., and Lee, C.L. (2000). Spine loss and other dendritic abnormalities in epilepsy. *Hippocampus* 10, 617-625.
- Takasu, M.A., Dalva, M.B., Zigmond, R.E., and Greenberg, M.E. (2002). Modulation of NMDA receptor-dependent calcium influx and gene expression through EphB receptors. *Science* 295, 491-495.

Tanaka, K., Watase, K., Manabe, T., Yamada, K., Watanabe, M., Takahashi, K., Iwama, H., Nishikawa, T., Ichihara, N., Kikuchi, T., *et al.* (1997). Epilepsy and exacerbation of brain injury in mice lacking the glutamate transporter GLT-1. *Science* 276, 1699-1702.

Tang, Y.P., Shimizu, E., Dube, G.R., Rampon, C., Kerchner, G.A., Zhuo, M., Liu, G., and Tsien, J.Z. (1999). Genetic enhancement of learning and memory in mice. *Nature* 401, 63-69.

Thomas, G.M., and Huganir, R.L. (2004). MAPK cascade signalling and synaptic plasticity. *Nat Rev Neurosci* 5, 173-183.

Tolias, K.F., Bikoff, J.B., Burette, A., Paradis, S., Harrar, D., Tavazoie, S., Weinberg, R.J., and Greenberg, M.E. (2005). The Rac1-GEF Tiam1 couples the NMDA receptor to the activity-dependent development of dendritic arbors and spines. *Neuron* 45, 525-538.

Tolias, K.F., Bikoff, J.B., Kane, C.G., Tolias, C.S., Hu, L., and Greenberg, M.E. (2007). The Rac1 guanine nucleotide exchange factor Tiam1 mediates EphB receptor-dependent dendritic spine development. *Proc Natl Acad Sci U S A* 104, 7265-7270.

Tremblay, M.E., Riad, M., Bouvier, D., Murai, K.K., Pasquale, E.B., Descarries, L., and Doucet, G. (2007). Localization of EphA4 in axon terminals and dendritic spines of adult rat hippocampus. *J Comp Neurol* 501, 691-702.

Trotti, D., Rolfs, A., Danbolt, N.C., Brown, R.H., Jr., and Hediger, M.A. (1999). SOD1 mutants linked to amyotrophic lateral sclerosis selectively inactivate a glial glutamate transporter. *Nat Neurosci* 2, 427-433.

Tsien, J.Z., Chen, D.F., Gerber, D., Tom, C., Mercer, E.H., Anderson, D.J., Mayford, M., Kandel, E.R., and Tonegawa, S. (1996). Subregion- and cell type-restricted gene knockout in mouse brain. *Cell* 87, 1317-1326.

Tsuda, H., Han, S.M., Yang, Y., Tong, C., Lin, Y.Q., Mohan, K., Haueter, C., Zoghbi, A., Harati, Y., Kwan, J., *et al.* (2008). The amyotrophic lateral sclerosis 8 protein VAPB is cleaved, secreted, and acts as a ligand for Eph receptors. *Cell* 133, 963-977.

Tsui-Pierchala, B.A., Encinas, M., Milbrandt, J., and Johnson, E.M., Jr. (2002). Lipid rafts in neuronal signaling and function. *Trends Neurosci* 25, 412-417.

Tsukada, S., Iino, M., Takayasu, Y., Shimamoto, K., and Ozawa, S. (2005). Effects of a novel glutamate transporter blocker, (2S, 3S)-3-[3-[4-(trifluoromethyl)benzoylamino]benzyloxy]aspartate (TFB-TBOA), on activities of hippocampal neurons. *Neuropharmacology* 48, 479-491.

Turrigiano, G.G. (2008). The self-tuning neuron: synaptic scaling of excitatory synapses. *Cell* 135, 422-435.

- Turrigiano, G.G., and Nelson, S.B. (2004). Homeostatic plasticity in the developing nervous system. *Nat Rev Neurosci* 5, 97-107.
- Tzingounis, A.V., and Wadiche, J.I. (2007). Glutamate transporters: confining runaway excitation by shaping synaptic transmission. *Nat Rev Neurosci* 8, 935-947.
- Ullian, E.M., Sapperstein, S.K., Christopherson, K.S., and Barres, B.A. (2001). Control of synapse number by glia. *Science* 291, 657-661.
- van Dam, E.J., Kamal, A., Artola, A., de Graan, P.N., Gispen, W.H., and Ramakers, G.M. (2004). Group I metabotropic glutamate receptors regulate the frequency-response function of hippocampal CA1 synapses for the induction of LTP and LTD. *Eur J Neurosci* 19, 112-118.
- Ventura, R., and Harris, K.M. (1999). Three-dimensional relationships between hippocampal synapses and astrocytes. *J Neurosci* 19, 6897-6906.
- Volterra, A., and Meldolesi, J. (2005). Astrocytes, from brain glue to communication elements: the revolution continues. *Nat Rev Neurosci* 6, 626-640.
- Wadiche, J.I., Arriza, J.L., Amara, S.G., and Kavanaugh, M.P. (1995). Kinetics of a human glutamate transporter. *Neuron* 14, 1019-1027.
- Wadiche, J.I., and Jahr, C.E. (2005). Patterned expression of Purkinje cell glutamate transporters controls synaptic plasticity. *Nat Neurosci* 8, 1329-1334.
- Watase, K., Hashimoto, K., Kano, M., Yamada, K., Watanabe, M., Inoue, Y., Okuyama, S., Sakagawa, T., Ogawa, S., Kawashima, N., *et al.* (1998). Motor discoordination and increased susceptibility to cerebellar injury in GLAST mutant mice. *Eur J Neurosci* 10, 976-988.
- Wegmeyer, H., Egea, J., Rabe, N., Gezelius, H., Filosa, A., Enjin, A., Varoqueaux, F., Deininger, K., Schnutgen, F., Brose, N., *et al.* (2007). EphA4-dependent axon guidance is mediated by the RacGAP alpha2-chimaerin. *Neuron* 55, 756-767.
- Weiergraber, M., Henry, M., Krieger, A., Kamp, M., Radhakrishnan, K., Hescheler, J., and Schneider, T. (2006). Altered seizure susceptibility in mice lacking the Ca(v)2.3 E-type Ca²⁺ channel. *Epilepsia* 47, 839-850.
- Wenthold, R.J., Petralia, R.S., Blahos, J., II, and Niedzielski, A.S. (1996). Evidence for multiple AMPA receptor complexes in hippocampal CA1/CA2 neurons. *J Neurosci* 16, 1982-1989.
- Whitlock, J.R., Heynen, A.J., Shuler, M.G., and Bear, M.F. (2006). Learning induces long-term potentiation in the hippocampus. *Science* 313, 1093-1097.
- Xu, N.J., and Henkemeyer, M. (2009). Ephrin-B3 reverse signaling through Grb4 and cytoskeletal regulators mediates axon pruning. *Nat Neurosci* 12, 268-276.

- Yasuda, H., Barth, A.L., Stellwagen, D., and Malenka, R.C. (2003). A developmental switch in the signaling cascades for LTP induction. *Nat Neurosci* 6, 15-16.
- Yuste, R., and Bonhoeffer, T. (2001). Morphological changes in dendritic spines associated with long-term synaptic plasticity. *Annu Rev Neurosci* 24, 1071-1089.
- Zakharenko, S.S., Patterson, S.L., Dragatsis, I., Zeitlin, S.O., Siegelbaum, S.A., Kandel, E.R., and Morozov, A. (2003). Presynaptic BDNF required for a presynaptic but not postsynaptic component of LTP at hippocampal CA1-CA3 synapses. *Neuron* 39, 975-990.
- Zhang, H., Webb, D.J., Asmussen, H., Niu, S., and Horwitz, A.F. (2005). A GIT1/PIX/Rac/PAK signaling module regulates spine morphogenesis and synapse formation through MLC. *J Neurosci* 25, 3379-3388.
- Zhou, L., Martinez, S.J., Haber, M., Jones, E.V., Bouvier, D., Doucet, G., Corera, A.T., Fon, E.A., Zisch, A.H., and Murai, K.K. (2007). EphA4 signaling regulates phospholipase Cgamma1 activation, cofilin membrane association, and dendritic spine morphology. *J Neurosci* 27, 5127-5138.
- Zucker, R.S., and Regehr, W.G. (2002). Short-term synaptic plasticity. *Annu Rev Physiol* 64, 355-405.
- Zuo, Y., Yang, G., Kwon, E., and Gan, W.B. (2005). Long-term sensory deprivation prevents dendritic spine loss in primary somatosensory cortex. *Nature* 436, 261-265.

Curriculum vitae

PERSONAL DATA

Name Alessandro Filosa
Nationality Italian
Date of birth October 31, 1980
Place of birth Formia, Italy

EDUCATION

Sep 2005 - Present International Max Planck Research School for Molecular and Cellular Life Sciences, Munich, Germany.

Sep 2005 - Present PhD student position at the Max Planck Institute of Neurobiology, Martinsried, Germany.

Nov 2004 Laurea (Master equivalent) in Biology, *summa cum laude*, University of Naples “Federico II”, Italy.

RESEARCH EXPERIENCE

Sep 2009 - Oct 2009 Friedrich Miescher Institute, Basel, Switzerland.

Project Modulation of amygdala synaptic plasticity by Eph receptors and ephrin ligands.

Position Guest scientist

PI Prof. Andreas Lüthi

Sep 2005 - Present Max Planck Institute of Neurobiology, Martinsried, Germany.
Project The role of Eph tyrosine kinase receptors in hippocampal synaptic plasticity.
Position PhD student
PI Prof. Rüdiger Klein

Dec 2004 - Aug 2005 Telethon Institute of Genetics and Medicine, Naples, Italy.
Project The function of the COUP-TF transcription factors in oligodendrocytes and Cajal-Retzius cells development.
Position Telethon foundation graduate fellow
PI Dr. Michèle Studer

Mar 2003 - Nov 2004 Telethon Institute of Genetics and Medicine, Naples, Italy.
Project The role of the COUP-TF transcription factors in forebrain interneuron migrations.
Position Master student
PI Dr. Michèle Studer

TEACHING EXPERIENCE

Oct 2009 - Present Supervisor of a PhD student of the Graduate School of Systemic Neurosciences, Ludwig Maximilians University, Munich.

- Aug 2009** Lecturer for one week practical course for master students of the Graduate School of Systemic Neurosciences, Ludwig Maximilians University, Munich.
- Mar 2008 - Jun 2008** Supervisor of a PhD student of the Graduate School of Systemic Neurosciences, Ludwig Maximilians University, Munich.
- May 2005** Lecturer for the undergraduate neurobiology course held by Prof. Carla Perrone-Capano, University of Naples Federico II.

PUBLICATIONS

Filosa A.*, Paixão S.*, Honsek S.D., Carmona M.A., Becker L., Feddersen, B., Gaitanos L., Rudhard Y., Schoepfer R., Klopstock T., Kullander, K., Rose C.R., Pasquale E.B., Klein R. (2009) Neuron-glia communication via EphA4/ephrinA3 modulates LTP through glial glutamate transport. *Nat. Neurosci.* 12, 1285-1292.

Wegmeyer H., Egea J., Rabe N., Gezelius H., **Filosa A.**, Enjin A., Veroqueaux F., Deininger K., Schnuetgen F., Brose N., Klein R., Kullander K., Betz A. (2007) EphA4-dependent axon guidance is mediated by the RacGAP α 2-chimaerin. *Neuron* 55, 756-767.

Armentano M., **Filosa A.**, Andolfi G., Studer M. (2006) COUP-TFI is required for the formation of commissural projections in the forebrain by regulating axonal growth. *Development* 133, 4151-4162.

Studer M., **Filosa A.**, Rubenstein J.L.R. (2005) The nuclear receptor COUP-TFI represses differentiation of Cajal-Retzius cells. *Brain. Res. Bull.* 66, 394-401.

Tripodi M.*, **Filosa A.***, Armentano M., Studer M. (2004) The COUP-TF nuclear receptors regulate cell migration in the mammalian basal forebrain. *Development* 131, 6119-6129.

*Equal contribution.

HONOURS AND AWARDS

Nov 2009 Rosa Laura and Hartmut Wekerle Award

Sep 2005 Antonio Marzullo Award for the best master thesis in molecular and cellular biology, University of Trieste, Trieste, Italy.